LONG TERM DNA STORAGE EVALUATION AND METHODOLOGY

By

Ryan Lehto

A dissertation submitted in partial
fulfillment of the requirements of the
degree of
Doctor of Philosophy in Biotechnology

Biotechnology PhD Program, Lakehead
University Thunder Bay, Ontario, Canada

20 July 2021

Abstract

DNA preservation over the long term is a considerable problem for many fields that still lack a viable, cost-effective, long-term solution. The considerable amount of genetic material that is currently aging in facilities around the world continues to slowly degrade over time. New discoveries are being made based on genetic material recovered from ancient specimens, and new technologies are looking to store metadata in DNA; but all face this eventual problem of long-term stability. There is no "magic bullet" for preventing the various forms of DNA damage that accumulate over time, and all current technological solutions have tradeoffs. Each method of preparation, storage, and processing is chosen with the immediate downstream application as the priority, and all have shortcomings for overall preservation. Costs and space requirements continue to rise as more material is continuously accumulated, and furthermore, DNA damage studies often extrapolate their results into the future, giving models that may not be accurate. In this study, I investigate current methods and propose a potential new approach to address the problem. Chapter 1 briefly introduces DNA structure, damage mechanisms and storage conditions. Chapter 2 investigates common laboratory storage conditions with ultrapure reagents, to investigate whether DNA damage accumulation is predominantly due to contamination and processing rather than storage conditions and spontaneous reactions. This study was conducted in real time over five years, under controlled conditions. Chapter 3 investigates the efficiency of trehalose, a sugar commonly used in anhydrobioses as it is often seen as a panacea for DNA preservation. Trehalose has protective properties, but by itself was not a viable long-term solution since the samples were still prone to certain damage types, as demonstrated experimentally. In Chapter 4, several commercial DNA storage products are tested for efficiency, with all showing various protective qualities but falling short of halting damage accumulation or being a satisfactory long-term storage candidate. Chapter 5 is a preliminary investigation of harnessing biocrystallization for DNA storage. The use of DNA protection during starvation protein (Dps), which is often used by bacteria for cellular and nucleic acid protection, was investigated as a potential long-term DNA storage solution. Dps was found to have significant protective properties, and further investigation into biocrystallization therefore needs to be carried out as a possible solution to the long-term DNA degradation problem.

Acknowledgements

The very long journey that I undertook while doing this project had an incredible number of challenges; personal, professional, and academic. I had a severe heath crisis, a two-year ongoing pandemic at the time of this publication which shut down my research, and several research setbacks. In the end, the people who I met and collaborated with in my academic career inspired me and taught me that the journey is the goal in leaning, not the destination. Learning is a lifelong pursuit and higher learning is the pursuit, not just the current project one is doing. I would like to thank Dr. David Law in particular for stepping in to fulfill my supervisor role and really help shape the final research. I would like to thank Dr. Carney Matheson for his depth of knowledge and inspiration as my original supervisor; my committee member Dr. Christine Gottardo and my external examiner Dr Greg Moorhead; the amazing staff in the Biology Department at Lakehead University, especially Michael Moore; the staff at Genetic Health; and the Lakehead University Paleo-DNA Laboratory for all their technical support and data collection. Special thanks to Sigma–Aldrich, Fisher Scientific, GE Healthcare, and Biomeme for donating reagents for the long-term stability and commercial reagent studies. As always, I am always grateful for my children, Jordan, and Victoria, as I strive to be someone they can look up to.

Declaration

I hereby declare that this submission is my own work and that, to the best of my knowledge and belief, it contains no material previously published or written by another person, except where due acknowledgment has been made in the text.

Ryan Lehto

Table of Contents

List of Figures

List of Tables

List of Abbreviations

Abbreviation	Name
A	Adenine
aDNA	Ancient DNA
AGE	Agarose Gel Electrophoresis
AP	Apurinic/Apyrimidinic Sites
AMU	Atomic Mass Units
BER	Base excision repair
bp	Base Pair
C	Cytosine
DNase	Deoxyribonuclease
DNA	Deoxyribonucleic acid
DSB	Double-Strand Breaks
Dps	DNA Starvation Proteins
dsDNA	Double-Stranded DNA
DTT	Dithiothreitol
E. coli	*Escherichia coli*
EtBr	Ethidium Bromide
Fapy A	2,6-diamino-5-formamidopyrimidine
Fapy G	2,6-diamino-4-hydroxy-5-formamidopyrimidine
FFPE	Formalin fixed paraffin embedded
FTA	Flinders Technology Associates
G	Guanine
H_2O_2	Hydrogen Peroxide
ICLs	Interstrand Cross Links
mtDNA	Mitochondrial DNA
NER	Nucleotide excision repair
nm	Nanometer
PCR	Polymerase Chain Reaction
PAGE	Polyacrylamide Gel Electrophoresis
PK	Proteinase K
ROS	Reactive Oxygen Species
SDS	Sodium Dodecyl Sulfate
SSB	Single-Strand Breaks
ssDNA	Single-Stranded DNA
T	Thymine
Taq	*Thermus aquaticus*
TE	TE (Tris–HCl/EDTA)
TMOS	Tetramethoxysilane
UDG	Uracil-DNA Glycosylase

Introduction

The deoxyribose nucleic acid, or deoxyribonucleic acid, molecule (DNA) is the basis of the code for life as we understand it. Ever since the structure of its B form, also known as the Watson–Crick form, was first elucidated by Crick, Watson, and Rosen (Watson et al., 1953) in the 1950s, understanding the information it represents has continued to grow in importance and complexity. Previous research has shown that the DNA molecule exists in several structural forms, with a variety of intermediate forms *in vitro* and *in vivo* (Berg et al., 2002). Effects of the form of DNA have been implicated in gene expression and regulation, and protection from damaging mechanisms; however, a large gap has been acknowledged in the research in this area (Kim, 2020).

While inside the living organism, the DNA molecule is under constant attack from many different sources and must be promptly repaired and stabilized in order to maintain its function and the health of the organism (Chen et al., 2020). The ability of an organism to maintain an intact genome with minimal errors, and consequently pass that genome to its offspring, is what allows that species to thrive and drives evolution (Mayr et al., 1998). Once the DNA molecule is removed from the dynamic equilibrium of damage and repair in the *in vivo* environment of an organism, it becomes vulnerable to many forms of damage. The ability to store DNA in an undamaged, unaltered form that is readily available for testing or biotechnological applications, over a long period of time, continues to present a significant challenge that has been met with varying degrees of success. In addition, newly-emerging technologies aiming to use synthetic DNA for digital data storage now struggle to maintain this DNA with minimal degradation over the long term (Dong et al., 2020).

There is currently no consensus on the best method for long-term DNA sample storage, and there is wide variation in storage methodology between industrial, academic, forensic, and medical applications, all which have unique challenges and requirements. (Anchordoquy et al., 2000 ; Davis et al., 2000 ; Durmaz, 2002, Evans et al., 2000; Kim et al 2003; Villanueva et al.,1998). Since DNA is thought to possess a half-life of 521 years, it can be extrapolated that DNA will effectively have every bond destroyed after a maximum of 6.8 million years (Kaplan, 2012). Any DNA subject to this spontaneous damage rate would cease to be readable after

approximately 1.5 million years, when the remaining strands would be too short to give meaningful information (Kaplan, 2012). In contradiction to this understanding of DNA degradation, a 1.6-million-year-old mammoth large genome was successfully recovered in Siberia from mammoth teeth. This discovery suggests that environmental rates of degradation may not be as linear as previously thought (van der Valk et al., 2021). In fact, environmental conditions where DNA specimens have survived for hundreds to millions of years all have similar properties. The DNA was embedded in some sort of physical matrix such as bone, resin, or ice, at a stable temperature, usually low, and protected from ultraviolet (UV) radiation (Peris et al., 2020). A further condition, overlooked until quite recently, is the preservation of DNA in low oxygen environments (Matange et al., 2021). In some natural environments under low temperature and low oxygen conditions, water by itself is not as destructive as shown experimentally under laboratory conditions (Pajnič et al. 2019). For example, bog bodies completely submerged for hundreds to thousands of years have been recovered and the DNA analyzed successfully, which is contrary to laboratory results that anticipated complete degradation in a relatively short time (Latham et al., 2019). Damage experiments and short-term experiments have all led to damage models that suggest environmental DNA from lake beds and saltwater environments should degrade very rapidly (Borde et al., 2008), but studies in which viable DNA was recovered from seabed's and lake beds after thousands of years contradict these models and show the ability of DNA to survive intact for extreme lengths of time in the real-world environment (Marco et al., 2013). Recent studies have argued that intracellular staining seen in Cenozoic and Cretaceous fossils is consistent with the presence of organic endogenous DNA from 30- to 80-million-year-old samples, which would necessitate a complete reevaluation of DNA stability over time if proven true (Alida M et al., 2021).

1.1 The Problem

Today's requirements for DNA storage outside of the cell come with many problems that continue to cause issues for traditional disciplines such as medicine, forensic science, biology, and pharmacy, as well as new technologies such as DNA-based, long-term mass data storage that is currently under development (Extance, 2016). There is no consensus on, or proven method for,

DNA storage over decades or longer without noticeable degradation. Current methodologies require a significant quantity of DNA to begin with, with a high purity and in a stable environment. The current revolution driving DNA recovery from older samples has arisen from advances in sequencing technology, methodology, and chemistry – as opposed to better storage techniques – which allow DNA to be recovered more efficiently and sequenced in smaller fragments (Gutaker et al., 2017, Rohland et al., 2018). These technological advances have lowered the bar, in some ways, to the level and quality of DNA needed for storage and for future analysis. However, these advances should also make researchers rethink what the priorities are for DNA preservation over the long term (Xavier et al., 2021). Base modification, crosslinking or abasic sites may have more of an impact on DNA quality and interpretation than samples being in the form of short fragments, which we are now able to amplify and interpret with the aid of complex bioinformatics programs (Barba et al., 2017).

The challenge begins when storing DNA outside of the dynamic equilibrium of the homeostatic cellular environment, as outlined above. The intracellular environment contains the associated proteins and enzymes which support structural packing as well as maintaining the pH, hydration, and ionic balance in a dynamic equilibrium thus keeping the DNA in a flexible, stable state (Kool et al. 2000). After extraction, isolated DNA is exposed to a greater variety of damaging agents and mechanisms, beginning at the extraction/purification stage when the homeostatic environment is compromised. The preservation of this genetic material over the medium to long term has emerged as a significant problem, and as uses for this genetic information continue to grow, the integrity and quality challenges also increase. As a continually growing number and quantity of DNA samples accumulate and age under a variety of conditions, the problem becomes greater and greater. There are huge numbers of DNA samples currently stored in genetic banks, medical facilities, research facilities and industrial facilities, all slowly degrading over time (Malsagova et al., 2020).

The most prevalent method of preservation involves storing genetic material deep-frozen, in ultra-low temperature conditions. Freezing the material and keeping it in a constant state of deep freeze requires special freezers, a constant electrical supply, and substantial space, and such samples are always at risk of mechanical failure while still experiencing slow degradation in

many cases (Shabihkhani et al. 2014). The cost of maintaining genetic banks continues to rise, as the ongoing addition of new material increasingly requires ever larger amounts of space and energy to maintain operations. These facilities are necessarily restricted to areas with a well-developed infrastructure and reliable power grid (Shabihkhani et al. 2014). The increasing energy demands necessary to maintain these high energy use facilities also increase costs and contribute to climate change, so a substitute could make a significant impact in cutting energy usage and carbon emissions (Hartman et al., 2019).

The ability to store the genomic material at room temperature without sophisticated equipment would allow genetic banks to readily expand with growing demand, and to be maintained at a fraction of today's financial and environmental costs. This would also allow the proliferation of banking facilities to areas not currently able to support them, such as developing countries and smaller institutions, thereby enhancing the number and geographic diversity of such facilities, and creating more diverse and equitable access (Coppola et al., 2019). Regional or local biobanks could safeguard biodiversity at the local level. The added ability to be independent of sophisticated machinery would increase the dependability and security of the genetic material, as it would no longer be at risk of spoilage due to equipment failures, or subject to freeze–thaw cycles that degrade the genomic material over time.

In this project, DNA storage methods will be evaluated for their efficiency in protecting against common types of DNA damage, then refined and optimized to help enable dry room temperature-based storage. Using specific sugars and proteins, which show promising preservative qualities for genetic integrity in a room temperature storage environment, the optimal combination of reagents for long-term storage will be determined and tested. UV damage will not be investigated in this study due to time, cost, and logistical limitations. It is well studied, and samples stored in laboratories and related facilities are not routinely exposed to UV for long periods of time. However, recovered environmental or ancient DNA could have had a significant amount of UV exposure, which might affect the degradation rate upon preservation (Pang et al., 2007). Radiation of many forms has profound effects on the DNA molecule (Immel et al., 2016), but these are outside the scope of the present study.

1.2 DNA Alternative Forms

DNA exists in several structural forms, including many transitional forms, and undergoes conformational changes in a dynamic fashion within a cell or even *in vitro* as environmental conditions change (Svozil et al., 2008). Within the DNA molecule, many forms exist regionally, simultaneously, and interchangeably (Herbert et al., 2021). Many factors influence the form that DNA takes, including sequence-specific protein binding, nucleotide sequence, relative humidity, ionic strength, pH changes in the local environment, temperature, and superhelical tension (Potaman et al., 2013). The three major biologically-active, double helical forms are A-, B- and Z-DNA (Figure 1, Table 1), with subgroups and rarer forms existing as well (Svozil et al., 2008). Within these groups there are likely numerous unstable transitional states which contain properties of one another (Potaman et al., 2013). The B-form of DNA, also known as the Watson and Crick DNA model, is the most common form shown in the literature. However, DNA does not exist solely in this form in the cell, or therefore in a dried state. Each form has characteristics with important implications for DNA storage and preservation, affecting properties such as its rigidity, brittleness, and susceptibility to different mechanisms of DNA damage (Wood, 2016).

Much contemporary research has failed to consider the physical form of the DNA, in relation to either damage mechanisms *in vitro* or how it affects long-term storage. DNA is regionally rigid and will become more so without associated proteins that introduce bending, or the hydrating water shell present in the cellular environment (Laage et al., 2017). These differences will make the molecule more rigid, and more susceptible to fragmentation, when in the alternate conformational forms of A- or Z-DNA (Baker et al., 2007). This is significant, because protecting against fragmentation has been recognized as one of the most challenging aspects of DNA storage and recovery (Baker et al., 2007). There are other conformational forms of the DNA molecule, but each of these needs very specific conditions to form meaning they are far less common (Jayaram et al., 1998), and less likely to be significant factors for long-term DNA integrity *in vitro*.

Whether a DNA sequence will be in the A-, B-or Z-DNA conformation depends on at least three factors. The first is the ionic strength or hydration environment, which will dictate which form the DNA takes and to what degree. A-DNA is favored by low hydration, whereas Z-DNA is

preferentially formed under high salt conditions (Kim et al., 2017). The second factor which directly affects the conformation state is the DNA sequence, and the third is the presence or absence of proteins that bind to DNA in one helical conformation and force it to adopt a different form (Stefano et al., 2010). There are several such proteins that bind to B-DNA and drive it to either A- or Z-forms. In living cells, most of the DNA is in a mixture of A- and B-DNA conformations with a few small regions capable of forming Z-DNA. When extracted, the form DNA takes will depend on its storage buffer, hydration, and salt concentration. The B-form is unlikely to be the form found in dried samples or under many common storage conditions; rather, the A-form is likely to predominate, which may therefore affect the susceptibility of the sample to fragmentation, oxidation, and enzymatic attack (Waters et al., 2016). Also, the transition junctions between forms result in exposed nucleotides that are especially vulnerable to chemical and enzymatic damage, potentially impacting the stability of the DNA over time (Zhao et al., 2010).

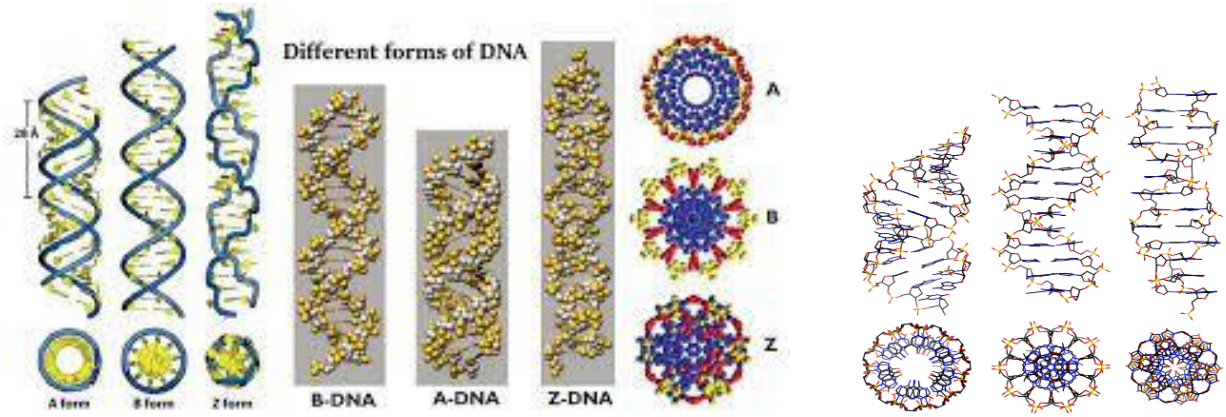

https://commons.wikimedia.org/wiki/User:Mauroesguerroto

Figure 1: Most Common Forms of DNA

X-ray diffraction images showing the different DNA structures: B-form (left), A-form (middle), and Z-form (right). B-form is the most biologically active form and most represented in the literature. A-form is a more compact version that occurs in lower humidity. Z form is an elongated version of DNA molecule and is sequence dependent and in the presence of high salt concentrations. All three forms exist within a DNA molecule and also various unstable transition states. Other forms do exist but are only present in small amounts and under specific conditions and don't contribute substantially to the composition of the DNA molecule as a whole.

Table 1: Geometry of the DNA Forms

A comparison of the structural variation of differing DNA conformations including A-form, B-form, and Z-form.

	A	B	Z
Helix sense	Right-handed	Right-handed	Left-handed
Repeating unit	1 bp	1 bp	2 bp
Rotation/bp	33.6°	35.9°	60°/2
Mean bp/turn	10.7	10.0	12
Inclination of bp to axis	+19°	−1.2°	−9°
Rise/bp along axis	2.3 Å	3.32 Å	3.8 Å
Pitch/turn of helix	28.6 Å	33.2 Å	45.6 Å
Mean propeller twist	+18°	+16°	0°
Glycosyl angle	anti	anti	C: anti, G: syn
Sugar pucker	C3′-endo	C2′-endo	C: C2′-endo, G: C2′-exo
Diameter	26 Å	20 Å	18 Å

https://en.wikipedia.org/wiki/Nucleic_acid_double_helix

1.2.1 A-DNA Form

The A-form of DNA is a right-handed (de Rosa et al., 2010) double helix made up of deoxyribonucleotides and can generally be viewed as a condensed or compressed version of the B-form (Table 1). It has more base pairs per turn and a reduced width of the major grove, where many proteins attach. It forms when the relative humidity is less than 75% and is therefore rarely present under normal physiological conditions; however, it would be the main form in a dehydrated sample (Kaczmarek et al., 2019). The two strands of A-DNA run in opposite directions—i.e., are antiparallel relative to one other—and the arrangement is not symmetrical. The molecule is asymmetric because the glycosidic bonds of paired bases are not diametrically opposite to each other, and therefore, major and minor grooves can be observed in each turn. One turn of the helix consists of 11 base pairs with a length of 28.6 Å (2.86 nm). The A-DNA

form is wider than the more common B-DNA structure. This makes it less flexible, but more robust and less susceptible to enzymatic attack because of its relatively more compressed form (de Rosa et al., 2010).

1.2.2 B-DNA Form

B-form DNA is a right-handed double helix, which was described by Watson and Crick based on the X-ray diffraction patterns (de Rosa et al., 2010). B-DNA forms in an intermediate ionic environment, where relative humidity is over around 75% (Ussery et al., 2002), and is the most common form of DNA under normal physiological conditions (Zhang et al., 2017). As with A-DNA, the two strands of B-DNA are organized in an antiparallel fashion and the structure is again asymmetrical, with alternating major and minor grooves present due to the asymmetrical arrangement of glycosidic bonds of each base pair (which are not diametrically opposite to each other, as for A-DNA). Each turn comprises 10 base pairs and has a length of 34 Å (3.4 nm). The distance between adjacent deoxyribonucleotides is 3.4 Å (0.34 nm). B-DNA is narrower than A-DNA, is less stable, and has more rigid off-center stacking of the bases. The minor groove is less susceptible to nucleases and more resistant to UV (Becker et al., 1989).

1.2.3 Z-DNA Form

The Z-form of DNA is markedly different from the A- and B-forms and can generally be described as a stretched version, or elongated form, of the B-DNA structure. The Z-DNA form is a left-handed double helix, and its backbone has a unique zigzag appearance which makes it easily distinguishable from other forms of DNA (Roy et al., 2021). The helix width is the narrowest of the three types, with an 18 Å (1.8 nm) diameter. The structure still has both major and minor grooves, but these are shallower than in the other two forms of DNA. One turn of Z-DNA has 12 base pairs, and the length is 45.6 Å (4.56 nm). The distance between adjacent deoxyribonucleotides is 3.7 Å (0.37 nm). Direct observation of Z-DNA is difficult since it is unstable and will change form in different conditions. Nonetheless, it has a possible role in regulation of gene expression for some genes, and in genetic recombination (Herbert A, 2019). Once thought to be rare, Z-DNA has now been identified in bacterial, eukaryotic, and viral genomes (de Rosa et al., 2010).

1.3 DNA Stability

The overall stability of the DNA double helix greatly depends on three major forces: hydrogen bonding, base stacking, and hydrophobic–hydrophilic interactions between the sugar–phosphate backbone and solvent molecules (Mak, 2016). Various studies have been made using a combination of physical methods—including X-ray crystallography, ultraviolet (UV) melting, and nuclear magnetic resonance (NMR)—to try and measure the overall contribution of these forces, but the relative contribution of each is still unclear as their individual contributions also depend on many changing variables that are influenced by environmental conditions (Aboul-ela, 1987; Cooper et al., 2008). The overall entropy of DNA is lower when double-stranded, in the biologically active state found within the cell, than when it exists in single-stranded form (Kool, 2001).

1.3.1 Factors Influencing DNA Duplex Stability

The DNA double helix is stabilized by hydrogen bonding, influenced by factors including the number of bonds, the relative angles of those bonds (strength), and the presence of other molecules that can form alternative hydrogen bonded structures or otherwise interfere with DNA hydrogen bonding (Kool et al., 2000). However, temperature is the most obvious destabilizing factor. The sequence of the DNA bases has a direct effect on stability since purines can form an extra hydrogen bond compared to pyrimidines (Driessen et al., 2014), when base pairing. Thus, the greater the GC content of the DNA sequence, the more thermally stable it will be. Base stacking is also a major factor, along with hydrophobic–hydrophilic solvent interactions, these factors all working together in a dynamic equilibrium. Hydrogen bonding and base stacking will now be discussed in greater detail.

1.3.1.1 Hydrogen bonding

A hydrogen bond is a primarily electrostatic force of attraction between a hydrogen atom which is covalently bound to a more electronegative atom or group, and another electronegative atom bearing a lone pair of electrons—the hydrogen bond acceptor. The electronegativity of the atoms involved

determines the strength of the hydrogen bond formed. Overall, hydrogen bonds are weak in comparison to covalent bonds, but cumulatively they can become a very strong bonding force especially between large molecules like DNA (Mohan et al., 1991), where many interstrand hydrogen bonds are involved. The most common hydrogen bonds on earth involve water, either with itself as in bulk water (Figure 2), or with other molecules. The hydrogen atom is attracted to the negatively polarized oxygen atom of the adjacent water molecule, thereby increasing the partial positive charge of the hydrogen atom (δ^+). As the hydrogen atom is pulled towards the oxygen atom of the adjacent water molecule, there is an increase in the polarization of the oxygen atoms of both the adjacent and companion water molecules. This not only strengthens the bond between the water molecules, but also makes the hydrogen available for deprotonation when the temperature or pH changes.

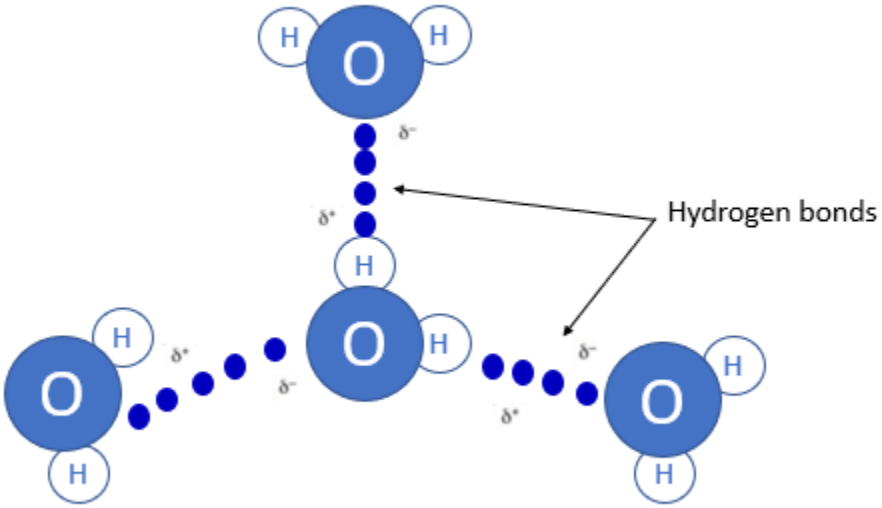

Figure 2: Hydrogen Bonding in Water

A water molecule contains a highly electronegative oxygen atom linked to the hydrogen atom. Oxygen atom attracts the shared pair of electrons more and this end of the molecule becomes negative whereas the hydrogen atoms become positive.

The angle of the hydrogen bond is also important, within a fixed macromolecule like DNA, for determining its strength. The directionality is most favorable, and the hydrogen bond is

strongest, at an angle of 180°. There are a large number of hydrogen bonds in DNA, but many of them are not at 180°. Such variations in directionality place strain on these bonds, making them slightly weaker. The larger the distortion, the weaker the bond; and as such, the structural form of the DNA and the base sequence both have major effects on its overall stability. The length and angle of the hydrogen bonds are affected by local structural changes and distortion, and the tolerable level of distortion in a hydrogen bond, measured between the vector of the bond and the angle of the X–H bond, is less than 20° (Gyuri et al., 2021). The form the DNA takes, e.g., the elongated Z-form or the compacted A-form, therefore has important effects on the angle of the hydrogen bonds and, by implication, their strength. The B-form of DNA has the least distortion and is therefore the most stable under physiological conditions.

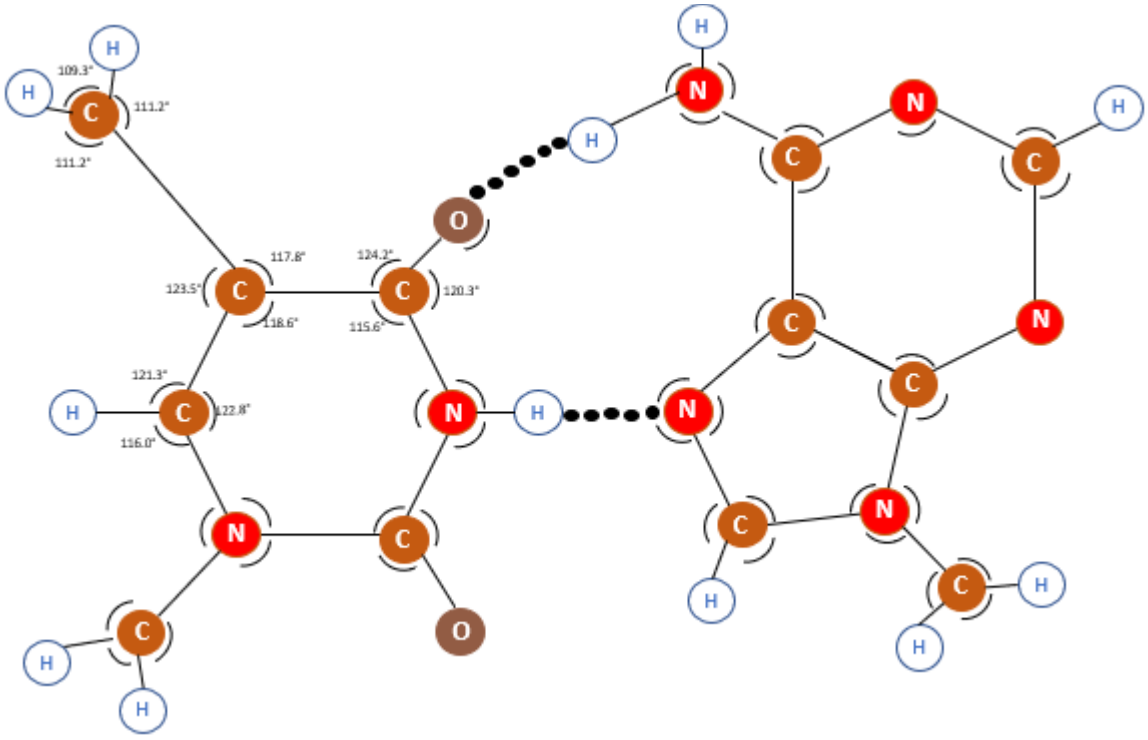

Figure 3: Hydrogen Bond Angles in DNA (B-Form)

The number of hydrogen bonds are not the only factor in the stability of the DNA molecule as each bond relative strength will depend on its geometry within the DNA and its length which distorts as DNA changes from B-form to A-form, to Z-form and the transition states in between. The angle and length of the hydrogen bond within the DNA base pairing will determine their relative strength. The optimal bond

angle is 180° so any twisting or distorting of the DNA molecule distorts the bond angles and either strengthens or weakens them.

1.3.1.2 Base stacking

Base–base stacking (or, more simply, base stacking) is usually considered to be the most important overall enthalpic contributor to the stability of double-stranded DNA (dsDNA) (Beyerle et al., 2021). Base stacking refers to the attractive forces that exist between adjacent base pairs in the DNA structure, and in fact, base stacking effects are generally thought to be the most important factor from which the double helical structure of B-form DNA arises. These stacking effects are governed by London dispersion forces (Yakovchuk et al., 2006), a type of van der Waals forces.

The optimum distance at which two atoms or molecules have the strongest attraction for each other is known as the van der Waals distance. This attraction, termed a van der Waals interaction or van der Waals force, is analogous to a gravitational force since it is distance dependent. If the distance is too small, the electron clouds of the two closely-approaching molecules overlap, causing electrostatic repulsion, but above this distance an attractive force exists. At any given instant, the electronic charge distribution within atoms or atomic groups (i.e., molecules) is asymmetric due to electron fluctuations, creating momentary dipoles. These dipoles created in one group of atoms polarize the electronic systems of the neighboring atoms or molecules, thus inducing parallel dipoles that attract each other. These forces are additive and are extremely distance-dependent. If the molecules are held close together in an ordered structure, the polarization of electrons can occur over a large number of molecules, creating an overall polarity across all the molecules.

Since DNA contains 5- and 6-membered aromatic rings, these rings can stack on top of each other with the p-clouds forming dipoles that attract each other. This stacking of nucleobases thus requires aromaticity to generate the attractive or repulsive forces that dictate the arrangement of bonds and formations, and nonaromatic bases do not display these stacking interactions. The strength of stacking interactions depends on the polarizability of the p-electron cloud, and since all nucleobases have different substituents, their stacking potential differs. It

follows that the stacking potential of a base can additionally be influenced by chemical modification, such as alkylation or halogenation. DNA intercalators—that are mostly polycyclic, aromatic, and planar—can also affect the base stacking forces in either a positive or negative fashion (Shen et al., 2009).

Stacking is dependent on both base composition and base sequence. Stacking interactions of base paired nucleotide dimers containing G–C base pairs are more stable than those containing A–T base pairs. Interestingly, recent studies have indicated that individual base pairing may be a much stronger force for DNA duplex stability than the base stacking interactions alone, which were previously considered to be the dominant factor (Zacharias, 2020).

One important function of base stacking, relevant to long-term DNA stability, is that it protects the DNA duplex from unravelling around single-strand nicks when the sugar backbone is compromised (Protozanova et al., 2004).

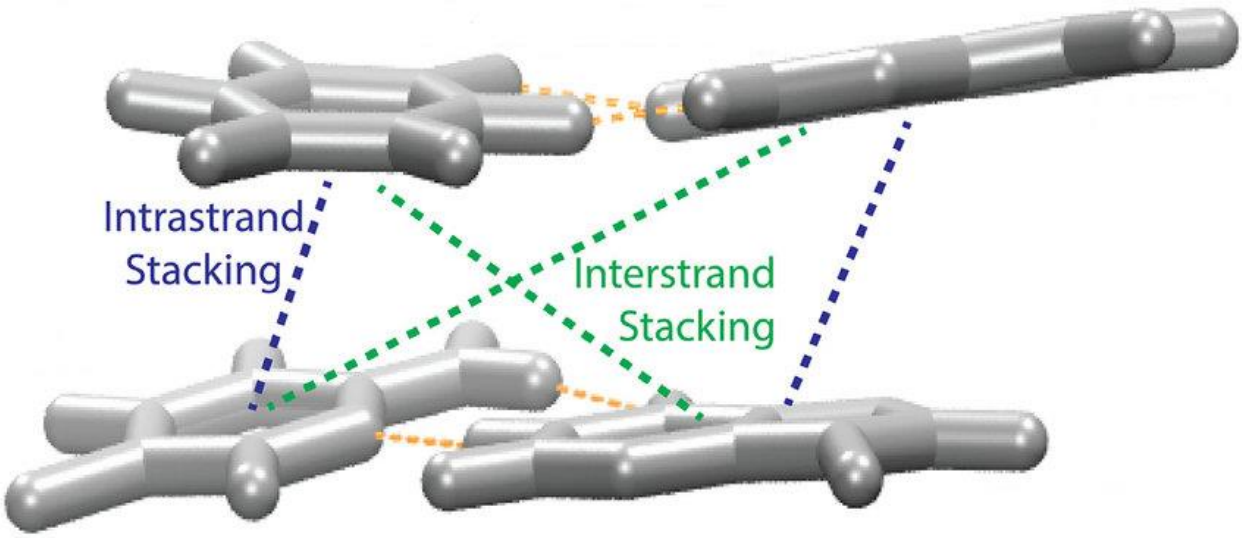

https://www.researchgate.net/figure/Schematic-of-bases-involved-for-calculated-hydrogen-bonding-energies-and-intra-and_fig3_344065074

Figure 4: Base Stacking van der Waals Interactions Between Bases

DNA bases stack upon one another at their van der Waals distance. The electronic charge distribution within the aromatic ring becomes asymmetric due to electron fluctuation. This creates dipoles on the one group which then polarizes the electronic system of the neighboring bases thus inducing parallel poles that attract each other over multiple bases. The blue dashed line represents the attraction forces of induced

dipoles of the polarizable p electron cloud of the DNA base pairs. The electronic structure of a base and its polarizable p electron cloud can be modified by chemical modification-e.g., alkylation, halogenation affecting the stacking forces. All bases also have different substituents making stacking attraction force of the bases all different. The yellow dashed line represents the hydrogen bonds between nitrogenous bases and the dashed green line represents the interstrand stacking forces.

1.3.1.3 Lack of hydroxyl group at the 2′ position of ribose

There are specific reasons why DNA, as opposed to other nucleic acids, has become the information storage molecule for organisms. One major reason is that DNA is more resistant to hydrolytic damage, which is a common form of damage at physiological levels of ionic strength and hydration. The loss of an oxygen atom in DNA (*deoxy*ribonucleic acid) compared to RNA translates to the lack of a hydroxyl group at the 2′ position of ribose. This lack of a nucleophilic, potentially hydrolytic group provides DNA with resistance to intramolecular hydrolytic degradation of the phosphodiester backbone over a wide range of pH conditions. In contrast, although the 2′-hydroxyl group of RNA increases its sensitivity to hydrolytic damage, it also helps to stabilize the base stacking forces in RNA. This raises the melting temperature of RNA and makes it more resistant to oxidative damage when adopting an A-form structure (Lodish et al., 2000).

1.4 DNA Damage

Within a living cell, DNA damage occurs continuously, but there are many mechanisms that exist to help keep the DNA intact and error free (Huang et al., 2021). When extracting DNA from a metabolically active tissue, enzymatic damage occurs more rapidly after the cell dies and its membranes rupture since this allows digestive enzymes to spill out of their segregated organelles (Alaeddini et al., 2010). To preserve the integrity of the DNA molecule, this process must be halted or inhibited rapidly, using techniques such as rapid desiccation, freezing, or treatment with an inhibitory agent (Pusch et al., 2003). Even with minimal degradation from cellular death and the extraction process, nucleic acids are thought to gradually degrade over time through spontaneous processes, such as hydrolysis and oxidation, which occur even under ideal preservation conditions (Hofreiter et al., 2001). DNA damage in older samples is typically characterized by an overrepresentation of strand breaks, abasic sites, miscoding lesions, modified

bases, and crosslinks (Lindahl, 1993), all of which can confound downstream analysis such as PCR or sequencing applications.

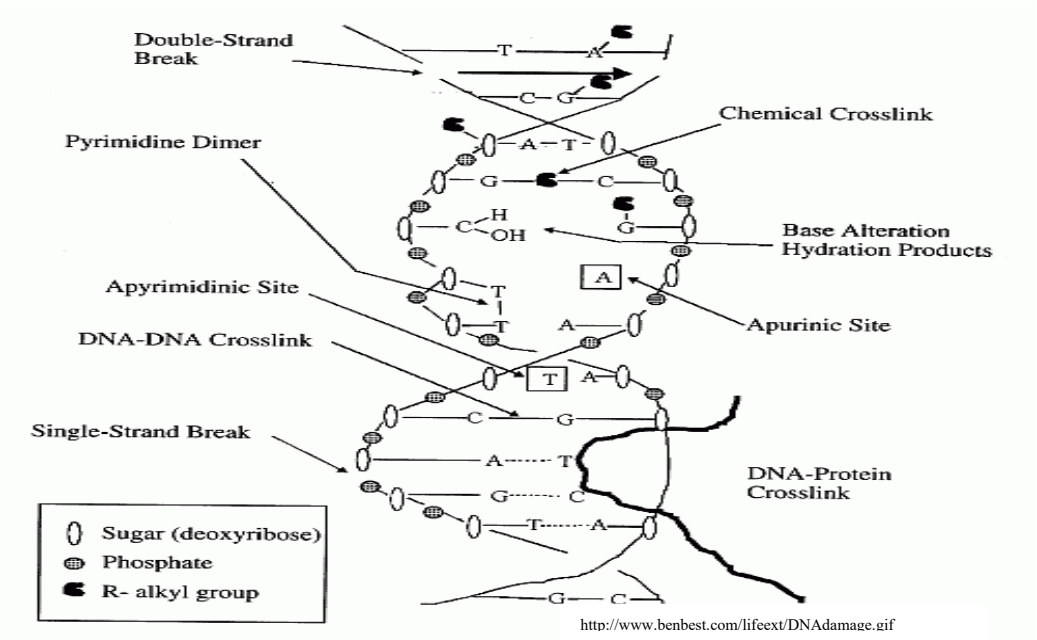

Figure 5: Forms of DNA Damage

Figure 5 shows a DNA molecule, demonstrating possible forms of DNA damage including double-strand breaks, pyrimidine dimers, apurinic/apyrimidinic sites, DNA–DNA or chemical crosslinks, single-strand breaks, base-altering hydration products, and DNA–protein crosslinks. These most common types of DNA damage can be caused by multiple sources, both endogenous and exogenous, and each source may induce more than one type of damage.

1.4.1 Strand Breaks

The term “strand break” can be applied to a wide range of diverse chemical structures. Single-strand breaks (SSB) are lesions that are created on one side of the DNA helix, while double-strand breaks (DSB) have lesions adjacent to each other on both strands or in the very near vicinity, causing a blunt or sticky end shearing of the helix into two fragments. Strand breaks are generally characterized by loss or modification of the phosphodiester bond in the sugar–phosphate backbone of DNA, resulting in a loss of integrity (Karimi-Busheri et al., 1998).

The phosphodiester bond is vulnerable to hydrolysis and is therefore a common site of strand breakage. Such breakages occur at a slow and steady rate, and are constantly being repaired in metabolically active tissue. However, over time and without repair pathways, strand breaks will accumulate in stored DNA samples (Lindahl & Wood, 1999). Oxidative damage and enzymatic attack can also cause breaks in the DNA backbone.

DSBs are much more deleterious than SSBs as they cause the DNA molecule to break into two fragments at the damage site, making repair more difficult (Cannan et al., 2016). There are many chemically distinct 3′ and 5′ modifications, but to complete the DNA repair process, the 3′-termini of the fragments must be returned to a hydroxyl group and the 5′-termini to a phosphate group, in order for DNA polymerases and ligases to initiate repair. Repairing DSBs involves either homologous recombination (HR) or non-homologous end joining (NHEJ), both of which rejoin the broken ends directly but may also incorporate errors and deletions (Dobbs et al., 2008). The presence of DSBs will inhibit both nucleotide excision repair (NER) and base excision repair (BER) *in vitro* prior to the denaturation step, and this is one of the major obstacles in repairing postmortem DNA *in vitro* (Calsou et al., 1996).

1.4.2 Abasic Sites

The chemical bond between a DNA base and its respective deoxyribose sugar, called the glycosidic bond, is subject to chance cleavage by a water molecule in a process known as spontaneous hydrolysis. The result of hydrolysis of the glycosidic bond is the creation of an abasic site, as the nucleobase is released. The formation of an abasic site can occur with any of the four bases (A, T, G, and C), and therefore for both purines and pyrimidines, but depurination (loss of adenine or guanine) happens at a higher rate than depyrimidination (loss of thymine or cytosine). An estimated 10,000 depurination events occur per day in a mammalian cell, with depyrimidination also occurring but at a 20- to 100-fold lower rate (Boiteux et al., 2004; Lindahl and Andersson, 1972). Abasic sites can generate ribonucleotide misincorporation lesions preventing DNA replication if enough of them accumulate, where they become blocking lesions preventing PCR amplification (Kitsera et al., 2019).

1.4.3 Modified bases

Nucleobases can be chemically modified from their chemical structure in a multitude of ways, and each base has many sites that are susceptible to attack or modification (Figure 6). The carbon–nitrogen bonds in the heterocyclic ring structure are less stable than carbon–carbon bonds. The presence of heteroatoms, such as nitrogen, results in significant changes in reactivity of the cyclic molecular structures due to the availability of unshared electrons and the difference in electronegativity between the heteroatoms and carbon. Due to their bicyclic structure, purines contain more heteroatomic sites that are chemically reactive, meaning they are the most modified bases in DNA (Table 2). Guanine (G) is the most reactive base with an extra cyclic oxygen, at the O6-position, which is also reactive and exposed to certain attacks (Garcia-Valverde & Torroba, 2005).

The susceptibility of DNA bases to chemical modification depends on their environment. The most common damage types that occur within the cell are alkylation/methylation, oxidation, deamination (hydrolysis), and hydrogenation. Methylation is the most common form of alkylation in DNA and is simply the addition of a methyl group to a DNA base, most commonly cytosine (C). This process is the most harmful to living organisms because of its gene silencing consequence and transcriptional mutations (Razin & Riggs, 1980). *In vitro*, methylation can also prove problematic by inhibiting PCR, preventing amplification through acting as a blocking lesion, or by inducing sequence changes to copies in the PCR reaction.

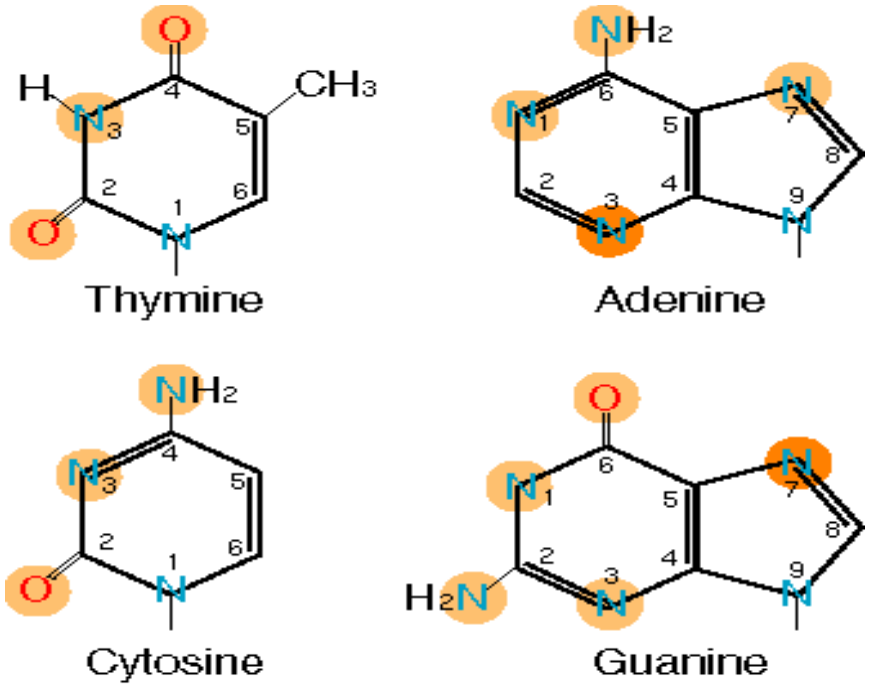

Figure 6: Heteratoms in DNA Bases Most Susceptible to Chemical Modification.

The most reactive sites on the four main DNA bases that are subject to modifications, particularly oxidative damage, are highlighted in orange. Alkylation-prone nucleophilic positions are highlighted in yellow.

Early on, radiation biologists discovered that the attack of hydroxyl radicals (·OH) generated by radiolysis of water resulted in significant alterations to all four bases and the deoxyribose sugar (Teoule, 1987). Hydroxyl radicals are also produced through cellular oxidation and enzymatic processes, and it has been estimated that as much as 2% of the oxygen consumed through respiration is converted to free radicals such as ·OH. Hydroxyl radicals accumulate rapidly upon cell death, causing major damage to the DNA (Aust & Eveleigh, 1999).

Reactions of the hydroxyl radical can be classified into three main types: hydrogen abstraction addition, and electron transfer. Reactions of ·OH with the deoxyribose sugar proceed by hydrogen abstraction, forming carbon-centered radicals. All five carbons in the deoxyribose are vulnerable to this attack. Under anaerobic conditions, the C4′ radical can undergo β-

elimination of the phosphate ester group leading to a single-strand break and causing sugar modification (Dizdaroglu et al., 1975). Under aerobic conditions, peroxyl radicals are formed by the addition of molecular oxygen. This results in the cleavage of a carbon–carbon bond and the creation of an alkali-labile site. C5′ can again undergo β-elimination, generating a strand break followed by the release of an intact base and the production of an altered sugar. Aldehyde formation at C5′ can also occur while generating a strand break (Goldberg, 1987).

The heterocyclic bases in the DNA can be modified through addition reactions. In pyrimidines, the hydroxyl radical adds to the C5=C6 double bond creating base radicals that rapidly undergo additional chemical reactions, resulting in multitudes of modified bases (O'Neill, 1983). In purines, ·OH adds to the C4, C5, and C8 positions, which can create both oxidizing and reducing types of radicals, expanding the additional modification products that may be created (Cadet et al., 1999). Addition to C8 can also lead to unimolecular opening of the imidazole ring, again offering the opportunity for many possible modifications from further reaction, depending on the species present and the environmental conditions (Dizdaroglu et al., 2008). The oxidized purine bases 2,6-diamino-5-formamidopyrimidine (FapyA) and 2,6-diamino-4-hydroxy-5-formamidopyrimidine (FapyG) are potentially lethal lesions to cells *in vivo*, effectively stopping replication one base prior to the ring-opened residue. *In vitro* analyses have shown both Fapy modifications to be blocking lesions to the Klenow fragment of *E.coli* DNA Polymerase I, as well as phage T4 DNA Polymerase, effectively inhibiting PCR analysis (O'Connor et al., 1988).

Deamination is the hydrolytic release of an amine group from A, C, or G that results in a modified base (Table 2). An acidic, moist environment and elevated temperatures will increase the rate of hydrolysis (Wolfenden et al., 1998). Although deamination of DNA bases occurs more frequently in pyrimidines than in purines, both are equally mutagenic (Mol et al., 1999). In the hydrolysis reaction, an oxygen atom is donated from a water molecule. The spontaneous deamination products of A and G are readily recognizable as unnatural when they occur in DNA and thus are efficiently repaired (Table 2).

Table 2: Products of Oxidative DNA Modification and the Mutations Induced

A comparison of oxidized modified DNA products and the resulting mutations identified in both mammalian and plant genetic studies.

DNA modification	Mutation (base change)	Reference
5-formyluracil	C→T	1, 2
	G→T	1, 2
	T→C	1-4
	T→A	1-4
	T→G	2, 5
5-hydroxyuracil	C→T	2, 6-8
5,6-dihydrouracil	G→A	2, 9
5,6-dihydroxyuracil	C→T	2, 7
	G→A	
5-hydroxy-6-hydrouracil	C→T	2
5-hydroxymethyluracil	C→T	2, 7, 10, 11
uracil glycol	C→T	2, 6, 8
5-hydroxymethylcytosine	C→T	11, 12
5-hydroxycytosine	C→T	2, 6-8
5,6-dihydroxycytosine	C→T	2
5-hydroxy-6-hydrocytosine	C→T	2
5-formylcytosine	C→T	8, 13
	C→A	8, 13
cytosine glycol	C→T	2
8-hydroxyguanine (8-oxoguanine)	G→T	2, 4, 7, 8, 14, 15
	G→C	2, 4, 14, 15
	G→A	14, 15
	A→C	8, 16
8-hydroxyadenine (8-oxoadenine)	A→G	2, 14, 17
	A→C	14, 17
2-hydroxyadenine	A→G	2, 8, 15
	A→T	8, 15
	A→C	8, 15
5-hydroxy-6-hydrothymine	T→C	2
thymine glycol	Blocking	2, 8, 18
5,6-dihydrothymine	T→C	2
5-hydroxy-5-methylhydantoin	Blocking	2, 7
trans-1-carbamoyl-2-oxo-4,5-dihydroxyimidazolidine	Blocking	2
5-hydroxyhydantoin	Blocking	2, 7
alloxan	Blocking	2
4,6-diamino-5-formamidopyrimidine (FapyA)	Blocking	2, 7
2,6-diamino-4-hydroxy-5-formamidopyrimidine (FapyG)	Blocking	2, 7
oxazolone	G→T	2, 8

References: 1 (Anensen et al., 2001), 2 (Cooke et al., 2003), 3 (Miyabe et al., 2001), 4 (Zhang, 2001), 5 (Zhang et al., 1997), 6 (Kreutzer & Essigmann, 1998), 7 (Kasprzak et al., 1997), 8 (Evans et al., 2004), 9 (Liu, Zhou et al., 1995), 10 (Cannon-Carlson et al., 1989), 11 (Hori et al,. 2003), 12 (Baltz et al., 1976), 13 (Karino et al., 2001), 14 (Tan et al., 1999), 15 (Kamiya, 2004), 16 (Cheng et al., 1992), 17 (Tuo et al., 2003), 18 (Basu et al., 1989).

Approximately 3% of the C nucleotides in vertebrate DNA, and up to 25% in plant DNA, are methylated as a means of regulating of gene expression. In mammalian cells, cytosine is most often methylated at C5 for the gene regulation and silencing function. The most common mutagenic pathway from 5-methlycytosine (5meC) is deamination to form the natural nucleotide A hydrogen bond is a primarily electrostatic force of attraction between a hydrogen atom which is covalently bound to a more electronegative atom or group, and another electronegative atom bearing a lone pair of electrons—the hydrogen bond acceptor thymine (Waters & Swann, 2000). T nucleotides formed by deamination of 5meC would be paired with G on the opposite strand, forming a mismatched T–G base pair that could persist in the sequence (Horst & Fritz, 1996) and lead to a C–G → T–A transition mutation upon replication.

The addition of one or more hydrogen atoms to a compound, usually at the site of a C=C double bond, is referred to as hydrogenation. This addition reaction reduces the double bond to a single bond. On some occasions, intramolecular hydrogenation of cytosine C4=C5 can lead to the formation of a radical anion and, ultimately, strand cleavage (Dabkowska et al., 2005). The pyrimidine bases are the most susceptible to these modifications, at the C4=C5 double bond. Resonance stabilization by the C4=C5 double bond gives the C–N glycosidic bond its resistance to acid hydrolysis, but bases modified such that the double bond is lost then become susceptible to depyrimidization and/or strand breakage (Dabkowska et al., 2005). Many divalent metals can increase the rate of hydrogenation, especially if the DNA is exposed, as is the case in buried or treated remains (Cano, 1996). Finally, oxidative damage can alter bases in many different ways, generating subsequent replication and transcription errors (Table 1) (Anensen et al., 2001; Cooke et al., 2003; Kamiya, 2004; Tan et al., 1999).

1.4.4 Crosslinks

Crosslinking of DNA involves the formation of covalent bonds between two bases within the same strand (intrastrand crosslink), or on adjacent strands (interstrand crosslink, or ICL). Crosslinking can also occur between DNA and proteins, or DNA and sugars. All three types of crosslink have deleterious effects in living organisms and can occur through involvement of a

variety of exogenous and endogenous agents (Stützer et al., 2020). Intrastrand DNA crosslinking can cause kinking in the DNA strand, A hydrogen bond is a primarily electrostatic force of attraction between a hydrogen atom which is covalently bound to a more electronegative atom or group, and another electronegative atom bearing a lone pair of electrons—the hydrogen bond acceptor which prevents regulatory proteins from binding or creates a blocking structure for a DNA polymerases, inhibiting replication and amplification both *in vivo* and *in vitro.* ICLs are an extremely problematic type of DNA damage that arise during normal metabolism and accumulate spontaneously in aging DNA samples (Mitchell et al., 2005). ICLs prevent strand unwinding of duplex DNA as they covalently tether the strands together, thereby limiting the access of DNA polymerases to the strands during transcription or PCR amplification (Hashimoto et al., 2016). In kinetic studies performed by Hansen et al. (2006), on nucleic acids from Siberian frozen sediment core samples from the permafrost within layers ranging from 10,000 to 600,000 years old, ICLs were found to accumulate approximately 100 times faster than SSBs. Although this prevents amplification and retrieval through PCR, it may well preserve the integrity of the biological molecule over long periods of time (Hansen et al., 2006). The mechanisms for covalent bond formation *in vitro* are thought to involve exogenous agents acting via a free radical mechanism that requires no molecular oxygen to be present (Greenberg, 2005).

Proteins can also become crosslinked to DNA by a variety of agents including UV radiation, metals, various aldehydes, and environmental chemicals. This most often occurs through an oxidative free radical mechanism, but it can also be initiated by various chemical agents in combination with a metal ion, such as Cr^{3+} or Ni^{2+} (Barker et al., 2005).

1.5 Major DNA Damaging Agents

There are many mechanisms and combinations of chemical and physical damage pathways that can affect the DNA molecule over time. Eventually, their accumulation degrades the DNA into unrecoverable fragments, or modifies the bases, thereby blocking or altering the DNA sequence sufficiently to prevent amplification or complicate analysis.

1.5.1 Nucleases

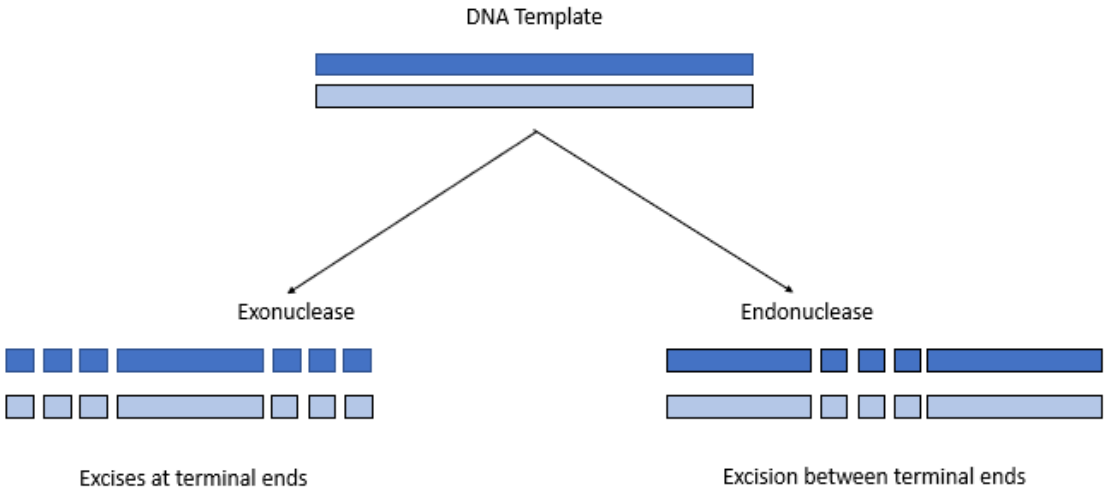

Figure 7: Endonuclease and Exonucleases

A representation of the two primary types of nucleases, including exonuclease (acting at strand termini) and endonucleases (acting anywhere between the termini).

Nucleases can be regarded as “molecular scissors” that hydrolytically cleave phosphodiester bonds between the sugar and the phosphate moieties of DNA. Their activities are normally tightly regulated, but if aberrant or excessive nuclease activity occurred, physical damage is caused to the DNA. This can be gaps (arising from nucleotide excision), single-strand nicks, or double-strand breaks, all of which can lead to significant degradation of the DNA within a short period of time.

Nucleases contain conserved minimal motifs, which usually consist of acidic and basic residues forming the active site (Nishino et al., 2002). These active site residues coordinate catalytically essential divalent cations—such as magnesium, calcium, manganese, or zinc ions—as cofactors (Nishino et al., 2002). The precise requirements for hydrolytic cleavage, such as the type and number of metal ions, are complex, often debated, and not uniform among the nucleases (Sinha et al., 2016). It appears that the major role of the metal ions is to stabilize intermediates, thereby

facilitating the phosphoryl transfer reactions. Cleavage reactions occur either at the end of, or within, DNA strands and DNA nucleases are thus categorized as exonucleases or endonucleases, respectively (Figure 4). Exonucleases can be further classified as 5′-end processing or 3′-end processing enzymes, according to their polarity of processive cleavage (Mimitou et al., 2009; Nishino et al., 2002).

Most nuclease damage to isolated DNA samples occurs at the time of extraction, or through nucleases persisting as impurities in the sample, but there are also ubiquitous environmental nucleases that can damage DNA integrity over time if they are introduced during processing, or the sample is exposed to them over time. Even a small amount of nuclease can cause major damage over the long term (Oh et al., 2018).

1.5.2 Physical

Physical damage to DNA is most often referred to as shearing or breakage, and is distinct from SSBs, DSBs, or abasic sites, which are chemically-induced events that can lead to downstream breakage. When supercoiled inside the cell and hydrated, genomic DNA is resistant to breakage from physical processes. When removed from the hydrated cellular environment and the associated protective structures, it can become susceptible to physical damage (Paleček, 1991). Essential steps in sample preparation, including vortexing, centrifugation, and pipetting, all cause some physical damage to DNA. Calculations by Vanapalli et al. (2006) showed that the pull on a DNA molecule stuck in two vortices at the same time is sufficient to break the strand in half and that this is the primary cause of fragmentation under most hydrodynamic conditions. The breakage rate is a function of the shear rate rather than the shear stress; and as such, over-processing of DNA can cause substantial fragmentation (Anchordoquy et al., 2007).

Furthermore, DNA can become very brittle after drying, suggesting that even mild extraction methods can cause extensive physical damage if the DNA is over-processed or not properly hydrated. Once the DNA is extracted, if it is not bound to a physical matrix, it can also be subject to physical breakage in the storage vessel during handling. Experimental observations have established that the inclusion of cryoprotectants—which break up the extreme rigidity of pure ice and slow ice crystal formation—prevents shearing of the DNA strand through repeated

freeze–thaw cycling and can reduce fragmentation and preserve DNA quality (Röder et al., 2010).

1.5.3 Oxygen

Oxygen is a highly reactive molecule within the cell, which can cause major DNA damage through free radical formation. The damage induced by exposing stored DNA, in its extracted form, to oxygen over time was often overlooked until relatively recently, when ancient DNA samples were analyzed and found to contain large amounts of oxidatively-modified bases but good DNA preservation overall (Lamers et al., 2008). Historically, much of the research around oxygen and reactive oxygen species (ROS) has focused on their deleterious effects on living cells and their consequential DNA mutations (Kowalska et al., 2020). It was discovered that DNA recovered from dry locations, which had not suffered hydrolytic or UV damage, could not be amplified by PCR for analysis. Through further investigation, a large variety of modifications were found in the DNA, including some arising from oxidative damage mechanisms. Many of these modifications did not just induce mutations or base mismatches; they also created blocking lesions, preventing polymerase amplification of the DNA downstream of those sites (Poetsch, 2020).

1.5.4 H_2O

As water is found everywhere, it is common for DNA to be exposed to it in almost all environments. When a sample is immersed in water for extended periods of time, DNA degradation occurs through strand breakage, microbial attack, and chemical modifications, based on the relative humidity and sterility of the environment. The biggest factor leading to DNA degradation in these aqueous environments is hydrolytic damage, which refers to the breakage of chemical bonds through nucleophilic attack of water (Lathamand & Madonna, 2013). The resulting processes of deamination (the loss of an amine group), depurination, and depyrimidination all cause DNA damage that inhibits downstream application of PCR (Dabrowska et al., 2017). Since DNA has a high affinity for water, the longer a sample is exposed to an aqueous environment, the higher the chances that the DNA will suffer hydrolytic

damage. In addition to this, aquatic environments allow many organisms to thrive, including bacteria. This can lead to increased microbial interaction with DNA, further exacerbating DNA degradation.

Hydrolytic damage to DNA occurs because the molecule is unstable in water, to some extent. While the process is slow in comparison to other common chemical reactions, the monomeric components of initial degradation are further subject to a range of hydrolytic reactions (Shapiro, 1981). Water is an ideal medium for chemical reactions, and many other damaging agents are soluble in water, thereby driving other damage processes (Dabrowska et al., 2017). Both acidic and alkaline environments influence the rate of hydrolytic reactions. Acidic environments function to convert DNA into a more reactive protonated form, while alkaline environments reduce the reactivity by converting thymidine and guanosine to their anionic forms (Shapiro, 1981).

1.5.5 Temperature

Temperature itself appears to have a secondary effect on DNA storage, as it accelerates or inhibits chemical processes associated with other damage vectors. The availability of free water as a medium is most directly impacted by temperature. Very high temperatures can affect the stability of the DNA molecule itself, with destruction occurring from dry heat under extreme conditions.

The helical structure of double-stranded DNA is destabilized by increasing temperature until it reaches a critical temperature, the melting temperature (T_m), at which the two strands of duplex DNA become fully separated. Below this temperature, thermal structural effects are localized, but may become more profound when combined with variations in pH or hydration. Experimental studies of purified DNA have indicated that it degrades linearly at around 130°C, with complete degradation occurring at 190°C (Karni et al., 2013). Forensic studies on biological materials, such as burnt bones, have revealed varying degrees of degradation even at temperatures of 500°C. This indicates that interactions of DNA with the surrounding biological matrix are also a factor, though there is limited research on the upper limits of stability in environmental conditions (Kadunc et al., 2009).

1.6 Common DNA Preservation Methods

Millions of DNA samples are stored each year. Storage methods are chosen based on considerations such as cost, convenience, materials at hand, ease of collection, shipping restrictions, and the lowest quantity needed for downstream application. This stands in contrast to choosing methods based on their reliability or efficiency. Furthermore, even though they are inefficient, many methods are used simply because they have become commonplace and are seen as "good enough."

In a laboratory setting, DNA is most often stored at 4°C, −20°C, or −80°C, but to avoid chemical and enzymatic degradation is often stored as a precipitate in ethanol at −80°C. Under these conditions, nucleic acids are stable for prolonged periods but must be separated from the ethanol, transferred to aqueous buffers, and typically quantified prior to use. These manipulations render ethanol precipitation undesirable for applications where the samples are needed on a regular basis. Aqueous solutions of DNA would be the most convenient, but nucleic acids are sensitive to depurination, depyrimidination, deamination, and hydrolytic cleavage, limiting the usefulness of prolonged storage under these conditions. It is possible to inhibit these acid-catalyzed degradation processes by storing DNA in alkaline solutions, such as the commonly-used TE buffer (Tris–EDTA, pH 8.0). The ionic strength of the solution also affects depurination rates, so storage in salt solutions—as opposed to a low ionic strength buffer—is preferable. Assuming the absence of nucleases when DNA is stored in a saline solution at pH 8.5, the most common form of damage occurs via oxidation. The rate of oxidation is enhanced by the presence of trace metal ions (e.g., Fe^{3+}, Cu^{2+}), due to the production of free radicals via Fenton-type reactions (Dabrowska et al., 2017).

1.6.1 Freezing

Storing DNA at −20°C or −80°C may well provide adequate conditions, depending on the quality and quantity of DNA desired and the time frame over which the sample is stored. However, over extended time periods (i.e., decades), neither of these conditions will maintain DNA quality equivalent to storage at liquid nitrogen temperatures. The DNA storage medium, contaminants, quantity, and other environmental conditions also have an impact, reinforcing the

point many factors potentially influence the viability of the DNA sample. The main purpose of ultra-low temperature storage is to halt or slow down chemical reactions, as well as removing free water, which acts as a vector for chemical reactions (Liu, 2019).

1.6.2 Anhydrobiosis

Anhydrobiosis is a state of dehydration in which all cell metabolic functions are reversibly paused (Rapoport et al., 2014). Organisms can stay in this state for decades, or until the conditions are favorable. They are then able to absorb water and, in some cases, thaw out and resume metabolic activity. This process occurs in fungi and yeast as a resistance mechanism against dehydration (Kacmareek et al., 2019). When some animals, such as tardigrades, undergo this phenomenon, they fill with a sugar, such as trehalose, to preserve DNA and other cellular contents. The trehalose forms a glassy matrix that retards chemical reactions and is thought to protect cellular structure (Rae et al., 2018). These molecular changes can prevent protein denaturation and fatal changes to membrane conformation (Wang, 2014). DNA is preserved, but is subject to damage through the initial dehydration or freezing processes, as well as the reverse process. This damage is mitigated, though, by the cells' repair mechanisms, which act to repair the DNA once metabolic activity resumes (Leprince et al., 2015).

1.6.2.1 Anti-freeze and Glassy State

Glass formation, or vitrification, is the creation of a liquid solution that has the viscosity of a solid. Glassy states combine properties of both crystals and liquids, and can be formed either by increasing the solute concentration or by lowering the temperature. In frozen aqueous samples, glasses are formed by a combination of the two (Woak, 2010). Glasses are usually supersaturated, and thus metastable, but the high viscosities and activation energies required for phase separation may prevent decomposition for long periods, the duration of which is dependent on composition and temperature. The formation of glasses is normal for substances that remain liquid over a wide temperature range and can be induced for most liquids if cooling is fast enough to bypass crystallization (Zanotto & Mauro, 2017). Storing DNA in substances that can enter a glassy state at higher temperatures is becoming a popular method for DNA storage (Wang et al. 2020).

1.6.3 Drying

In contrast to storing DNA in solution at very low temperatures, it is also possible to store it in dried form, and this can be a practical alternative for long-term storage. In addition to reducing molecular mobility, dehydration also removes water that can participate in hydrolytic reactions and function as a catalyst for UV-induced damage. There are several methods of removing water from liquid preparations, and these include spray drying, vacuum drying, spray freeze drying, air drying, and lyophilization (Zhang et al., 2017). Spray drying DNA is perhaps the least popular option as it has been associated with major damage caused by shear stress (Morgan et al., 2020).

1.6.4 Salt

The DNA backbone is negatively charged and the presence of salts, especially Na^{+} and Mg^{2+} ions, has a stabilizing effect wherein the cations neutralize negative charges on the phosphate groups of the DNA strand. This reinforces the hydrogen bonds that connect complementary strands of the double helix, and enhances the overall stability of the DNA by providing some degree of physical protection via the displacement of solvating water molecules and by shielding vulnerable bonds (Singh and Singh, 2015a; Weber et al., 2009). There is an optimum concentration range up to which the molecule will be stabilized, and this is dependent on relative humidity. When the concentration exceeds this point, the ions reverse roles and then can force DNA conformational changes from B-form to A- or Z-forms (Hormeño et al., 2011, 2012), resulting in instability (Khimji et al., 2013). Therefore, simply storing DNA at high salt concentrations would inhibit enzymatic damage and help prevent UV damage. However, there is a limit beyond which the concentration and pH become detrimental and destabilize the hydrogen bonding structures and integrity of the molecule. In addition, another potential disadvantage might require desalting depending on the downstream application (Schlaak et al., 2005).

1.6.5 Ethanol

To prevent degradation by chemical and enzymatic processes, DNA is often stored as a precipitate in ethanol at −80°C, as mentioned above. Since DNA is not soluble in ethanol, it is

therefore precipitated, segregated, and physically protected from damage by various agents. In addition, storage at −80°C also greatly inhibits any spontaneous chemical reactions (Evans et al., 2000). Storing DNA in ethanol above −80°C is also effective, but the ethanol tends to evaporate over time. A potential substitute at higher temperatures is propylene glycol as this substance has a much higher boiling point, and therefore does not evaporate readily (Nakahama et al., 2019).

1.6.6 Membranes

A DNA preservation technique that is gaining in popularity – and does not involve freezing – involves binding the DNA to a matrix, which reinforces its structure, prevents fragmentation, and provides physical barriers to UV radiation and enzymatic attack. Simple laboratory filter paper is the most basic form that has been used, with varying success, but many new variations now exist.

The most widely used commercial storage membranes for DNA samples are Whatman FTA® Cards, which are used extensively in the medical and forensic fields, although there are a range of similar competitor products that all use the same premise. Cells are lysed directly upon application to the card, and the nucleic acids are immobilized, so DNA from tissue or biological material is stored directly on the cards.

Studies have shown that genomic DNA stored on FTA® Cards at room temperature for over 17 years can be successfully amplified by PCR (Santos et al., 2018). The cards are supplied with a reagent that enables high molecular weight DNA to be released from the matrix for use in many molecular biology applications. There is, however, a problem with DNA becoming entrapped in the matrix, which lowers the amount of recoverable DNA (Green et al., 2019).

1.6.7 Storage Buffers

Many varieties of storage buffer exist, depending on the type of sample and desired downstream application. Choosing an ideal storage buffer largely depends on the available resources during sampling, such as the availability of freezing conditions and low-temperature storage facilities (Choo et al., 2015). Selecting optimal storage buffers is dependent on the compatibility of the buffer with all downstream analyses, including the extraction method. TE

(Tris–EDTA) buffer is a universally accepted buffer for DNA storage that has been demonstrated to preserve DNA over a range of conditions and sample types. There is much variety in DNA storage buffers, but they typically contain various salts dissolved in water to inhibit nucleases and provide ionic support for the DNA backbone (Williams, 2007).

1.6.8 Tetramethoxysilane (TMOS)

A sol-gel prepared by mixing tetramethoxysilane, or tetramethyl orthosilicate (TMOS), with TE buffer has recently been tested as a DNA storage matrix, and initial studies have shown great promise. Embedding the DNA inside a gel matrix without water can mimic the glassy state, protect the DNA from oxidative damage, and reinforce the DNA structure, thus protecting it from physical and chemical damage. Long-term studies are needed to evaluate the efficiency of this approach over extended time periods, but initial results seem promising (Narvaez et al., 2021).

1.6.9 Biocrystallization

Historically, the crystalline state was thought to be incompatible with biological processes. This has since been found to be untrue, and biocrystals are now considered to provide vital storage, sequestering, and protective roles in many living organisms. Biocrystallization has been found in all kingdoms of life, and the importance of these structures continues to grow as research advances. In many of these structures, proteins interact with minerals or other proteins to form a highly ordered crystalline state (Nürnberger et al., 2017; Vayssié et al., 2000).

Viruses use biocrystallization as a mechanical protection mechanism, to encapsulate virons in late-stage infections within a robust crystalline coat that is resistant to very harsh conditions and can lie dormant in soils for years (Coulibaly et al., 2007). This coat can then be dissolved in the midgut of a host, which has a specific pH, allowing for infection of the host (Payne & Mertens, 1983).

In prokaryotes, biocrystals are involved in cell wall stabilization, compartmentalization, and nucleic acid protection. One function of biocrystalline structures in bacteria is the formation of microcompartments, called metabolosomes, which provide a specialized reaction environment

for catabolic functions (Kerfeld & Erbilgin, 2015). Such confinement of enzymatic reactions protects the cell from potentially harmful reaction intermediates (Plegaria & Kerfeld, 2017). Another important function of biocrystallized structures is formation of cytoplasmic protein–nucleic acid complexes to protect bacterial DNA against stress (Luijsterburg et al., 2006). In *E. coli*, where the histone-like Dps (DNA protection during starvation) proteins were first discovered, crystalline complexes can form in the cytoplasm that contain this protein as the main component, and that protect the bacterial DNA from a multitude of damaging agents (Karas et al., 2015).

1.6.10 Formalin-Fixed Paraffin-Embedded

A standard clinical method of tissue preservation and storage is formalin fixation and paraffin embedding. Formalin-fixed paraffin-embedded (FFPE) tissue samples are used widely in clinical pathology laboratories and there is a large reservoir of older samples in storage. This method of tissue preservation is ideal for pathology as it preserves the cellular morphology, but it also has major limitations for nucleic acid preservation (Hewitt et al., 2008).

An extreme range of factors can affect the quality and quantity of recoverable DNA for downstream analysis. These include the duration of fixation and the storage conditions of paraffin blocks (time, temperature, and humidity) (Nam et al., 2014). Studies have found that formalin initiates DNA denaturation in AT-rich regions of dsDNA and creates sites for chemical interaction (Reid et al., 2017). DNA and proteins can become crosslinked during the embedding process, making subsequent extraction and amplification of the DNA highly variable with considerable fragmentation and damage (Do & Dobrovic, 2015). Several alternative fixation protocols have been developed and tested, but there is still no optimal method to consistently recover high quality DNA from FFPE tissues (Reid et al., 2017). Despite being a readily available method, the commonly-practiced FFPE method is not a reliable way to preserve DNA, and it should therefore not be used for samples that may require downstream molecular analysis.

1.7 Rationale and Objectives

While a considerable amount of information has been gathered over the past few decades about the DNA molecule and its importance, much of the fundamental work has been performed around decoding the information it stores. There are major gaps in our understanding of how the physical molecule reacts to long-term storage and damage, and how to preserve the encoded information. The DNA molecule is vulnerable to many classes of damaging agents, all of which have been studied extensively; however, there are still significant gaps in both the scientific knowledge and consensus concerning the rates and types of damage that accumulate over long time periods. The ability to identify and proactively mitigate this damage can allow the DNA molecule to survive intact for longer without compromising the information it contains. The ability to preserve DNA with its accompanying regulatory proteins would allow the DNA to be stored in a bioactive state with its natural structure and form, rather than as a simple chemical entity.

During the course of these studies, we developed, evaluated, enhanced, and utilized novel biotechnologies—including the use of new storage methodologies and proteins—to enhance DNA storage. We also challenged some of the degradation rates that were established by previous accelerated damage studies. Chapter 2 evaluates common types of storage conditions against temperature over a longer time period than a typical study, while Chapter 3 focuses on the evaluation of commercially available DNA storage products and their efficiency. Chapter 4 evaluates the protective effects of trehalose, which has become a major DNA preservative in recent years, against common damage mechanisms. Finally, Chapter 5 introduces a potential new protein-based DNA preservation method. Overall, this work contributes to the body of DNA storage knowledge by describing a comprehensive comparative study that furthers existing knowledge and advances the field through development of a promising new technique.

Chapter 2: Evaluating common DNA storage methods against temperature and pH over a multi-year study

2.1 Abstract

DNA storage in the laboratory continues to be a major issue. Loss of quality and quantity of sample DNA over time is a problem every laboratory faces. Accelerated time and damage studies have often shown that DNA degrades rapidly under many common storage conditions. Conversely, extremely old samples have recently been recovered and analyzed successfully, suggesting that the actual stability of the DNA molecule may be more robust than laboratory damage studies have indicated through future extrapolation of their results. In this work, general trends were consistent with these prior studies, over a five-year span, but DNA preservation was significantly greater than predicted by the damage models. Ultrapure reagents and extraction procedures significantly reduced damage and increased preservation under multiple storage conditions that are usually considered less optimal (e.g., room temperature, water). It was concluded that much of the damage, and damaging agents, were introduced or present at the time of processing. Damage may have also occurred during the analysis stage after storage. If the DNA is kept in a static, stable environment with ultrapure reagents, it can last for significantly longer than previously thought under a range of laboratory conditions.

2.2 Introduction

The DNA molecule has been the subject of many damage experiments and short-term accelerated damage replications in the laboratory, all aimed at examining which damage types are most deleterious to the molecule. Such knowledge is helpful for the development and modification of common laboratory DNA storage techniques. These previous explorations have resulted in a consensus that may not, in fact, be an accurate representation of how DNA samples degrade or react to environmental conditions in real time. The experimental accelerated damage conditions artificially generated for the sake of time and cost savings, and convenience, may actually cause greater DNA degradation and modifications, lead to false extrapolations, and not therefore provide an accurate, real-time picture. Room temperature storage is not recommended without additives as this results in rapid decay and degradation (Colotte et al., 2014).

In this study, several common laboratory storage techniques were evaluated separately, in parallel, and over a much longer time period compared with many existing studies that were performed without accelerated damage agents or techniques. Mitochondrial DNA samples were extracted under clean room conditions and stored in ultrapure reagents to evaluate, in real time, whether degradation rates were consistent with those in reported accelerated damage studies. Three different amplicons were evaluated by PCR and assigned weighted values to measure DNA quality by the size of the recoverable amplicons. The total amount of DNA degradation over time was measured with a dsDNA Qubit quantification assay, as this can detect both damaged and undamaged DNA. The Qubit system was also chosen for its accuracy, its cost effectiveness, and its ability to process a large number of samples in a very short time span – approximately two minutes per sample. These approaches were chosen to provide a more comprehensive view of the effectiveness of common storage methods, compared directly in a real-world situation.

Samples simply left in water or in a high humidity environment degrade very rapidly. This is reported to be a consequence of impurities such as nucleases and divalent metal ions, which in combination can damage the DNA (Narvaez et al., 2021). Studies have shown that samples stored in various buffers or nuclease-free water can last a significant amount of time, with various degrees of success at different temperatures (Latham & Miller, 2019). It is believed that DNA molecules are better preserved in more basic solutions: A pH range of 5–9 is considered the acceptable range for DNA integrity, with a slightly more basic solution considered optimal for stable sample storage (Hedges & Millard, 1995; Latham & Miller, 2019). With the addition of heat or other agents, the degradation process may be accelerated significantly above its original rate, causing damage to accumulate at a magnified rate rather than a natural rate; and when such results are extrapolated, this error is compounded (Latham & Miller, 2019). Thus, using accelerated damage techniques and extrapolating the results into the future may not be an accurate method of measuring or predicting the efficiency of a storage method. DNA damage is most likely accelerated or multiplied by the concentrated or enhanced damaging agents, which may not have the same efficiency in damaging the DNA molecule as in a static environment under equivalent conditions (Matange et al., 2021).

2.3 Materials and Methods

2.3.1 Collection and Extraction

All samples were extracted and purified in a designated clean room with appropriate protocols, PPE, and equipment to minimize any external contamination which could affect the DNA storage over the long-term (positive pressurized room I 6500B AllerAir double HEPA filter/activated charcoal air purification; HEPA-filtered biological safety cabinet with UV, Microzone Corporation, model # BK-2-6, cabinet type A2). All equipment, tubes, and reagents were exposed to UV crosslinking, autoclaving (where appropriate), and acetone glass washing along with bleach, water, and ethanol, to wash, remove or inactivate contaminants. The clean room had constant sterilizing UV exposure when not in use, during the entire extraction and aliquoting procedure. Samples were taken by buccal swabs and air dried for 20 min before extraction. Due to the large volume of DNA needed, buccal samples were taken from three individuals over a seven-day period, not under the clean room conditions in which they were processed. Samples were extracted in a 2 mL microcentrifuge tube (crosslinked/autoclaved) with 400 µl of extraction buffer—comprising 290 µL TNE (10 mM Tris, 100 mM NaCl, 1.0 mM EDTA, pH 8), 40 µL 20% SDS (Fluka, catalogue # 05030), 0.39 M DTT (Fisher Scientific, catalogue # BP17225), 5 µL Proteinase K (20 mg/mL, EN ISO 9001/07/94, Qiagen, catalogue # 19131), and 25 µL water (ultrapure RNase/DNase-free water, Invitrogen, catalogue # 10977-23)—followed by a 3 h incubation at 56 °C on a thermomixer (Eppendorf Thermomixer R 5355 Mixer Shaker) with agitation at 350 rpm.

At the end of the incubation step, samples were centrifuged 12,000 *g* speed for 1 min and the supernatant was transferred to a sterile 1.5 mL microcentrifuge tube (crosslinked/autoclaved). Then, 4 M guanidine thiocyanate (1 µL, Sigma, Catalogue # G9277) and 15 µL of silica beads (Sigma, Catalogue # 119H0212) were added to the tube and the sample was mixed, using a vortex mixer, for 30 seconds. The tubes were placed on ice for 6 h, following which they were centrifuged at high speed for 1 min then the supernatant carefully removed and discarded. Each sample was then resuspended in 500 µL of wash buffer (50 mM Tris–HCl pH 7.5, 50 mM NaCl, 1 mM EDTA in EtOH–H_2O (1:1); prepared using ultrapure, DNase/RNase-

free distilled water, Invitrogen, catalogue # 10977-23), then vortexed until the silica beads were resuspended, centrifuged on high speed for 1 min and the supernatant removed. To remove any residual salts, 500 µl of ice cold 75% EtOH was added and the sample vortexed again until the silica beads were resuspended, then centrifuged on high speed for 1 min and the supernatant removed and discarded. An additional wash step was carried out using 200 µL of cold 100% EtOH, with vortexing, centrifugation and aspiration steps as before.

Samples were then dried overnight in a forensic drying cabinet (DrySafe forensic evidence drying cabinet, AirClean Systems, model 300) at 28°C. After 24 h, 50 µL of ultrapure water (Invitrogen) was added and the sample was vortexed. The tubes were incubated for 1 h, with 350 rpm agitation, at 56°C, then the purified extracts were pooled and diluted to a concentration of 10 ng/µL in 50 µL of ultrapure water and aliquoted into individual 0.5 mL microcentrifuge tubes. Samples were again dried, overnight in a forensic drying cabinet at 28°C as before. The dry storage samples required no further treatment. For the other samples, ultrapure water or individual buffers were added up to a volume of 50 µL, as appropriate. The samples in ultrapure water, acidic solution, basic solution, and TE buffer required no further processing at this point. The other samples were vortexed for 1 min, then filter paper punches (Harris Micro Punch 3 mm punching device, GE Healthcare Life Sciences) were inserted into the tubes to soak up the solution, then allowed to air dry in a forensic drying cabinet prior to storage. A total of 1,155 tubes were aliquoted with the buffers, dried, and processed using filter paper punches.

2.3.2 Purification

QIAquick columns (Qiagen, QIAquick PCR purification kit, Catalogue # 28104) were used to purify DNA and remove alkaline and acidic storage buffers. This process was important to ensure the storage buffer components were removed from the samples, since they could affect downstream PCR analysis. The sample to be purified was diluted with five volumes of PB Buffer (supplied with the purification kit) and quickly vortexed. The mixture was pipetted onto the center of the column membrane and the column then centrifuged for 1 min at 17,900 *g*. The eluate was discarded, then 750 µL of PE Buffer (as supplied) was pipetted into the column, which was again centrifuged for 1 min at 17,900 *g* and the eluate discarded. The column was

transferred to a sterile 1.5 mL microcentrifuge tube and 50 µL of ultrapure, DNase/RNase-free distilled water, Invitrogen, catalogue # 10977-23), was added to the center of the membrane within the column, which was then allowed to incubate for 1 min at room temperature (18°C). The column was centrifuged at 17,900 *g* for 1 min to elute the DNA. Purified samples were used immediately in PCR amplification experiments.

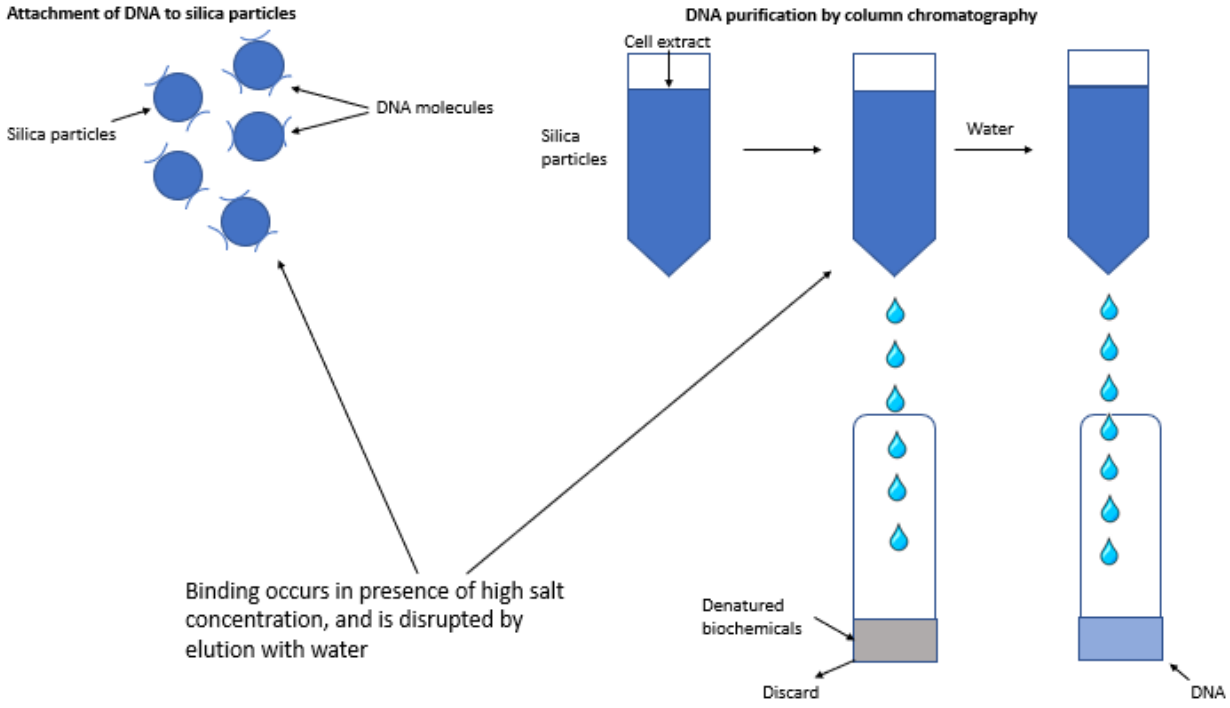

Figure 8: Binding of DNA to silica matrix in QIAquick mini columns

Following cellular digestion with proteinase K, extraction, and membrane disruption, DNA is isolated by adsorption on silica while the cellular debris is washed away. The DNA is then released from the silica matrix with a change in ionic conditions, and eluted. Lower volumes of water or elution buffer can be used to increase the concentration of the recovered DNA sample.

2.3.3 DNA Storage

The DNA samples were all stored in controlled environments throughout the duration of the study. Daily temperature logs of the fridges and freezers showed that their temperatures did not vary outside of the acceptable normal variations verified by the manufacturer. The samples were all stored in a dedicated, temperate-controlled clean room that had restricted access, regular cleaning, and a defined decontamination schedule. All work surface areas were bleached, and

UV treated on a monthly basis, while benchtops and work hoods were cleaned, and UV treated after every use.

All samples were stored in standard 50-well microcentrifuge tube plastic freezer boxes and in sterile, screw top 0.5 mL microcentrifuge tubes (Fisher Scientific, 517SFIS) to minimize evaporation and contamination. Room temperature samples were stored out of direct sunlight, under counter laboratory cabinets, with a thermometer that recorded temperatures with a variation of 17–24°C between seasons (the experiment occurred in northern Canada, where there are four distinct seasons and very large variations in relative humidity).

Due to evaporation, all liquid samples stored at room temperature were topped up every three months with storage buffers. Some liquid samples at 4°C, in refrigerator storage (General Electric laboratory refrigerator, model TB15SPFR, GE Healthcare Life Sciences), had to be topped up several times with storage solutions. The freezer samples (−30°C laboratory refrigerator/freezer, model ULT3030-A, Revco) did not require topping up, but a small amount of volume loss over time in the ethanol and buffer solutions was observed by the end of the study. The freezer unit operated within the manufacturer's specifications over the time frame of the study.

Storage Solutions and Materials

Ultrapure distilled water, DNase/RNase-free, Invitrogen, catalogue # 10977-23. TE buffer, DNase/RNase-free, Invitrogen, Catalogue # AM9849. Whatman qualitative filter paper, Grade 1, Sigma–Aldrich, catalogue # WHA10016508.

Acid solution was prepared with ultrapure, DNase/RNase-free distilled water (Invitrogen) with HCl titration to pH 5.0, while basic solution was prepared using the same grade of water with titration to pH 10 using NaOH. Alcohol, Sigma–Aldrich, catalogue # 676829 (95 parts of specially denatured ethyl alcohol 3A, 200 proof, with 5 parts of isopropyl alcohol. Final composition was ~90% ethanol, ~5% methanol, and ~5% isopropanol).

2.3.4 DNA Amplification

Thermostable DNA polymerase from *Thermus aquaticus* (*Taq* polymerase) was used to amplify DNA samples after extraction and following storage at various temperatures over the appropriate time intervals. Standard reactions were performed in 20 µL volume in 0.2 mL tubes, and used the mitochondrial DNA primers listed (Table 3) to generate three amplicons with sizes 800, 425, and 230 bp. Separate PCR reactions were run in duplicate, for each set of primers, to evaluate the quality of the DNA. All reaction mixtures were prepared on ice. The PCR reaction, after optimization, contained: 200 µM dNTPs, 0.2 µM of each primer, 1.0 mM $MgCl_2$, 1× PCR buffer (750 mM Tris–HCl pH 8.8, 200 mM $(NH_4)_2SO_4$, 0.1% Tween-20), 0.5 U *Taq* DNA polymerase, and 10 ng of DNA template. The remaining volume was made up to 20 µL using ddH_2O. Tubes were vortexed, spun down, and placed in a 96-well Gradient Mastercycler (Eppendorf).

Table 3: Mitochondrial DNA Primers Used

Mitochondrial DNA primers used during polymerase chain reaction (PCR) on DNA storage samples.

Primer	Sequence	Amplicon
MtF16210	TTT TCT ATT TTT AAC CTT TAG GAC	800 bp
MtR408	CAG CAA TCA TCA ACC CTC AAC TAT	
Mt14724F	CGA AGC TTG ATA TGA AAA ACC ATC GTT G	425 bp
Mt15149R	AAA CTG GAG CCC TCA GAA TGA TAT TTG	
Mt16 190F	CCC ATG CCT ACA AGC AAG TA	230 bp
Mt16 420R	TGA TTT CAC GGA GGA TGG TG	

The cycling parameters included an initial denaturation at 94°C for 2 min followed by 30 cycles of 94°C for 30 sec, 60°C for 1 min, and 72°C for 2 min. On completion, the reaction was placed at 4°C on hold. This PCR protocol was adapted and optimized from Lorenz (2012).

2.3.5 PCR Score

Three different mitochondrial amplicons were generated in order to estimate DNA quality by the size of the recoverable amplicon over different time periods and with different storage conditions. These three amplicons were 800, 425, and 230 bp in length. The size of the PCR product fragment can often be used as a proxy for DNA damage (Deagle et al., 2006). All samples were run in duplicate, and each amplicon was given a weighted value depending on its size, enabling integration of the multiple PCRs into a chartable format. The weighting was as follows: The 800 bp fragment was assigned a numerical value of 4 for amplification success, the 425 bp amplicon was assigned a value of 2, and the 230 bp amplicon was assigned a value of 1. For each amplification, the number of positive amplicons was added together for analysis and comparison. For example, a successful amplification of all three amplicons in duplicate would have a value of (4+4+2+2+1+1) = 14. This facilitated easy comparison of many samples, and multiple PCR amplicon sizes, allowing them to be visually displayed and graphed over time.

2.3.6 Electrophoresis Protocol

For agarose gel electrophoresis (AGE), PCR products were applied to a 2% agarose gel containing ethidium bromide (EtBr, ~1% in H_2O, Sigma–Aldrich, catalogue # 46067) for detection, and viewed with a transilluminator under UV light. One well was loaded with a molecular marker (5 μL) and the remaining wells with 3 μL of 6× loading buffer (Invitrogen) and 5 μL of sample. Gels were run for 30 minutes at 110 V in 1× TBE buffer, then removed from the running buffer and subsequently viewed on the transilluminator (UVB wavelength) and photographed.

2.3.7 Qubit Fluorometer Quantification

The large number of samples that needed to be quantified on a regular basis made quantitative PCR (qPCR) costs prohibitive, from both labor and monetary standpoints. As such, the Qubit system was chosen for this study for its rapid workflow, accuracy, and low cost.

The Qubit fluorometric system was highly accurate even at low concentrations. It detected all damaged DNA types that might not be accurately measured through quantitative

PCR where DNA may be of low quality and unamplifiable (Sedlackova et al., 2013). Qubit fluorometers detect fluorescent dyes that are specific to the target of interest; in this case, dsDNA, and emit only when bound to the target molecules. Qubit fluorometers are orders of magnitude more sensitive than UV absorbance, which measures any species present that absorbs at 260 nm: DNA, RNA, protein, free nucleotides, or excess salts. This could be problematic in a study looking for small changes in concentration over time, and furthermore, UV spectrophotometry often does not have sufficient sensitivity to accurately measure low concentrations of DNA and RNA (Ponti et al, 2018). Conditions where the Qubit system is known to have inaccuracies, such as FFPE tissue or Trizol–DNA extractions (Nakayama et al., 2016), were not present in this study.

The Qubit QuDye dsDNA HS (high sensitivity) assay kit (Lumiprobe, Catalogue # 531020) was used, in conjunction with the Qubit Flex fluorometer (ThermoFisher Scientific, Catalogue # Q33327), allowing for only the measurement of dsDNA. The assay is highly selective for dsDNA over RNA and is designed to be accurate for sample concentrations over the range 10 pg/µL to 100 ng/µL.

Quant-iT working solution was made by diluting the Quant-iT reagent 1:200 in Quant-iT buffer in a 5 mL Falcon tube. A volume of 200 µL of working solution was required for each sample to be quantified, including the standards, and the solutions were prepared as per the details in Table 4. Prior to quantification, all tubes were vortexed for 2–3 s then incubated for 2 min at room temperature, away from direct light. Following this, tubes were inserted into the Qubit quantometer, and after 5 s, a measurement for the nucleic acid concentration was obtained in nanograms per microliter (ng/µL).

Table 4: Qubit Standards / Working Solutions

Values of working solution volumes, and total tube volumes, for standards and samples used for DNA quantification using the Qubit quantometer.

	Standards	**Samples**
Working solution	190 µL	180–199 µL
Standard	10 µL	–
Sample	–	1–20 µL
Total volume per tube	200 µL	200 µL

2.4 Results

Figure 9 shows the results for PCR amplification analysis of samples stored at room temperature. Samples kept in alkaline solution (pH 10) displayed a steady decline in PCR amplification scores over time, with complete failure occurring at just over 500 days. DNA stored in acidic solution had complete PCR failure at only 150 days, whereas samples maintained in ultrapure water failed PCR at day 420. Storage in TE buffer (pH 8) proved successful for PCR until day 1,530. Dry storage gave successful amplification of the shortest 230 bp amplicon up until day 1,800, and for EtOH storage, PCR amplification occurred until day 1,440. Storage on dry filter paper had the greatest PCR score at 1,800 days

2.4.1 Room Temperature DNA Storage

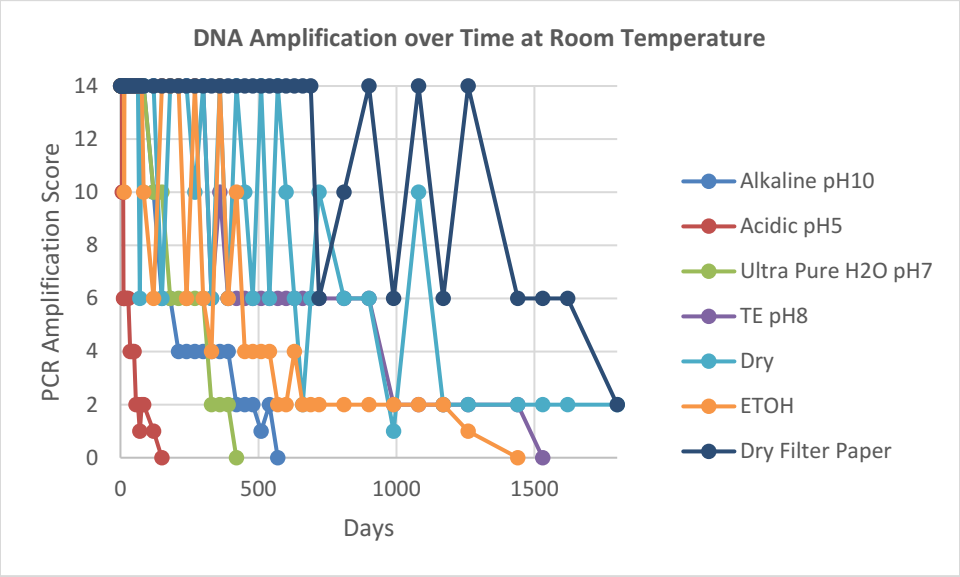

Figure 9: DNA Amplification over Time at Room Temperature

PCR amplification scores, over time, for DNA samples stored under the following conditions: in alkaline solution, in acidic solution, in ultrapure water, in TE buffer, in ethanol, dried, and dried on filter paper. Testing occurred over the range 150–1,800 days on samples stored at room temperature. Acidic conditions rapidly degrade the DNA while increasing pH increased the length of time viable DNA was recovered. Dried samples increased preservation lengths most overall.

When examining the storage of DNA at room temperature in greater detail, acidic conditions (pH 5) were associated with a sharp decline in PCR amplification during the first 90 days (Figure 9). These conditions performed the worst out of all the storage conditions tested.

Ultrapure water, ethanol, and alkaline storage conditions displayed a step-down decline in PCR amplification success after solutions were topped up due to evaporation loss (Appendix A. top up dates are marked in blue). Storage in TE buffer showed a sharp decline in PCR amplification after day 900. Storing the samples dry in tubes, or on dry filter paper, were the techniques that displayed the longest period for amplification success. Here, the volatility in amplification accelerated after approximately 600 days, with both dry and dry filter paper storage conditions recovering smaller amplicons by the 1,800-day mark.

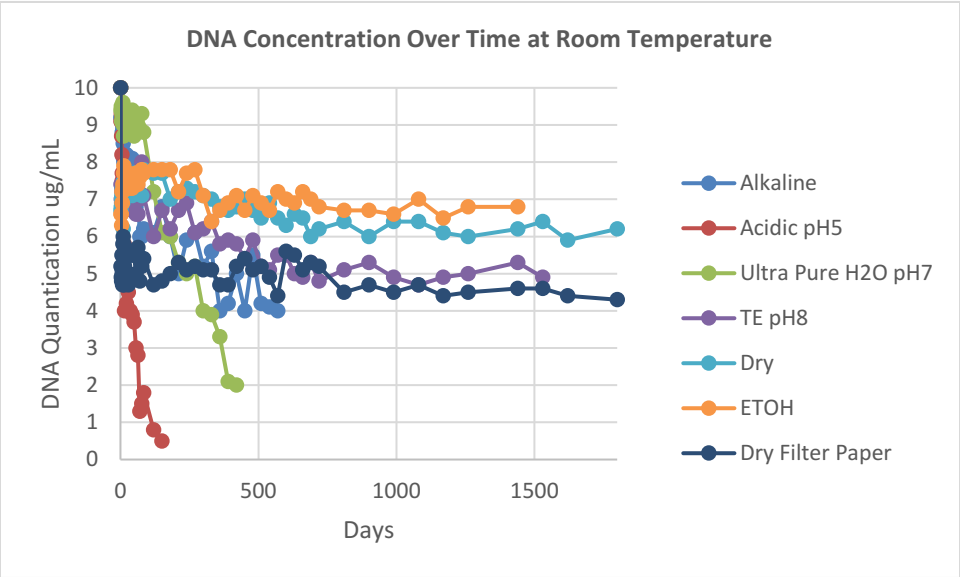

Figure 10: DNA Concentration over Time at Room Temperature

A Qubit fluorometer was used to measure the DNA concentration of samples (µg/mL) stored under the same conditions as for Figure 9: in alkaline solution, in acidic solution, in ultrapure water, in TE buffer, in ethanol, dried, and dried on filter paper. Testing occurred over the range 150–1,800 days and samples were stored at room temperature. Acidic conditions showed rapid degradation while higher pH solutions had greater preservation. Ethanol stored and dried samples had excellent preservation with relative high-quality DNA preserved over the experimental period.

The observed DNA concentration of the samples was also followed over time. Figure 10 shows that the concentration of samples stored in the alkaline buffer declined steadily up to day 500, whereas the DNA concentration in acidic solution rapidly declined up to the 150-day mark. In ultrapure water, the concentration of DNA displayed a stepwise decline in concentration up until day 420, beyond which the PCR amplicons were no longer recoverable. The DNA concentration

in TE buffer initially declined, over approximately the first 500 days, then remained steady until day 1,440. The dry samples showed an initial drop in concentration followed by slow decline to day 1,800 but remained relatively stable overall. The DNA stored in ethanol displayed high concentrations, following an initial drop, but again remained stable until day 1,440. The DNA concentration of samples stored in dry filter paper displayed the largest initial drop, but then remained constant until day 1,800.

When examining the DNA concentrations results for room temperature (Figure 10) in greater detail, acidic conditions (pH 5) were seen to be associated with a sharp decline in the measurable quantity of DNA during the first 150 days, making such conditions the worst performing of all those tested. Ultrapure water storage showed the second largest decline, with no measurable quantity of DNA present after 420 days. This was followed closely by alkaline storage, where there was no measurable quantity of DNA remaining after 570 days. This stair step decline in concentration readings occurred after the samples were topped up to compensate for evaporation losses. The TE buffer, ethanol, dry storage, and dry filter paper storage techniques all showed large initial drops in DNA concentration but then settled at values that remained steady for the rest of the experiment. Ethanol storage proved to be the most stable approach, as it produced the highest measurable quantities of DNA, while dry filter paper had lower measurable quantities of DNA despite being a stable form of storage. The DNA concentration for dry filter paper storage remained steadily with a narrow range to day 1,800, following a large initial drop of around 50%.

2.4.2 DNA Storage at 4°C

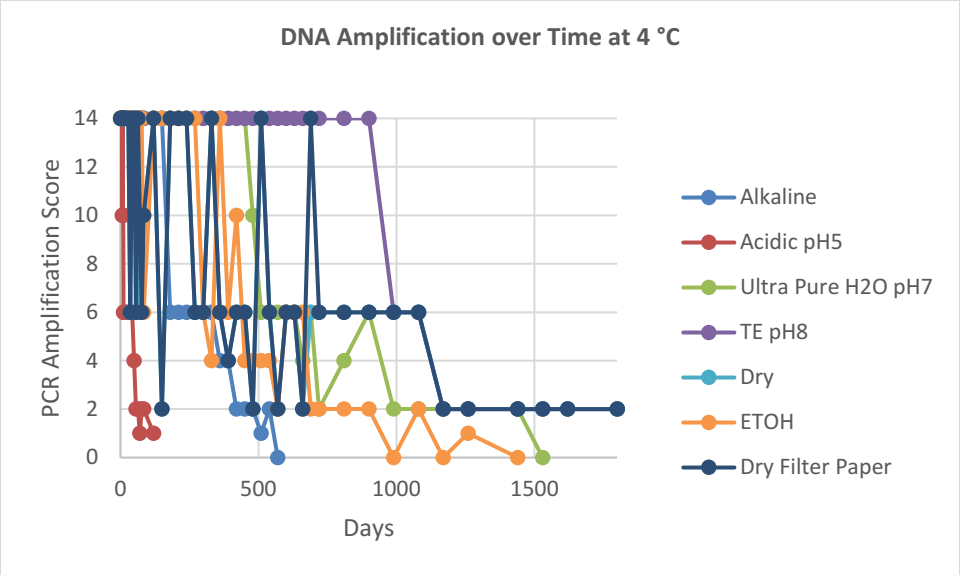

Figure 11: DNA Amplification over Time at 4°C

The PCR amplification score of DNA samples stored under the same range of conditions as previously: in alkaline solution, in acidic solution, in ultrapure water, in TE buffer, in ethanol, dried, and dried on filter paper. Testing occurred over a range of 120–1,800 days and the samples were stored at 4°C.

Figure 11 shows that DNA samples stored at 4°C in alkaline solution failed in PCR amplification at just over 500 days. Samples maintained in acidic solution showed a more rapid decline in amplification, with PCR failure at 120 days, whereas amplification was successful up to day 1,530 for samples stored in ultrapure water. TE storage buffer showed successful PCR amplification of the smallest 230 bp amplicon up to the 1,800-day mark, and dried samples amplified the 425 bp fragment successfully up until the same time point. Ethanol storage displayed variability over the first 1,000 days, with complete PCR failure at 1,440 days. Samples stored dry on filter paper maintained successful amplification of the 230 bp amplicon up to the 1,800-day mark.

When examining the storage of DNA at 4°C (Figure 11) more closely, it is apparent that acidic conditions were associated with a sharp decline in PCR amplification. Such conditions were the worst performing of all the storage conditions tested (Figure 11). Alkaline, dry, and dry filter paper storage conditions had lower PCR amplification scores at 4°C than the equivalent

room temperature samples, but with less evaporation and fewer top-ups required. Ethanol and ultrapure water storage produced higher PCR amplification scores over time at 4°C than at room temperature, but produced lower scores than the dry and TE buffer-based storage techniques. Dry filter paper had the longest period of amplification; however, recovery consisted of strictly small amplicons at the 1,100-day point. Storage at 4°C in TE buffer solution showed the best performance improvement in comparison with room temperature conditions.

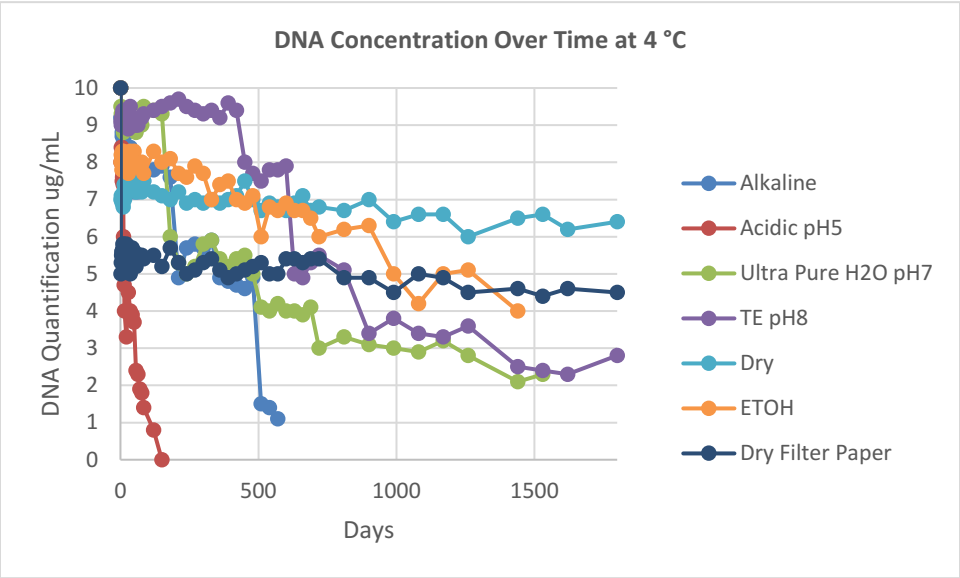

Figure 12: DNA Concentration over Time at 4°C

The DNA concentration of samples (µg/mL) measured using a Qubit fluorometer stored under the same conditions as in Figures 9–11: in alkaline solution, in acidic solution, in ultrapure water, in TE buffer, in ethanol, dried, or dried on filter paper. Testing occurred the range 150–1,800 days, and the samples were all stored at 4°C. Acidic conditions pH 5 had a rapid degradation while increasing pH had increasingly better preservation until pH 10 where it had a rapid decline much like the acidic pH 5.

Figure 12 shows there was a decline in the measurable quantity of DNA in samples stored in alkaline solution up to the point at which PCR failure occurred, at day 570. Similarly, samples stored in acidic solution displayed a steep decline in DNA concentration up to the point at which PCR failed at 150 days. With storage in ultrapure water, the DNA concentration of these samples showed a steep initial decline over approximately the first 200 days, followed by a slower but continuing decline up to the point of eventual PCR failure at day 1,530. The DNA

concentration in the TE solution was initially stable for the first ~400 days, and then underwent several large downward steps between days 500–1,000 before stabilizing for the rest of the experiment, remaining viable for PCR analysis at day 1,800. Under dry storage conditions, the DNA concentration initially declined more steeply before settling into a phase of slower decline, and again remaining viable at day 1,800. The concentration of DNA stored in ethanol showed a slow, steady decline up until the point of PCR failure at day 1,440. Dry filter paper storage was associated with ~50% initial decline in DNA concentration before the concentration stabilized, with little change up to day 1,800, where the sample remained viable for PCR.

When considering the storage of DNA at 4°C (Figures 11,12) in greater detail, it is apparent that acidic conditions were associated with a sharp decline in the measurable quantity of DNA during the first 150 days, and that these conditions showed the greatest and fastest drop in concentration; however, the drop was slightly slower than at room temperature. Nonetheless, acidic storage again showed the worst performance of all the conditions investigated. Under alkaline storage conditions, the DNA concentration remained stable until it had to be topped up due to evaporation at around the 500-day mark. Ultrapure water storage of DNA performed considerably better at 4°C than at room temperature, showing a lesser decline in concentration and a longer preservation period, with measurable DNA lasting up until day 1,530 (about three times as long as for room temperature storage). Ethanol, TE buffer solution, dry storage conditions, and dry filter paper storage all showed larger declines in measurable DNA concentration in comparison to equivalent room temperature storage.

2.4.3 DNA storage at −20°C

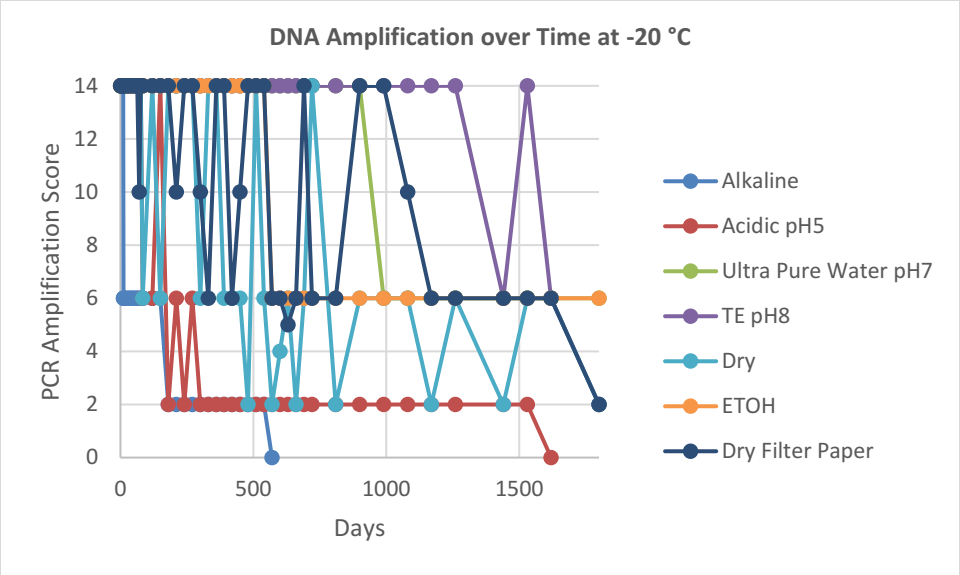

Figure 13: DNA Amplification over Time at −20°C

PCR amplification scores of DNA samples stored under same range of conditions as previously: in alkaline solution, in acidic solution, in ultrapure water, in TE buffer, in ethanol, dried, or dried on filter paper. Testing occurred over a range of 570–1,800 days, and all of the samples were stored at −20°C. The alkaline (pH 10) sample rapidly lost recoverability and the acidic (pH 5) remained viable but only with the lowest amplicon recoverable. Ethanol had the most consistent and longest preservation rate at −20°C.

At −20°C, DNA stored in alkaline solution showed a stepwise decline in PCR performance with failure occurring at 570 days (Figure 13). For the acidic solution, amplicon size declined rapidly over approximately the first 200 days, but the 230 bp fragment remained recoverable until day 1,620. DNA stored in ultrapure water showed no degradation until day 1,000 but then dropped down to success for 425 bp as the longest amplicon, which was recoverable up to day 1,800. The DNA stored in the TE solution maintained a high degree of integrity until day 1,500; following that, amplification was variable, but the 425 bp amplicon was recoverable at day 1,800. Dried DNA displayed considerable variability in performance over time, but nonetheless remained viable until day 1,800. Ethanol storage was associated with a drop in amplicon size at day 500, but the DNA again remained stably viable for PCR until day 1,800. Finally, the DNA stored on

dry filter paper showed large variability, with amplicon size fluctuating considerably over time and ending with the 230 bp amplicon recoverable at day 1,800.

When examining the storage of DNA at −20°C further, it was observed that all storage media performed significantly better than at room temperature or 4°C, as expected. Under acidic storage conditions, a significantly larger amount of amplifiable DNA was preserved at this temperature. Contrary to room temperature and 4°C, acidic storage of DNA at −20°C led to higher PCR amplification scores than for alkaline conditions. Ultrapure water storage performed significantly better, with larger DNA amplicons even at 1,800 days. TE solution was the most effective storage medium overall for preservation at −20°C, with high quality large amplicons retrievable after 1,500 days.

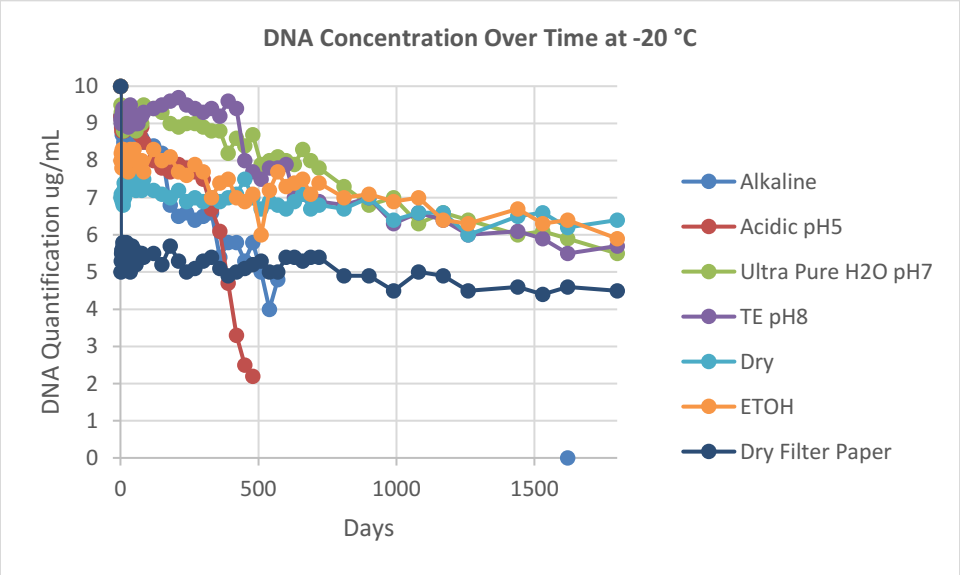

Figure 14: DNA Concentration Over Time at −20°C

The concentration of DNA samples (µg/mL) measured using a Qubit fluorometer, with storage under the following conditions: in alkaline solution (pH 10), in acidic solution (pH 5), in ultrapure water, in TE buffer, in ethanol, dried, or dried on filter paper. Testing occurred over a range of 480–1800 days and samples were stored at −20°C. Acidic (pH 5)had a steady rapid decline while the other storage solutions had a gradual decline but remained relatively stable.

Figure 14 shows that the concentration of samples stored in alkaline solution at −20°C declined initially, but then remained stable up to day 1,800. In acidic solution, the samples

displayed a steady decline in DNA concentration up until day 480, beyond which only the smallest amplicon was recoverable with PCR. Samples stored in ultrapure water showed a slow, steady decline in DNA concentration over the course of the experiment, but the DNA remained viable for PCR at day 1,800 with only a 30% decline from the initial concentration. The DNA stored in TE buffer displayed no noticeable change in concentration until day 500, after which point the concentration declined slowly, but the DNA remained viable at day 1,800. Dry storage showed an initial 30% decline in concentration before remaining stable, without additional decline, until day 1,800. The concentration of DNA stored in ethanol dropped a small amount initially, but then displayed a very slow decline over time, also remaining viable until day 1,800. Dry filter paper storage was associated with an initial 50% decline in DNA concentration, similarly to storage at the other temperatures, but there was then no noticeable decline up until day 1,800.

When examining these results further, it is apparent that a higher measurable quantity of DNA was retained under acidic storage conditions than at the previously-examined temperatures (room temperature and 4°C). By day 480, there was no detectable quantity of DNA under acidic storage conditions at −20°C, in comparison to the disappearance of measurable DNA by day 150 under the other temperature conditions tested. Ultrapure water, TE buffer, ethanol, dry, and dry filter paper storage techniques all showed large initial drops in DNA concentration but then settled, remaining within a narrow concentration range. These reductions in concentration occurred after the samples were topped up following evaporation. The measurable quantity of DNA at the end of the storage period, at −20°C, showed smaller variation between storage conditions than for the other temperatures investigated.

2.5 Discussion

Comparison of the time course data from the different storage conditions provides validation for the expected general trend: Frozen samples are the most stable, and retain the most viable DNA, at the highest concentrations. However, the data shows significant anomalies that may have interesting implications for better understanding DNA storage and developing best practices.

Using ultrapure water storage as a baseline for comparison, a steady increase in efficiency can be seen as the temperature is lowered. After the tubes were topped up with storage medium following evaporation, a major drop in DNA amplification occurred. This was evident in the room temperature storage samples, with sharp drops occurring after every event, and such drops were also apparent after a few years under the 4°C storage conditions. When stored frozen at −20°C, without the evaporation and top-up cycles, the DNA slowly declined in viability but without sharp drops. The amount of DNA remained stable but the declining sample quality—as shown by the drop in recoverable amplicon size—indicates accumulation of damage that can inhibit PCR, or simply increase fragmentation.

Across all the storage media evaluated, acidic conditions can be viewed as the worst conditions under which to store DNA, and there is a direct correlation between increasing temperature and increased damage. This is probably related to the well-known hydrolytic damage mechanisms which cause abasic sites and strand nicks, inhibiting PCR and degrading the DNA over time (Lathan & Miller, 2019).

Alkaline storage of DNA is generally considered to be a good approach. However, our results show that in a moderately basic environment (pH 10), alkaline storage underperformed in comparison to all other storage media except for the acidic environment. The quality of the DNA, assessed by the amount of amplifiable product, dropped rapidly, but the measurable DNA concentration was preserved as well as in other media over a long period. The highly basic environment interferes with the hydrogen bonding network that holds the DNA molecule in its structure, causing it to unwind and the strands to separate. This makes it highly susceptible to fragmentation, which would explain the inability to obtain larger amplicons upon extended storage.

The extra purification step with QIAquick columns that was used to purify out the DNA from alkaline and acidic storage buffers, immediately prior to PCR, could impact the downstream PCR analysis and might be expected to contribute to more fragmentation.. It was potentially a factor in the major drops that occurred after samples had evaporated and had to be

refilled, although the water storage showed a similar pattern but did not have the extra QIAquick purification step and the control samples did not have a drop after QIAquick purification.

Pelletized DNA under 100% ethanol performed similarly to DNA stored neat, as a dry sample, or dried onto filter paper conditions, at both room temperature and 4°C. However, evaporation loss of ethanol from the room temperature tubes was significant, and after top-up there was a decline in quality. This suggests that the ethanol is not a real preservative of the DNA but rather that it acts as a physical barrier protecting the DNA from enzymatic damage, atmospheric moisture, and oxygen (Gaudêncio da Silva Sales et al., 2020). In a lower temperature environment, at −20°C, using ethanol showed better preservation than the dry or dry filter paper storage conditions. This is probably due to the ethanol maintaining a physical barrier, and it did not have the same evaporation problem at −20°C that was experienced over time at room temperature and 4°C. In addition, the DNA stored under ethanol was not subjected to damage from ice crystal formation, as for the aqueous storage media.

Storage of DNA as dried samples, or on dry filter paper, both performed very well as preservation methods but experienced a higher degree of variability over time. Older samples occasionally had better amplification than younger samples stored under the same conditions. Atmospheric oxygen and water are both known to damage and modify DNA molecules over time, creating blocking lesions in a random fashion; and as such, the accumulation of these lesions occurs in a random pattern (Cadet et al., 2017). Exactly where the damage accumulates within the DNA will affect the apparent randomness of the amplifiable product. Furthermore, many blocking lesions can be created through oxidative damage—even in a frozen environment—contributing to the variable recovery of samples over time. Being in a dry state also creates a degree of fragility and brittleness, as discussed earlier, since much of the DNA may be in the A-form, which is more unstable, rigid, and susceptible to fragmentation (Baker et al., 2007). Overall, the dry filter paper method showed better amplification and had the greatest DNA preservation. There was a 50% initial drop in measurable DNA quantity, which occurs when the sample DNA is stuck in the matrix of the filter paper; this is recognized as a major

problem, even with commercial filter paper storage materials such as FTA cards (Tillmar et al., 2019).

In addition, some of the sample DNA could have stuck to the walls of the storage tubes. This has also been recognized as a problem with laboratory plastic tubes (da Cunha Santos et al., 2018), but did not appear to be a major contributor in this study. Relatedly, the starting material quality, reagents, and purity of the extracted materials also impact preservation, as shown in one study which concluded that the type of extraction kit used can contribute to the integrity of DNA samples in storage over time (Hallmaier-Wacker et al., 2018).

2.6 Conclusions

When extracted with ultrapure reagents and processed in an ultraclean environment, DNA was found to last significantly longer in real time than indicated by the results of many similar studies using accelerated damage experiments, without the need for specialized treatments. The conclusion from our study is, therefore, that DNA is a relatively stable molecule when it is maintained in a static and stable environment. It is therefore no surprise that DNA has been successfully recovered from environments that have had stable conditions for tens of thousands to hundreds of thousands of years, such as ice cores and frozen tundra (Liang et al., 2021). DNA has also displayed excellent preservation in dry and hot climates, with well-known Egyptian genetic studies having demonstrated a high degree of preservation in bones and teeth that were several thousands of years old (Watson et al., 2017).

In contrast, many published studies report significant degradation of DNA under laboratory conditions over a timescale of weeks or months; whereas in our study, this period was considerably longer. However, DNA molecules did suffer from significant degradation in quality, in terms of PCR viability, even when the measurable quantity was significantly higher after manipulation or rehydration. This suggests that DNA fragmentation might be a major problem, on a par with other damaging agents, during DNA storage. At any rate, much of the accumulated damage comes from the original sample itself (impurities or environmental contaminants), from fluctuations in the storage conditions, and from reagent contaminants; and also from processing steps before or after extraction, including manipulations involved in

purification or PCR amplification. The various pH conditions and temperature regimes used are adopted in an effort to inhibit these damaging agents during storage.

In this study, DNA molecules were found to be very stable until they had to be rehydrated or opened due to evaporation. Locally, the DNA molecule is very rigid, and the nucleotide sequence has a significant effect on this rigidity, but when in solution, the hydration shell that forms helps to create some flexibility, both local and regional. Hydrated B-form DNA is therefore more flexible, but after dehydration, much of the DNA takes on other forms. This is mostly the A-form but can include the Z-form, which is more fragile and rigid in a high ionic strength environment. When dried DNA is hydrated quickly with agitation, this can cause significant fragmentation. Even gentle agitation will exert significant shearing forces on the DNA. Miroshnikova et al. (2016) showed that for DNA, the amount of time spent in a vortex is more important than the force of the vortex, and DNA sheared at certain locations regardless of the force of the agitation. It thus seems apparent that hydrating DNA slowly after a long storage period, without agitation or heat, may aid sample recovery by restoring the B-form and hydration shell that make the DNA more flexible, and conferring resistance shearing and fragmentation. Therefore, a gentler method of mixing, rather than vortexing, may serve to minimize shearing damage.

An evaporation issue occurred during this study that forced the storage tubes to be opened at regular intervals to be topped up. It is unknown whether potentially damaging environmental agents like nucleases were introduced at this time, contributing to the rapid step declines described above, or whether the observations were the result of a hydration/fragmentation problem instead. Only double stranded DNA was probed in this study and some of the lower concentrations over time may be related to the denaturing of the DNA helix into single strands which may not be an overall loss or if the fragmentation of the backbone into base pair fragments to small for fluorometric binding and detection by qubit quantification. Further investigation is needed.

Chapter 3: Effectiveness of Trehalose for DNA Preservation Against Common Damage Types in Solution

3.1 Abstract

Trehalose, a disaccharide consisting of two α-D-glucose units, is a common sugar that is often touted as a panacea for DNA preservation and is an integral part of anhydrobiosis. The ability of trehalose to help protect DNA in a dried state is well known, and its ability to support DNA structure and prevent degradation have been extensively studied. In this work, we evaluated whether trehalose could function as an effective preservative at room temperature, for DNA samples stored in solution form, against specific experimentally induced damage types. In its lyophilized state, the protective properties of trehalose are known. DNA samples were treated with a concentration gradient of trehalose and subjected to damage experiments that included acid hydrolysis, oxidative damage, and enzymatic damage. Samples with increasing trehalose molarity and, consequently, viscosity, showed significant improvements in the preservation of DNA in the damage experiments, relative to control. Resistance to enzymatic damage increased 66% over control at the highest trehalose concentration of 0.4 M. Protection against hydrolytic damage showed the largest change, increasing 86% over control at 0.4 M trehalose, indicating very effective protection against this type of damage. Both hydrolytic and enzymatic damage resistance had a direct correlation with increasing concentration. Oxidative damage resistance was increased by 21% relative to control, but increasing trehalose concentration showed diminishing returns above 0.1 M. Thus, trehalose is an effective additive to room temperature solution samples of DNA, to help protect against all three DNA damage types investigated, but its efficiency in protecting against oxidative damage is lower. Trehalose is therefore unsuitable as a stand-alone preservative; however, if used in an optimized blend or mixture, it could be an integral part of such a storage mixture that acts synergistically with other protective agents.

3.2 Introduction

Trehalose is a multifunctional non-reducing disaccharide that can be found in plants, microorganisms, and some animals such as shrimp, insects, and bees, where it normally serves

the purpose of a principal blood sugar. In microorganisms, it acts as a carbon source (Kosar et al., 2018). As a response to abiotic stresses, cells will overproduce trehalose in very high concentrations, where it has many protective qualities (Ruhal et al., 2013). Once produced, it is able to enter a glassy state that stabilizes the key structural components of the cell when frozen, dehydrated, or subjected to large changes in salinity (Vinayykumarr et al., 2019). One of its major functions, in cooperation with anti-freeze proteins, is therefore to prevent or mitigate cellular freezing thereby protecting tissues from ice crystal formation (Zhang et al., 2019). In fact, trehalose has unique chemical properties that enable it to fulfil this role: it is the only sugar that forms amorphous non-hygroscopic crystals, and is very stable at high temperatures (Iturriaga et al., 2009). Trehalose can also allow the survival of cells under dehydrating conditions in a process known as anhydrobiosis. Additionally, it offers protection from large changes in pH and temperature, which are often faced by insects or microorganisms, and it contributes to the ability to undergo long states of dormancy (Vanaporn & Titball, 2020). Along with the ability to preserve cellular structures, such as membranes and proteins, it has been shown that trehalose is an effective nucleic acid protectant under several environmentally stressful conditions (Spiess et al., 2004). Depending on the concentration of trehalose present, DNA degradation—when dried and subjected to accelerated damage experiments with heating—can be slowed greatly (Lee at al., 2012). Trehalose can also regulate the rehydration process, preventing cells from rupturing as water molecules are reintroduced (Morano et al., 2014).

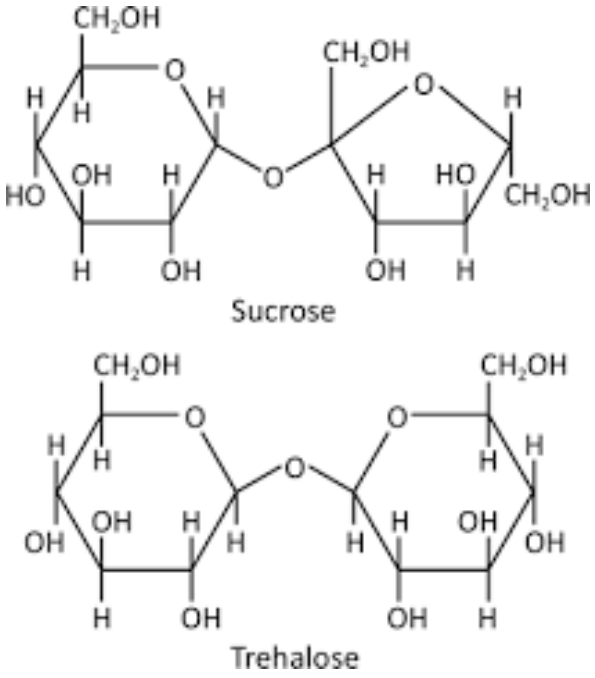

Singh S.K. (2018)

Figure 15: The Chemical Structures of Sucrose and Trehalose

Chemical structures of Sucrose and Trehalose both disaccharide molecules with similar molecular structures. Each molecule contains the same amount of energy 16.7 kJ/g but have different solubility and glassy state temperatures which affect their preservative ability.

Figure 15 shows the chemical structures of sucrose and trehalose, both which are well-known lyoprotective (Woo et al., 2021) and cryoprotective agents for nucleic acids (Ball et al., 2016). The chemical properties that allow trehalose to be a more superior protectant than other sugars, such as sucrose or maltose, have been well studied in solution. The ability for it to hydrogen bond with the DNA backbone and with other trehalose molecules substitutes the hydration shell usually supplied by water molecules. Trehalose can also incorporate water molecules into these structures, and prevent clumping and crystal formation (Olgenblum et al., 2020).

In the dried state, where DNA converts to the A-form, the presence of trehalose substitutes for the primary hydration shell; for the water molecules that are lost from around the DNA. This helps prevent hydrolytic degradation and promotes maintenance of the DNA in the B-form, which is more flexible and offers some protection from physical forces, thereby preventing fragmentation (Brogna et al., 2021). Its ability to protect nucleic acids *in vivo* has led

to the use of trehalose as a preservative, or protective agent, when storing and transporting nucleic acids *in vitro*. Many commercial protective agents have some concentration, or variant, of trehalose in their preservative mix (Organick et al., 2021). Trehalose is readily soluble in water (Yuan et al., 2017), and is not thought to have a negative impact on downstream applications like PCR, making it an attractive option as a preservative. It has a glass transition temperature 60 °C higher than that of sucrose, which has the same molecular weight. This high glass transition temperature makes it very stable, and it can easily enter the glassy state (Zhang et al., 2017).

There are some conflicting reports regarding the efficiency of the glassy state in protecting DNA, as this can be affected by temperature, sample purity, moisture content, and concentration. In a study by Zayed & Roos (2004) using stored cells, it was found that the residual moisture level left in freeze-dried cells at the time of desiccation directly impacted the amount of DNA damage that occurred. Furthermore, Zhang et al. (2017) showed that temperature was a factor in determining DNA damage, with temperatures of 4°C or lower preserving the DNA best. This contradicts research of Smith & Morin (2005), who investigated the dry state at room temperature, and showed there was no significant loss of quantity at 4°C or −20°C in the glassy state over the duration of the study. Whereas the protective abilities of trehalose are well documented with regards to its physical ability to reinforce vital structures like proteins, membranes, and nucleic acids during dehydration and freezing events (Zhang et al., 2017), there is less clarity around what protection it provides against specific damaging insults such as oxidation, enzymatic damage, UV radiation, and pH- or heat-induced hydrolytic damage.

One additional feature that makes trehalose attractive as an additive for DNA preservation is that, not only does it not interfere with PCR, but it can also enhance the efficiency of PCR for GC-rich templates. This is due to the ability of trehalose to (a) lower the melting temperature of DNA, and (b) give thermostabilization to the *Taq* DNA polymerase (Spiess et al., 2004).

Even outside of the glassy state, trehalose still appears to have protective and preservative value for DNA (Olgenblum et al., 2020). This may be due to its ability to interfere with hydrogen

bonding while replacing and sequestering water molecules. If trehalose replaces water molecules around the DNA molecule in the hydration shell, this can prevent or inhibit chemical attack or UV radiation damage (Liu et al., 2017). As the concentration of trehalose increases, this physical shell around the DNA molecule will be further protected from fluctuations in pH (Spiess et al., 2004). In figure 16 the trehalose molecule is shown binding to different positions on the DNA molecule through one glucose units while figure 17 shows how both glucose units of the trehalose molecule bind to the various positions of the DNA molecule.

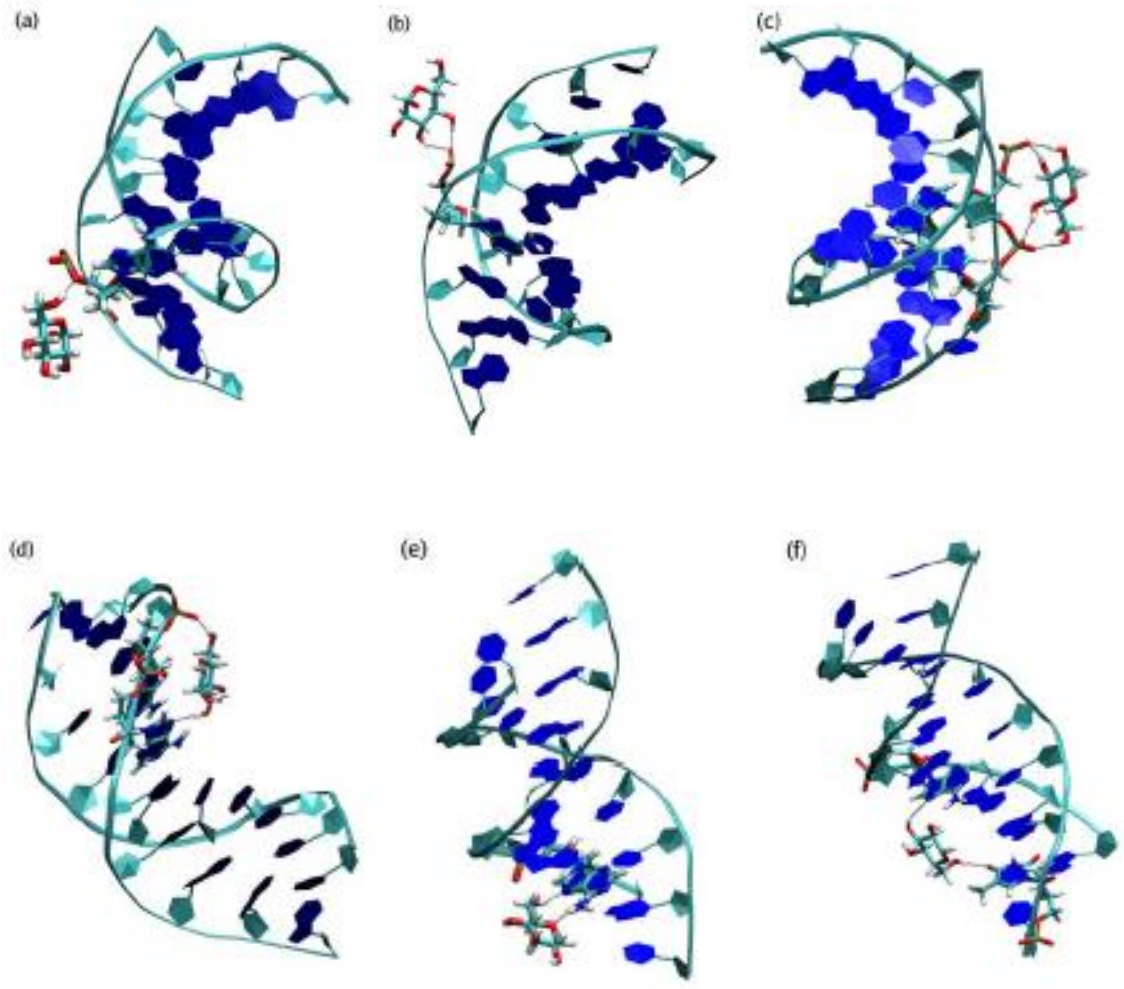

(Fu, 2008)

Figure 16: Trehalose Hydrogen Bonds in Multiple Formations to DNA, with One Glucose Unit

Trehalose can hydrogen bond with DNA through one glucose unit of the molecule (the other glucose unit not forming hydrogen bonds is not shown), by forming (a) one bond to a phosphate group; (b) multiple bonds with one phosphate group; (c) bonds with two phosphate groups; (d) bonds with one phosphate group and one base pair; (e) bonds with one base pair; or (f) bonds with two base pairs.

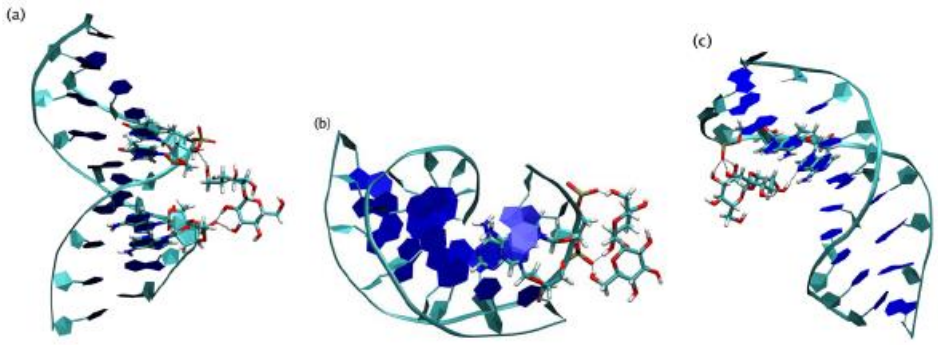

(Fu, 2008)

Figure 17: Trehalose Hydrogen Bonds in Multiple Formations to DNA, with Both Glucose Units

Trehalose interacting with DNA through both glucose units, by forming hydrogen bonds with (a) two phosphate groups on different strands; (b) two phosphate groups on the same strand; or (c) with one phosphate group and one base pair.

The ability of trehalose to form hydrogen bonds with the DNA molecule in many ways, and with itself, allows it to build a lattice network with multiple binding sites. This reinforces the DNA molecule in a hydrated state, replacing the water molecules lost in a dehydrated state.

3.3 Materials and Methods

As before, various-sized target areas were amplified to assess DNA preservation or protection. A set of 230 bp, 425 bp, and 800 bp DNA amplicons was optimized for PCR. The conditions, exposure time, and concentration of damage-inducing treatments were used and modified from the previously-published Lakehead University Master's thesis titled, "Assessing *in vitro* DNA repair methods" (Lehto, 2012).

3.3.1 Initial DNA Purification and Extraction

The protocol followed for initial DNA extraction and subsequent silica/guanidium purification was taken from the Lakehead University Paleo DNA Laboratory Methods for Forensic Testing (PDL 001, Sections 4.1.7 and 4.3.6). Samples were extracted in a 2 mL microcentrifuge tube (crosslinked/autoclaved) with 400 µL of extraction buffer consisting of: 290 µL TNE (10 mM Tris, 100 mM NaCl, 1.0 mM EDTA), 40 µL 20% SDS (Fluka, catalogue # 05030), 40 µL 0.39 M DTT (Fisher Scientific, catalogue # BP17225), 5 µL proteinase K (20 mg/mL, Qiagen, EN ISO 9001/07/94, catalogue # 19131), and 25 µL water (ultrapure RNase/DNase free distilled water, Invitrogen, catalogue # 10977015). This was followed by a 3 h incubation at 56°C on a thermomixer (Eppendorf, Thermomixer R) with agitation at 350 rpm.

After this time, samples were centrifuged at 12,000 *g* for 1 min and the supernatant was transferred to a sterile 1.5 mL microcentrifuge tube (crosslinked/autoclaved). A volume of 1 mL of 4 M guanidine thiocyanate (Sigma, catalogue # G-9277) and 15 µL of silica beads (Sigma, catalogue # 119H0212) were added into the tube. This mixture was vortexed for 30 s, then the tubes were placed on ice for 6 h. They were then centrifuged at 12,000 *g* for 1 min, before the supernatant was carefully removed and discarded. Then, 500 µL of working wash buffer was added (50 mM Tris–HCl pH 7.5, 50 mM NaCl, 1 mM EDTA in EtOH–H_2O (1:1); prepared using ultrapure, DNase/RNase-free distilled water, Invitrogen, catalogue # 10977-23). The mixture was vortexed until the silica beads were resuspended, centrifuged at 12,000 *g* for 1 min and the supernatant was removed. To remove any residual salts, the silica beads were resuspended in 500 µL ice cold 75% EtOH by vortexing. The samples were then centrifuged at 12,000 g for 1 min and the supernatant was removed and discarded. An additional wash step was similarly carried out using 200 µL of cold 100% EtOH.

Samples were then dried overnight at 28°C in a forensic drying cabinet (AirClean Systems, DrySafe Forensic Evidence Drying Cabinet Model 300) and dissolved in 50 µL of ultrapure water (ultrapure RNase/DNase free distilled water, Invitrogen, catalogue # 10977015). The purified extracts were pooled and diluted to a concentration of 10 ng/µL using Qubit Quantification system in 50 µL of ultrapure water and aliquoted into individual 1.5 mL

microcentrifuge tubes for total concentration of 500 ug/mL. Samples were then dried back down in forensic biosafety cabinets, as above. Individual buffers, as appropriate, were added to each sample and they were subjected to damage protocols in a final assay volume of 50 µL. The samples were then vortexed for one minute.

3.3.2 Purification

QIAquick columns (Qiagen, QIAquick PCR purification kit (50), catalogue # 28104) were used to purify DNA to remove buffers and treatment agents, as they could potentially affect downstream PCR. The buffer solutions supplied with the commercial kit were used with the columns. Each sample to be purified was first diluted with five volumes of PB Buffer and quickly vortexed. The mixture was pipetted onto the center of the column membrane, and the column centrifuged for 1 min at 17,900 *g*. The eluate was discarded, then 750 µL of PE Buffer was pipetted into the column, which was again centrifuged for 1 min at 17,900 *g*. The eluate was again discarded. The column was transferred to a sterile 1.5 mL centrifuge tube and 50 µL of sterile ddH_2O was added to the center of the membrane within the column. After incubation for 1 min at room temperature (18°C), the column was centrifuged at 17,900 *g* for 1 min to elute the DNA. Purified samples were then used immediately in PCR amplification experiments after quantification.

3.3.3 Qubit Fluorometer Quantification

The large number of samples that needed to be quantified on a regular basis and at various steps made qPCR cost-prohibitive from a labor and monetary standpoint. As such, the Qubit system was chosen for its suitability of workflow, accuracy, and cost.

The Qubit fluorometric system is highly accurate even at low concentrations and detects all damaged DNA types that might not be accurately measured through qPCR (Sedlackova et al., 2013). Qubit fluorometers detect fluorescent dyes that are specific to the target of interest. These fluorescent dyes emit only when bound to the target molecules, even at low concentrations. Qubit fluorometers are orders of magnitude more sensitive than UV absorbance, which measures any species present that absorbs at 260 nm—including DNA, RNA, proteins, free nucleotides, or excess salts. This is problematic in a study looking for small changes in concentrations over

time. UV spectrophotometry often does not have the sensitivity to accurately measure low concentrations of DNA and RNA (Ponti et al., 2018). Conditions where the Qubit system is known to have inaccuracies, such as FFPE tissue or Trizol–DNA extractions, were not present in this study (Nakayama et al., 2016).

The Qubit dsDNA HS (high sensitivity) assay kit (Lumiprobe, catalogue # 531020) was used in conjunction with the Qubit Fluorometer (ThermoFisher Scientific, Qubit Flex fluorometer, catalogue # Q33327), allowing for only the measurement of dsDNA. The assay is highly selective for dsDNA over RNA and is designed to have a wide dynamic range, covering initial sample concentrations from 10 pg/µL to 100 ng/µL. Quant-iT working solution was made by diluting the Quant-iT reagent 1:200 in Quant-iT buffer in a 5 mL Falcon tube. A volume of 200 µL of working solution was required for each sample to be quantified, including the standards. Solutions were prepared as per Table 5. All tubes were vortexed for 2–3 s then incubated for 2 min at room temperature, avoiding direct light. They were then inserted into the Qubit quantometer and a nucleic acid concentration was given after a 5 s wait time.

Table 5: Qubit standards and working solutions

Volumes of working solutions, and total tube volume, for standards and test samples used for DNA quantification using the Qubit quantometer.

	Standards	**Samples**
Working solution	190 µL	180–199 µL
Standard	10 µL	–
Sample	–	1–20 µL
Total volume per tube	200 µL	200 µL

3.3.4 PCR

Each PCR reaction was carried out in a total volume of 12.5 µL, and contained: 1.25 µL of 10× reaction buffer (Life Technologies, Invitrogen), 2.5 mM $MgCl_2$, 1.25 pmol each of forward and reverse primer (Table 6), 50 µM dNTP mix, 0.3 U Platinum *Taq* DNA polymerase (Life Technologies, Invitrogen), and 2 µL of template DNA at 10 ng/µL. The PCR cycle

consisted of incubating at 94°C for 1 min, then 5 cycles of 94°C for 40 s, 45°C for 40 s, and 72°C for 1 min. This was followed by 30 cycles of 94°C for 40 s, 51°C for 40 s, and 72°C for 1 min, with a final extension at 72°C for 5 min (deWaard et al., 2008; Hajibabaei et al., 2005). This PCR protocol was optimized for trehalose, such that if there was any residual trehalose in the purified products, the reaction would not be inhibited.

Table 6: Mitochondrial DNA Primers Used

Mitochondrial DNA primers used during polymerase chain reaction (PCR) on DNA samples treated with damaging agents with or without trehalose. All forward and reverse primers used were authenticated by Lehto (2012).

Primer	Sequence	Amplicon
MtF16210	TTT TCT ATT TTT AAC CTT TAG GAC	800 bp
MtR408	CAG CAA TCA TCA ACC CTC AAC TAT	
Mt14724F	CGA AGC TTG ATA TGA AAA ACC ATC GTT G	425 bp
Mt15149R	AAA CTG GAG CCC TCA GAA TGA TAT TTG	
Mt16 190F	CCC ATG CCT ACA AGC AAG TA	230 bp
Mt16 420R	TGA TTT CAC GGA GGA TGG TG	

3.3.5 PCR Score

Three different mitochondrial amplicons were generated to estimate DNA quality by comparing the size of the amplicon that was recoverable after different exposure times to the DNA-damaging conditions. The size of the PCR fragment can often be used as a proxy for DNA damage (Deagle et al., 2006, Figueroa-González et al., 2017). The three amplicons used were 800 bp, 425 bp, and 230 bp, and each reaction was duplicated consecutively plus a positive and negative control for each time period. Each successful amplification was assigned a weighted score depending on the amplicon size, to enable integration of the results of multiple PCRs into a chartable format. This score was calculated with the 800 bp amplification success assigned a numerical value of 4, the 425 bp amplicon assigned a value of 2, and the 230 bp amplicon assigned a value of 1. For each amplification, the number of positive amplicons (including

replicates) was added together for analysis and comparison. For example, a successful amplification of all three amplicons in duplicate would have a value of 4+4+2+2+1+1 = 14. This approach permitted easy comparison of the large quantity of samples and multiple PCR amplifications, in a format which could readily be visually displayed and graphed over time.

3.3.6 DNA Damage

DNA damage was induced experimentally via appropriate damaging agents, to introduce and accelerate the three most common forms of DNA damage: strand nicks; oxidation (which can lead to blocking lesions); and modified bases and hydrolytic damage, which can both lead to formation of abasic sites.

3.3.7 Experimental Formation of Strand Breaks

To artificially induce strand nicks without causing other forms of damage, the enzyme DNase was used because of its ability to remove bases while leaving the 3′- and 5′-ends of DNA intact. A series of concentration gradient solutions was tested over time intervals on a DNA template to induce damage to the point of *Taq* DNA polymerase inhibition but not to completely degrade the molecule to single base pairs (which is its intended commercial purpose). Lehto (2012) found that 0.5 U DNase was the optimum experimental concentration for inducing strand nicks over the exposure times used in this study.

3.3.7.1 DNase Treatment

The DNase treatments were applied to DNA samples in ultrapure water solution containing a gradient of trehalose concentrations (0.01 M, 0.05 M, 0.1 M, 0.2 M, 0.3 M, and 0.4 M).

The introduction of SSBs was achieved using DNase enzyme in the presence of Mg^{2+} ions, which cleaves each strand of dsDNA independently in a statistically random fashion (Sambrook & Russell, 2001). Specifically, this work used DNase I (RNase-free, Fermentas Life Sciences, 1 U/µL), where 1 U is defined as the amount of enzyme which completely degrades 1 µg of plasmid DNA in 10 min at 37°C. Reactions were carried out 1.5 mL microcentrifuge tubes in a final volume of 100 µL, as follows: Template DNA (0.5 µg) was added to the tube and

combined with 0.5 U (0.5 µL) DNase in storage buffer (50 mM Tris–OAc pH 7.5, 10 mM $CaCl_2$, 50% v/v glycerol). Then, 10 µL of 10× reaction buffer with $MgCl_2$ (100 mM Tris–HCl pH 7.5, 25 mM $MgCl_2$, 1 mM $CaCl_2$) was added and followed by ddH_2O up to a volume of 100 µL. Reactions were incubated for various time intervals at 37°C then transferred to a separate Eppendorf thermomixer preheated to 65°C for 10 min heat to inactivate the enzyme. Samples were cooled on ice and purified using QIAquick PCR purification columns, as above, then used immediately in PCR reactions.

3.3.8 Experimental Formation of Oxidative Damage

Oxidative processes modify DNA and are generated through reactions of DNA with ROS. In this study, oxidative damage was generated by addition of H_2O_2 (approximately 180 mM) to the DNA and incubation at 37˚C. H_2O_2 was chosen because of its reliable and well-studied induction of oxidative damage to DNA.

3.3.8.1 Hydrogen Peroxide

DNA template (approximately 0.5 µg) in 50 µL of ddH_2O was added to a 1.5 mL microcentrifuge tube along with 10 µL of 6% H_2O_2 (~1.8 M) and varying concentrations of trehalose, from a commercial 1 M stock solution (Life Sciences Technologies), with addition of ddH_2O (dependent on the amount of trehalose solution added) to achieve a final volume of 100 µL. The samples were vortexed for 15 s, followed by a quick spin in a microcentrifuge (approximately 30 s), and then incubated at 37°C for various time periods on Eppendorf thermomixer. The samples were again purified using QIAquick PCR kit spin columns, and immediately added to PCR reactions.

3.3.8.2 Trehalose Concentration Gradient

A 1 M trehalose solution was purchased from Life Sciences Technologies. Tubes were prepared with 0.5 µg of DNA in 50 µL and the trehalose solution was added to give the desired final concentration, then the solutions topped up with water to the final assay volume (100 µL). The oxidative damage treatments were applied to a gradient (0.01 M, 0.05 M, 0.1 M, 0.2 M,

0.3 M, and 0.4 M) of trehalose solutions containing DNA, ultrapure water, and 6% hydrogen peroxide solution, as well as the trehalose.

3.3.9 Experimental Formation of Hydrolytic Damage

Hydrolytic damage to DNA occurs through spontaneous chemical reactions that happen over time in the presence of water, heat, acidic environments, or various combinations of each. Strand breaks, abasic sites, and deamination are the common damage types that accumulate through hydrolytic mechanisms. The deamination of DNA bases occurs more frequently in pyrimidines than in purines, but both types are equally mutagenic (Mol et al., 1999). In this study, a heat treatment combined with an acid buffer was used to induce hydrolytic damage to DNA within a short experimental time.

3.3.9.1 Heat/acid Buffer

The heat/acid damage treatments were applied to a gradient (0.01 M, 0.05 M, 0.1 M, 0.2 M, 0.3 M, 0.4 M, and 0.5 M) of trehalose solutions composed of DNA, ultrapure water, acid buffer solution, and 1 M trehalose.

Following the method of Nakamura & Swenberg (1999), an acid buffer solution was prepared consisting of 10 mM sodium citrate, 10 mM NaH_2PO_4, and 10 mM NaCl at pH 5.0. Template DNA (approximately 0.5 µg) was placed in a 1.5 mL microcentrifuge tube and dried down in a SpeedVac. The DNA was dissolved in 50 µL of the acid buffer, followed by addition of 50 µL of varying trehalose/ddH_2O mixtures (of 2× final trehalose concentration); the samples were then vortexed for 30 s and centrifuged briefly. The samples were incubated at 70°C, with mixing at 500 rpm, for various lengths of time (Eppendorf thermomixer). Once incubation was completed, the samples were immediately placed on ice to slow the reaction until they could be purified. Once cooled, the samples were then purified via ethanol precipitation with a 75% EtOH wash included to remove any salts, the DNA was then redissolved in 50 µL ddH_2O. A temperature/time control containing sample and 100 µL of ddH_2O was run alongside the samples for the maximum reaction time to ensure results were from the damaging agent and that neither time nor temperature were factors. A negative control containing only acid buffer was also run for the maximum reaction time.

3.4 Results

3.4.1 DNase

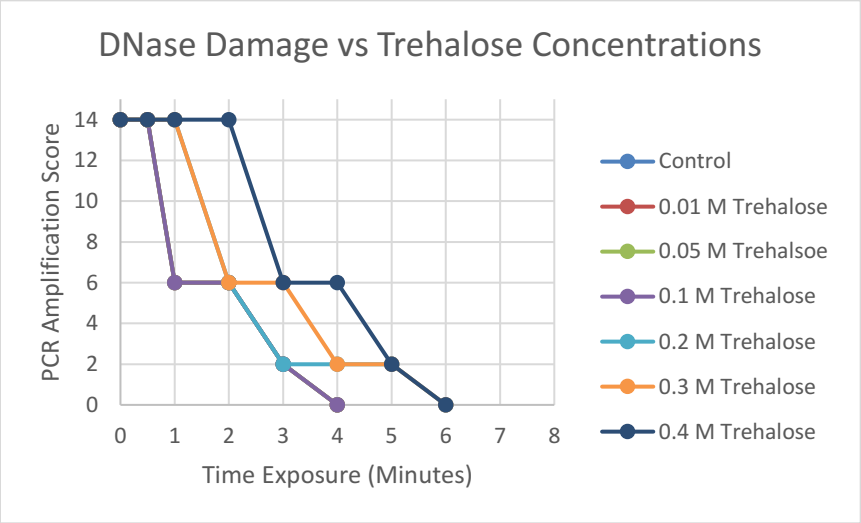

Figure 18: DNase Treatments vs Trehalose Concentration over Time

The PCR amplification score of DNA samples in a 0.01 M, 0.05 M, 0.1 M, 0.2 M, 0.3 M, and 0.4 M trehalose concentration gradient over a DNase exposure time of 0–8 min.

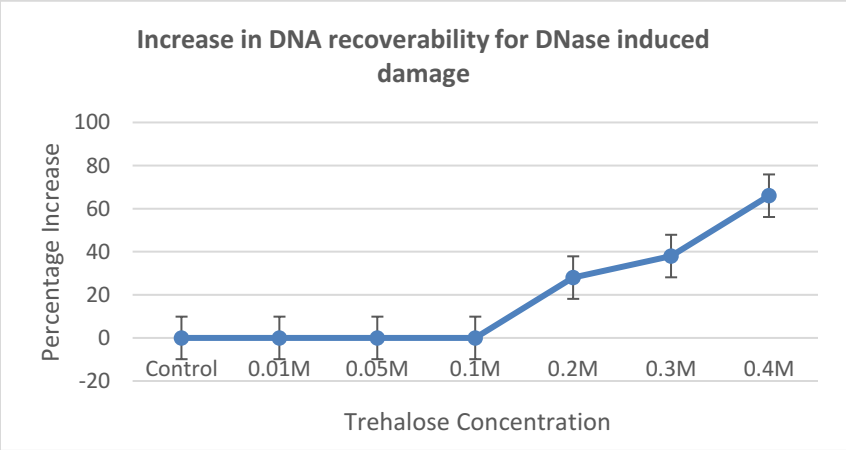

Figure 19: Trehalose Efficiency vs Enzymatic Damage

Efficiency of trehalose concentrations against control samples. PCR scores of concentrations divided by PCR control score expressed as percentage change.

For the control sample and trehalose concentrations below 0.1 M, there was no difference between treatments with different DNase exposure intervals, which all failed PCR amplification in every case (Figure 18). For samples with trehalose concentrations of 0.1 M, amplicon size consistently dropped from 800 bp at 30 sec to only 230 bp after 3 min of exposure, with PCR failure occurring at the 4 min exposure time. The 0.3 M and 0.4 M trehalose solutions were both able to maintain recoverable 800 bp amplicons to one- and two-minute exposure times, respectively; a treatment duration two and four times longer than for the lower concentration (0.1 M) and control solutions, respectively. At the highest trehalose concentrations (0.2 M and above), the ability to obtain PCR amplicons increased by at least 29% but only the smallest amplicon could be amplified at the 5 min time point. The 0.1 M trehalose samples failed to consistently amplify after exposure for four minutes, while the 0.2 M, 0.3 M, and 0.4 M trehalose samples completely failed to amplify after a 6 min exposure. There was a step-like correlation between trehalose concentration and PCR score with increasing exposure time, and in amplifiability of the DNA recovered after damage treatments.

Figure 19 shows that there was no recoverability of amplifiable DNA up to a trehalose concentration of 0.1 M, but at 0.2 M concentration this increased by 29%. The next highest concentration of 0.3 M gave an additional 10% increase in amplicon recoverability, with an additional 28% recovery in PCR efficiency when the trehalose concentration was increased to 0.4 M.

3.4.2 Oxidation

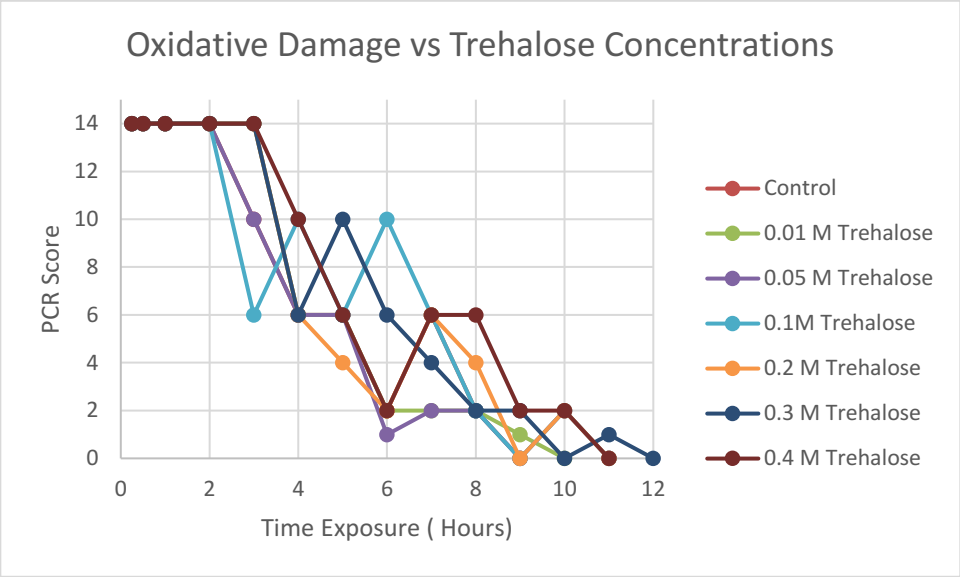

Figure 20: Oxidative Damage Treatments vs Trehalose Concentration over Time.

Trehalose concentrations and exposure times to oxidative induced damage. All concentrations have a sharp decline with the highest 0.4 M and 0.3 M having the greatest protective ability in the 10 to 12 hour range.

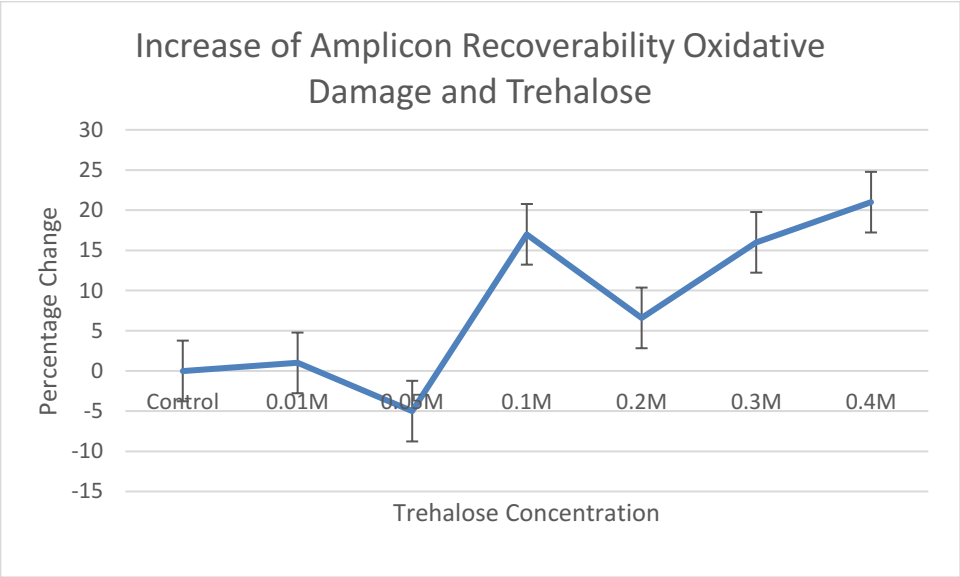

Figure 21: Trehalose Efficiency vs Oxidative Damage

Efficiency of trehalose concentrations against control samples. PCR scores of concentrations divided by PCR control score expressed as percentage change.

The PCR amplification score was measured for samples where oxidative damage had been induced, over a trehalose concentration gradient. Figure 20 shows the results for the solutions of DNA and H_2O_2 that were incubated at 37°C from 1–12 h. The control sample, and the 0.01 M and 0.05 M samples, all failed amplification completely after 9 h of exposure. At 0.1 M trehalose, variable results were obtained for H_2O_2 exposures of 3–6 h, but the 425 bp amplicon was the longest one recoverable, and beyond 6 h, only the 230 bp fragment could be amplified. The 0.2 M trehalose samples failed to consistently amplify beyond the 9 h time point. For the 0.3 M trehalose samples, this occurred after 10 h, and for the 0.4 M trehalose samples, amplification failure occurred at 11 h.

Only the higher concentrations of trehalose inhibited oxidative damage, with a 15% increase in recoverability, on average, over the range 0.1–0.4 M (Figure 21). For the highest trehalose concentration of 0.4 M, there was a 21% increase in recovery relative to the control sample. All conditions displayed a large decline in amplicon size after 2 h, indicating an accumulation of DNA damage. Despite failing amplification at 10 h exposure, the 0.3 M trehalose samples showed partial amplification at 11 h, with the 230 bp amplicons being recovered in one of the duplicate reactions.

3.4.3 Acid / Heat

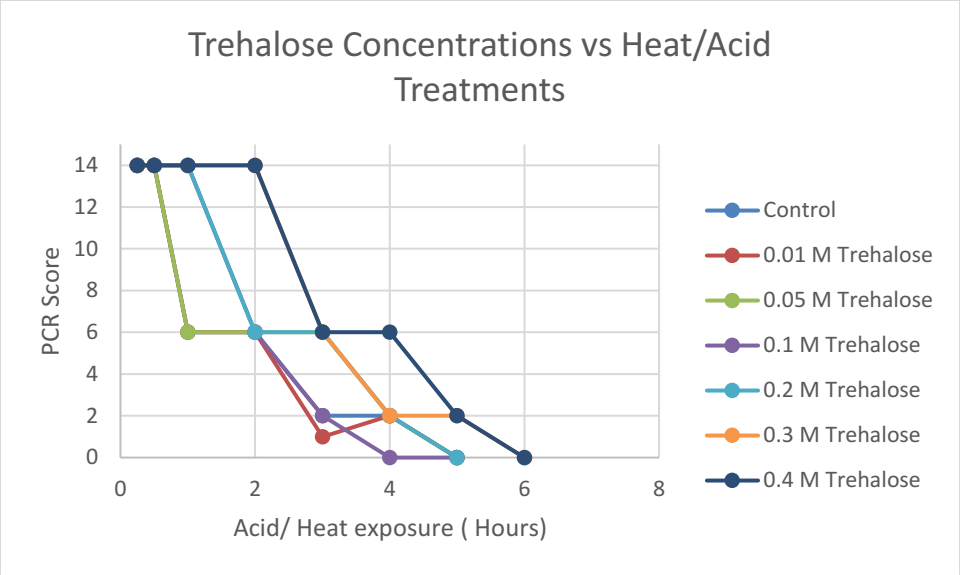

Figure 22: Graph of PCR Results over Time with Acid/Heat for Different Trehalose Concentrations

Trehalose and DNA solutions exposed to hydrolytic damage via heat acid treatments. The control up to the 0.1 M concentrations had very low protective ability or variation. 0.1 M to 0.3M concentrations showed stairstep increases in protective ability with each 0.1 M increase.

After damage was induced by acid and heat, the PCR amplification score was again measured over a trehalose concentration gradient (Figure 22). The 0.05 M and 0.1 M trehalose solution showed declining PCR score with time, with amplification failing completely after a 4 h exposure. The control sample also failed amplification at 4 h. In comparison, the 0.2 M, 0.3 M, and 0.4 M samples solutions all failed to amplify at 6 h exposure.

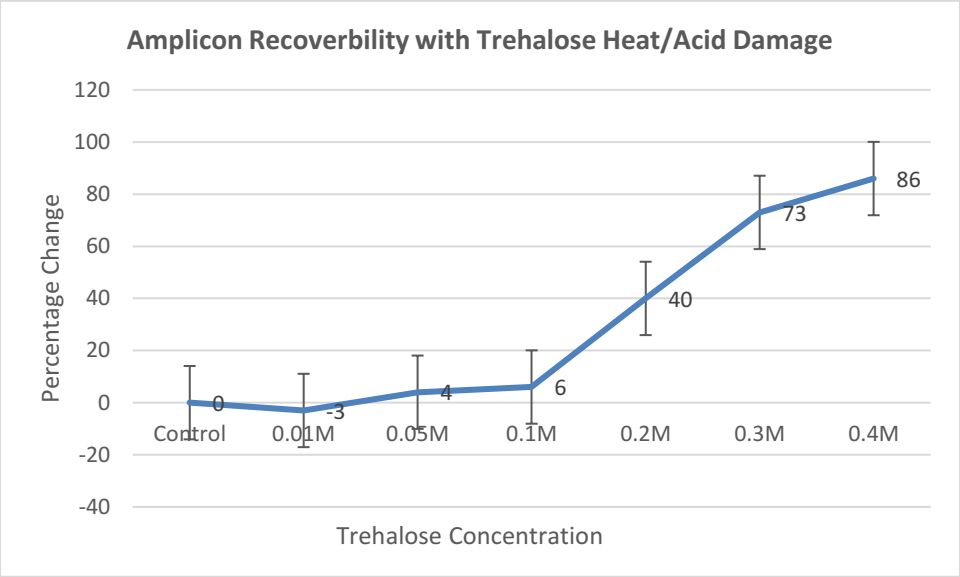

Figure 23: Trehalose Efficiency vs Hydrolytic Damage

Efficiency of trehalose concentrations against control samples. PCR scores of concentrations divided by PCR control score expressed as percentage change.

There was no real increase in efficiency with trehalose concentrations of 0.1 M or below, with the trendline virtually static until the 0.2 M concentration where it increased 34% relative to the 0.1 M samples. The 0.3 M concentration then increased in efficiency by another 33%, after which the trendline then begins to approach a plateau with the 0.4 M concentration only producing an additional increase of 13%. Between 0.1 M and 0.4 M trehalose, there was an overall 80% increase in efficiency for PCR recoverability, over the untreated DNA control, under conditions of hydrolytic damage.

.

3.5 Discussion

Trehalose can efficiently protect DNA from fragmentation during desiccation, freeze drying, and osmotic pressure changes by supporting the macrostructures within the cell and the nucleic acid structures themselves (Hussain et al., 2016). This is beneficial because fragmentation is one of the major problems associated with DNA preservation over time, and is a major obstacle to the recovery of older samples. The genetic information loses relevance when

the sequence becomes unreadable, as the fragments become too small to amplify and lose context within the macromolecule (Klingström et al., 2018). Recent advances in recovering and reading small fragmented sequences, from sources such as ancient DNA samples, are a direct result of advanced sequencing improvements, which allows these smaller fragments to be analyzed and pieced together (Arriola et al., 2020; Knapp & Hofreiter, 2010).

The main protective function of trehalose is to act as a blocking agent to physically wrap around the DNA and enter a glassy state, thereby providing a physical barrier. This ability has been well studied. In aqueous solution, the protective shell formed by trehalose will displace solvating water molecules and can therefore protect the DNA against various damaging mechanisms, such as hydrolytic reactions. This protective ability is directly proportional to trehalose concentration.

Without a chelator like EDTA to directly inhibit nuclease ability (Barra et al., 2015), the ability of trehalose to protect from enzymatic damage is restricted to it forming a physical barrier and blocking access to the DNA. The amount of trehalose needed to achieve a suitable level of inhibition of enzymatic damage is far greater in solution than in a frozen or dried state, where the molecule is in a glassy state (Smith et al., 2005). Nucleases can attack the DNA molecule in an aqueous environment but are inhibited, though a combination of viscosity and physical competition for vulnerable sites on the DNA, as trehalose concentration rises. These extreme molarity requirements may inhibit downstream analysis by affecting concentrations in the PCR, necessitating an additional purification step to remove the trehalose before amplification or sequencing.

The ability of trehalose to protect against oxidative damage was significant in this study, with the higher molar concentrations allowing an approximately 30% increase in recoverability of amplifiable DNA. These higher concentrations also gave the ability to recover larger amplicons over longer exposures to oxidative stress than the control. This indicates a reduction in base modifications by ROS that can prevent amplification by functioning as, or turning into, blocking lesions (Santos et al., 2002). Again, this is assumed in part to be due to physical competition and displacement of water molecules from the hydration shell around the DNA. Additionally, the ability of trehalose at higher concentrations ability to directly scavenge ROS

and outcompete H_2O_2 likely contributed, and this is well documented in living organisms (Luo et al., 2008). Similarly to what was seen in the damage experiments, the ability to scavenge ROS is directly correlated with the concentration of trehalose in living cells (Wang et al., 2018).

Trehalose showed moderate protective abilities against acid and heat damage that was used to induce strand breaks in the DNA. This effect was only significant at the highest concentrations (0.2 M and above), which showed an increase in preservation ability, but no concentration offered significant protection as both the frequency of amplification success, and the size of recoverable amplicon (indicating DNA quality) diminished with time, reaching zero after six hours' exposure. The ability of the higher concentrations to impart some protection to the DNA likely reflects the ability of trehalose physical displacement of water molecules when the concentration of solute is high, and allowing the DNA to remain stable at high temperatures (Matros et al., 2015).

The main protective ability of trehalose, outside of the glassy states, appears to be significant protection from oxidative damage. If this ability was combined with a chelator of divalent metal ions to suppress nuclease activity, significant protection from enzymatic attack of the DNA backbone would be provided. Hydrolytic, temperature, and pH-induced damage remain major obstacles to preserving DNA damage while using trehalose alone as a protective agent for DNA storage at normal concentrations. It is effective at millimolar concentrations when combined with desiccation and/or freezing (Hara et al., 2017). In the dried state, DNA fragmentation was reduced, possibly by substituting for water molecules in the hydration shell around the DNA strand. This keeps more of the DNA in its B-form, which is more flexible and less prone to fragmentation (Al-Badry et al., 2018). However, substantially higher trehalose concentrations are required to achieve significant protective results in solution (Hara et al., 2017), as is evident from the results of this work.

The concentrations of trehalose needed to achieve substantial protection of DNA in a room temperature liquid buffer are unsuitable for routine shipping and processing. The high molar concentration needed will inhibit downstream reactions, necessitating additional purification steps that can in turn lead to additional damage and sample loss. Overall, trehalose is an effective preservative that helps reduce damage to DNA from various damaging agents and

mechanisms, but is unsuitable as a standalone preservative/protectant. Trehalose has the potential to complement the action of a range of other preservative agents, and could thus be an important component in a complementary blend of preservatives.

Chapter 4: Evaluating Commercial DNA Preservation Products Against Common Damage Types

4.1 Abstract

There are many commercial DNA preservation products on the market that the manufacturers claim will prevent sample degradation and preserve DNA quality over a range of environmental conditions. These products are also claim to offer DNA preservation at room temperature, or over the long term. In this study, a number of these products—FTA Elute Cards, DNAstable, DNAgard, Biomeme's DNA/RNA Preservation Buffer, and DNA Shield—were all evaluated against trehalose, a common laboratory preservative, to test their efficiency. DNA samples were treated with the commercial preservative solutions and then subjected to DNA damage-inducing experimental conditions to induce acid hydrolysis, oxidative damage, or enzymatic damage, as were used previously in evaluating trehalose. DNA Shield showed the most effective protection overall and was especially effective against oxidative damage with a 60% increase in recoverability. DNAgard and DNAstable both displayed significant protection under all three experimentally induced damage conditions. For enzymatic damage DNAstable increased recoverability by 141% while DNAgard was the best at protecting against hydrolytic damage with an increase of 193%, in comparison to the control sample. Biomeme's DNA preservative and trehalose performed well overall, but the protection offered by these two agents was considerably less than for DNAgard, DNAstable, and DNA Shield. Results for the FTA Elute Cards were poor, but this was thought be more due to a problem with DNA elution than being directly related to the product's protective abilities. All of the products tested would be suitable for short-term storage or shipping; however, as they just slowed the rate of damage rather than halting it, none of them should be regarded as suitable solutions for effective long-term DNA storage.

4.2 Introduction

Long-term preservation of DNA samples has become an important priority for a variety of fields, agencies, and industries in many locations and under different conditions. As an understanding of "long-term DNA stability" might vary according to perspective, the time frame must first be defined. At one end of the spectrum, for pharmaceutical applications, two years may be considered an adequate time frame for DNA stability (Anchordoquy et al., 2007). Conversely, in evolutionary biology, the time frame for long-term DNA stability may be millions of years (Bailleul et al., 2021). In this study, we consider long-term storage to represent a multidecadal time frame, since this is consistent with what many medical and biorepository facilities consider as the long term (Lou et al., 2014). Many commercial products that were originally formulated for shipping and short-term storage are now being used by default for multiyear and multidecadal storage purposes, yet their long-term efficacy remains to be fully evaluated.

The ability to ship, store, and analyze DNA samples with minimal processing under different environmental conditions—and without significant quality or quantity loss—has become a growing challenge. DNA samples are often shipped to a central processing laboratory, or stored in different locations, creating another layer of difficulty in maintaining the integrity of the DNA throughout collection, storage, and final analysis. There are many commercially available DNA preservation solutions, which all claim to have significant preservative qualities relative to untreated samples, under non-extreme environmental conditions. Claims vary depending on the type of sample being stored; for example, whether the sample is extracted, or if the DNA is in a biological matrix, contained in a specimen like semen, blood, or saliva. Most studies evaluating the efficiency of these protectants have used accelerated heat experiments to damage the DNA and then measure preservative performance against untreated DNA samples, extrapolating the results far into the future (Frippet et al., 2010; Grey et al., 2012; Howlett et al., 2013; Hyde et al., 2020; Silva et al., 2020; Wolfgramm et al., 2003).

The exact formulations of many commercial products are proprietary, but they typically include a mixture of disaccharides, chelators, and buffers, all of which confer varying degrees of protection against common damaging agents, in a concentration-dependent fashion (Frantzen et al., 1998; Knebelsberger et al., 2012; Ohtake et al., 2011; Sharpe et al., 2020). Such products do

not explicitly list their protective efficiencies against specific damage types or environmental conditions, but provide a general range, with ambiguous definitions of environmental conditions, such as room temperature, frozen, or "non-extreme" conditions. In this study, we evaluated a panel of these products for protection of extracted/purified DNA against specific damage types, and using PCR, measured the ability of each test product to mitigate specific damage types over selected time intervals. The commercial products chosen were FTA Elute Cards, DNAstable, DNAgard, Biomeme's DNA/RNA Preservation Buffer, and DNA Shield. All of the commercial products tested did not list their efficiencies in mitigating each damage type, but made general claims regarding preservation, under general environmental conditions such as room temperature or "non-extreme" conditions. As controls, we used 0.4 M trehalose samples together with untreated DNA samples (in TE buffer, a standard laboratory buffer), to evaluate the claims made for each commercial product.

4.2.1 FTA Elute Cards

The FTA Elute Card, a filter paper product manufactured by GE Healthcare, was developed for biological fluids and their transport but this original usage has been extended to application as a long-term storage medium for nucleic acids. The product consists of a special type of filter paper impregnated with a proprietary formula, containing reagents that promote cell lysis and protein denaturation with subsequent release of nucleic acids that are entrapped within the matrix of the card and stabilized at room temperature. These features are thought to allow the product to be used for long-term DNA storage.

Over time, variations and competitor products of the FTA card have been developed, all of which aim to optimize the formulation for different sample types. Comparable products essentially contain the same core formulation, but with varying reagent concentrations and add-on features. The purported efficiency of these products for DNA storage and recovery has been well documented, and claims of storage for decades with little degradation can be found in the literature (Peluso et al., 2015; Rahikainen et al., 2016; Saieg et al., 2012). However, variable sample recovery has been reported. This relates to the problem of unbinding the DNA from the card matrix, which can cause deterioration in sample quality due to overprocessing (Siegel et al.,

2017). Some of the reported variability may also reflect differences in the storage conditions used, and an ability of the FTA cards to protect from certain damage mechanisms but not others (Harrel et al., 2021). Full manufacturer information can be found in Appendix B.

4.2.3 DNAstable

DNAstable is a storage medium that preserves genomic DNA, plasmids, bacterial artificial chromosomes (BACs), PCR products, and oligonucleotides at room temperature. DNAstable allows for long-term stabilization of DNA samples, with straightforward sample recovery by simple addition of water. Each tube or plate contains DNAstable provided as a coating at the bottom of the tube or well, which protects picogram to microgram quantities of DNA. The product is formulated so that upon application of liquid samples, the matrix dissolves and forms a protective coating around the DNA. The sample must then be completely dried for maximum protection and stability for storage at ambient temperatures (Howlett et al., 2013). Manufacturer information can again be found in Appendix B.

4.2.4 DNA Shield

DNA/RNA Shield is a DNA and RNA transport and storage medium for any biological sample. The product is claimed to preserve the genetic integrity and expression profiles of samples at ambient temperatures, and to completely inactivate infectious agents. Nucleic acids from samples maintained in this transport and storage medium can be isolated directly, using a suitable nucleic acid purification kit, without the need for precipitation or reagent removal (Bundgaard-Nielsen et al., 2018). As with the other products, manufacturer information is provided in Appendix B.

4.2.5 DNAgard

DNAgard Tissue is a DNA storage product based on Biomatrica's proprietary SampleMatrix technology. The product is claimed to stabilize and protect biological materials at room temperature without degradation. Reportedly, the SampleMatrix technology "was designed by combining extremophile biology that enables long-term survival of organisms in extremely

dry environments, with synthetic chemistry," most likely indicating that the product is based on a chemically-modified biomaterial. DNAgard is designed for immediate stabilization of DNA from intact cells and tissues with the convenience of shipping, processing, and storage at room temperature. The product, supplied as a liquid storage reagent, is reported to rapidly permeate cell membranes to stabilize and protect genomic DNA (Sigma-Aldrich, 2021). Manufacturer information can again be found in Appendix B.

4.2.6 Biomeme's DNA/RNA Preservation Buffer

Biomeme's DNA/RNA Preservation Buffer is used to collect and maintain samples during transport and before molecular analysis. When used to preserve and transport specimens in the field, this buffer is claimed to display significant preservative qualities relative to untreated samples, while transporting at room temperature. It has shown protective qualities when used as a storage medium in the short- to medium-term (Camacho-Sanchez et al., 2013; Hyde et al., 2020), and as for the other products, manufacturer information is included in Appendix B.

4.3 Materials and Methods

The samples were extracted with 400 µL extraction buffer, as specified in Chapters 2 & 3, in 2 mL microcentrifuge tubes with a 3 h incubation at 56°C and 350 rpm agitation on a thermomixer (Eppendorf, Thermomixer R). This was followed by a guanidium thiocyanate/silica purification and overnight drying, as detailed previously. Samples were taken up in 50 µL of ultrapure water (ultrapure RNase/DNase free distilled water, Invitrogen #10977-23), then the purified extracts pooled and diluted to a concentration of 50 ng/µL in ultrapure water and aliquoted (50 µL) into individual 1.5 mL microcentrifuge tubes. The DNAstable aliquots were further diluted to a concentration of 10 ng/µL. Samples were then dried back down in forensic biosafety cabinets (AirClean Systems, DrySafe Forensic Evidence Drying Cabinet Model 300) at 28°C. The individual buffers were re-added, as appropriate, up to a volume of 50 µL and the mixtures vortexed for 1 min.

4.3.1 DNA Damage

The same damage protocols outlined in Chapter 3 were replicated in experiments for Chapter 4, with slight modifications. The modifications included punching of the FTA card, and

the punched card was used in all the damage protocols prior to PCR and added directly to PCR reactions, alongside an untreated punched card that acted as a control.

4.3.2 Purification

QIAquick columns (Qiagen, QIAquick PCR Purification Kit (50), catalogue # 28104) were used to purify DNA by removing buffers after treatments, as the buffers could affect downstream PCR. The necessary buffer solutions were supplied with the columns. Five volumes of PB Buffer were added to the sample to be purified, which was briefly vortexed before being transferred by pipette to the center of the column membrane. The column was then centrifuged for 1 min at 17,900 g. The eluate was discarded. A volume of 750 µL of PE Buffer was pipetted into the column, which was again centrifuged for 1 min at 17,900 *g*, and the eluate again discarded. The column was transferred to a sterile 1.5 mL microcentrifuge tube and 50 µL of sterile ddH_2O was added to center of the column membrane. The column was then incubated for 1 min at room temperature (18°C) and centrifuged at 17,900 *g* for 1 min to elute the DNA.

The acid buffer samples were allowed to cool to room temperature, then purified via ethanol precipitation and dissolved in 50 µL ddH_2O. All purified samples were used immediately in PCR amplification experiments.

Qubit Fluorometer Quantification

The Qubit fluorometric system was again used for DNA quantification, for the reasons already outlined in Chapters 2 & 3. As before, the Qubit dsDNA HS (high sensitivity) assay kit (Lumiprobe, QuDye dsDNA HS assay kit, catalogue # 531020) was used in conjunction with the Qubit Fluorometer (Thermo Fisher, Qubit Flex Fluorometer, catalogue # Q33327), since this approach allows specifically for the measurement of dsDNA, over a wide dynamic range as already discussed. The Quant-iT working solutions were prepared analogously to the previous examples, as per Table 7. All tubes were vortexed for 2–3 s, then incubated for 2 min at room temperature, out of direct light. Samples were inserted into the Qubit Quantmeter, a 5 s wait period was permitted, and then a nucleic acid concentration measurement was given in ng/µL.

Table 7: Qubit Standards/Working Solutions

Working solution volumes and total tube volumes, for standards and samples used for DNA quantification using the Qubit quantometer.

	Standards	**Samples**
Working Solution	190 µL	180–199 µL
Standard	10 µL	–
Sample	–	1–20 µL
Total Volume per Tube	200 µL	200 µL

4.3.3 FTA Card

Using a small glass transfer pipette, 1 µg of DNA immediately after purification in solution was deposited slowly onto a 6 mm circle drawn on each FTA Elute Card (Qiagen, catalogue # WB120206). After drying, the FTA card was punched (Harris Micro-Punch 3 mm punching device, GE Healthcare Life Sciences) to make four punches from the circle (GE Healthcare, 2013). A total of 30 FTA Elute Cards were used, with four punches per card. The punches were removed and transferred to clean 1.5 mL tubes for damage experiments. The manufacturer's protocol was followed, as described in Appendix B, before undergoing a final QIAquick spin column purification and concentration to remove any residual damage buffers and to concentrate the DNA. In other words, the card punches had to undergo an elution wash after they were exposed to the damage experiments, but the amount of DNA recovered from each punch was significantly lower than the initial deposition by between 30–40% percent for the majority of the samples. The acid buffer treated samples were purified, after cooling, via ethanol precipitation with a 75% EtOH wash followed by resuspension in 50 µL ddH_2O.

4.3.4 DNAstable

A 50 µL aliquot of DNA solution in water, at 10 ng/µL, was slowly added to the center of each sample tube, giving a total amount of 0.5 µg DNA per tube. The tubes were then dried in a laminar flow hood, as per the manufacturer's protocol, for 28 h until completely dry. For the hydrolytic damage samples, the 100 µL acid buffer was added directly to the tubes without

agitation and heated for the time intervals indicated. For all treatments, negative control tubes were used that contained only water and DNAstable, while positive control tubes contained DNA extract in water with DNAstable.

4.3.5 DNA Shield

The manufacturer's protocol requires a 9× volume of buffer relative to DNA extract. As such, 10 µL of DNA, at a concentration of 50 ng/µL, was added to 90ul of DNA Shield solution then dried down keep the total amount of DNA in each tube at 0.5 µg. One tube for each treatment for each interval contained only water and DNA Shield as a negative control, while one had DNA extract in water, with DNA Shield, with no damaging-induing buffer as a positive control.

4.3.6 DNAgard

A volume of 10 µL of DNA sample at 50 ng/µL was added to each 1.5 mL tube to provide a total of 0.5 µg DNA per tube. As per the manufacturer's protocol, 100 µL of DNAgard was added to the tube. One tube for each treatment contained only water and DNAgard as a negative control, while one had extracted DNA in water with DNAgard but no acid buffer, as a positive control.

4.3.7 Biomeme's DNA/RNA Preservation Buffer

There is no standard protocol for Biomeme's buffer, with the only specification being that the sample should be fully submerged. As such, the protocol used for DNAgard was applied, with the same controls.

4.3.8 Controls

4.3.8. Positive Controls

Figure 24 shows the successful 800bp amplicon PCR optimized with primers without damage treatments

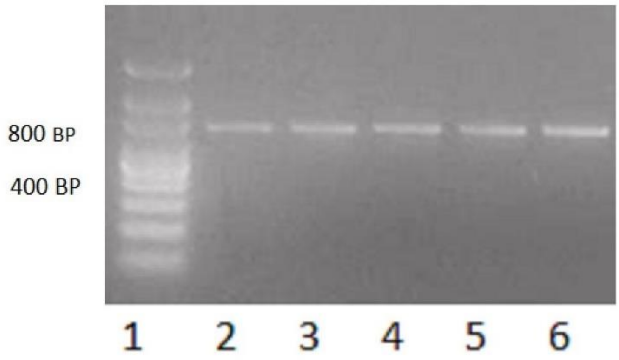

Figure 24: Positive Controls for Commercial Preservation Products
Lane 1: 100 bp ladder; lane 2: FTA Elute Card positive control; lane 3: DNAstable positive control; lane 4: DNAgard positive control; lane 5: Biomeme DNA/RNA Preservation Buffer positive control; lane 6: DNA Shield positive control.

4.3.8.1 DNase Treatment

For each commercial product, positive controls were run where the DNA sample was present but not subjected to the DNase treatment. Samples containing only water for each product (i.e., with no DNA) were run as a negative control. An aliquot of 2 µL was removed at each time interval and used in a PCR reaction. All positive controls successfully gave the longest 800 bp amplicon at every time interval, and all negative controls showed no amplification.

4.3.8.2 Oxidative Damage

Positive controls were run with each commercial product, where the DNA sample was present but was not subjected to the hydrogen peroxide treatment. Samples with only water (no DNA) were also run for each product, as a negative control. A 2 µL aliquot of sample was removed at each time interval and run in a PCR reaction. Again, all positive controls showed the 800 bp amplicon at every time interval, and all negative controls showed no amplification.

4.3.8.3 Hydrolytic Damage (Acid/Heat)

Positive controls were run for each commercial product, where the DNA sample was present and was subjected to only the heat treatment (without acid buffer). The positive controls were run alongside the acid heat buffer treatments. Samples containing only water (no DNA) were also

run for each product as a negative control. An aliquot of 2 µL was taken from each sample at each time interval, and run in a PCR reaction, with all positive controls showing the longest 800 bp amplicons at every time interval, and all negative controls showing no amplification. For purification from the acid buffer, the samples were purified via ethanol precipitation, once cooled, and redissolved in 50 µL ddH_2O. Purified samples were used immediately in PCR amplifications.

4.3.9 DNA Amplification

Thermostable DNA polymerase from *Taq* was used to amplify DNA samples after extraction and purification. Standard reactions were performed in 25 µL volume in 0.2mL thin-walled tubes using mitochondrial DNA primers (Table 8) for the same three amplicons as in previous examples. All reaction mixtures were prepared on ice. The PCR reaction conditions, after optimization, consisted of: 200 µM dNTPs, 0.2 µM of each primer, 1.0 mM $MgCl_2$, 1× PCR buffer (750 mM Tris–HCl pH 8.8, 200 mM $(NH_4)_2SO_4$, 0.1% Tween-20), 0.5 U *Taq* DNA Polymerase, and 50 ng of DNA template. The remaining volume was made up to 25 µL using ddH_2O. Tubes were vortexed, spun down, and placed in a 96-well Gradient Mastercycler (Eppendorf).

Table 8: Primers

Mitochondrial DNA primers used during PCR to amplify sequences for DNA damage assessment on DNA storage samples. All forward and reverse primers used were authenticated by Lehto (2012).

Primer	Sequence	Amplicon
MtF16210	TTT TCT ATT TTT AAC CTT TAG GAC	800 bp
MtR408	CAG CAA TCA TCA ACC CTC AAC TAT	
Mt14724F	CGA AGC TTG ATA TGA AAA ACC ATC GTT G	425 bp
Mt15149R	AAA CTG GAG CCC TCA GAA TGA TAT TTG	
Mt16 190F	CCC ATG CCT ACA AGC AAG TA	230 bp
Mt16 420R	TGA TTT CAC GGA GGA TGG TG	

The cycling parameters included an initial denaturation at 94°C for 2 min followed by 30 cycles of 94°C for 30 s, 60°C for 1 min, and 72°C for 2 min. On completion, the reaction was placed at 4°C on hold. This PCR protocol was followed for all samples.

4.3.10 Electrophoresis protocol

PCR products were subjected to 2% agarose gel electrophoresis (AGE) with gels containing ethidium bromide (EtBr) for detection. One well was loaded with molecular marker (5 µL), and other wells with 3 µL of 6× loading buffer (Invitrogen) mixed with 5 µL sample. Gels were run for 30 min at 110 V in 1x TBE buffer. The gel was removed after it was run then viewed on a transilluminator under UV light (UVB wavelength) and photographed.

4.4 Results

4.4.1 Preservation

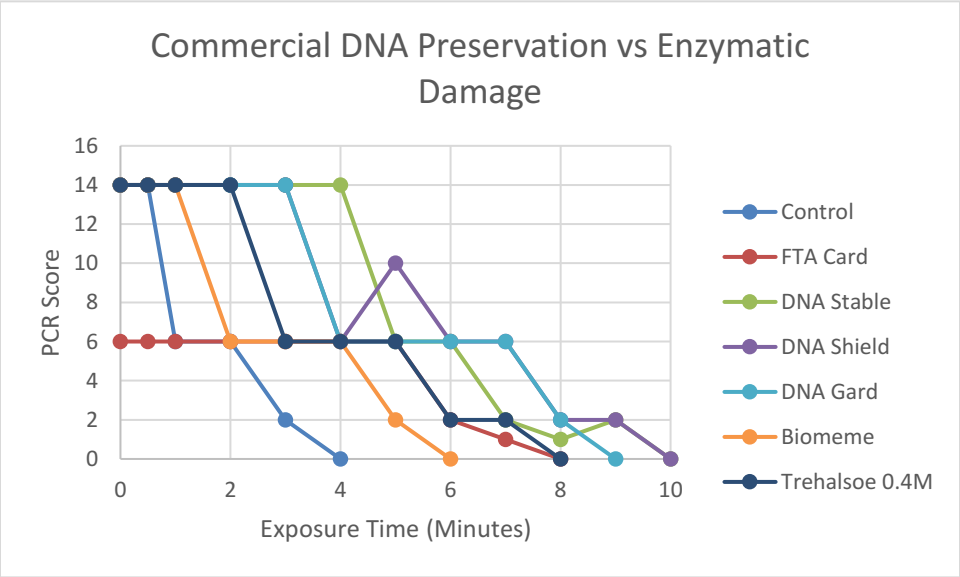

Figure 25: DNase Treatments over Time on Commercial DNA Preservatives.

PCR amplification scores, after induced enzymatic damage for a period of up to 10 min, for DNA samples stored using a range of commercial methods (FTA Elute Card, DNAstable, DNA Shield, DNAgard, Biomeme's solution) and 0.4 M trehalose.

Figure 25 shows that the DNA Shield sample produced a 230 bp amplicon after 9 min of DNase exposure, more than double the time at which this amplification failed for the control. Compared to the control, a larger amplicon was recovered for DNA Shield at every time point from

2 min onwards. DNA Shield was therefore very efficient at inhibiting enzymatic damage in this experiment. The next best performing preservatives were DNAstable and DNAgard, which performed relatively similarly, showing excellent inhibition or protection from enzymatic-induced DNA damage and enabling recovery of the smallest 230 bp for most of the duration of the experiment. Biomeme's DNA preservation solution showed a more modest ability to inhibit enzymatic damage, but was only 50% as effective compared to the top three preservatives. Trehalose, at a high concentration of 0.4 M, was comparable in performance to the commercial solutions and performed only slightly less effectively than the top three preservatives, while proving superior to the Biomeme product (Figure 26). The FTA Elute Card required an additional wash step and, from the start, mostly yielded smaller amplicons compared with the other methods. It was, however, able to produce amplicons comparable to 0.4 M trehalose for exposures of 3 min or longer.

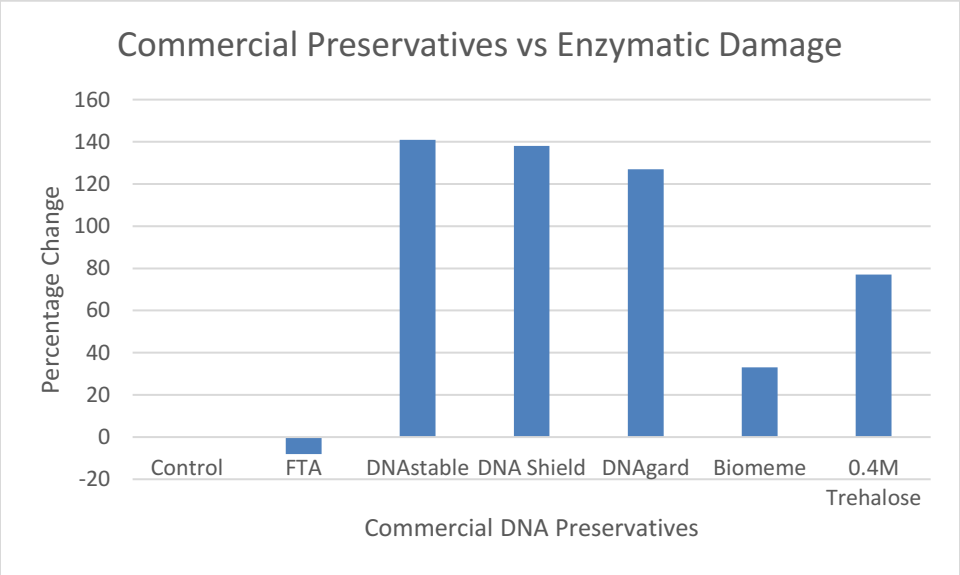

Figure 26: Commercial Preservatives vs Enzymatic Damage
Efficiency of commercial preservative concentrations against control samples. PCR scores of commercial preservative concentrations divided by PCR control score expressed as percentage change

Relative performance of DNA preservatives against DNase I degradation. DNAstable, DNA Shield, and DNAgard (Figure 26) all showed a large increase in protection against experimentally induced enzymatic

damage, with over 120% increase in recoverable DNA relative to control. Trehalose (0.4 M) also performed well, with a 77% increase in protective ability. Biomeme's preservative showed only a 33% increase in protection, with the FTA Elute Card proving ineffective and showing a small overall decline of 8% in protective ability.

4.4.2 Oxidation

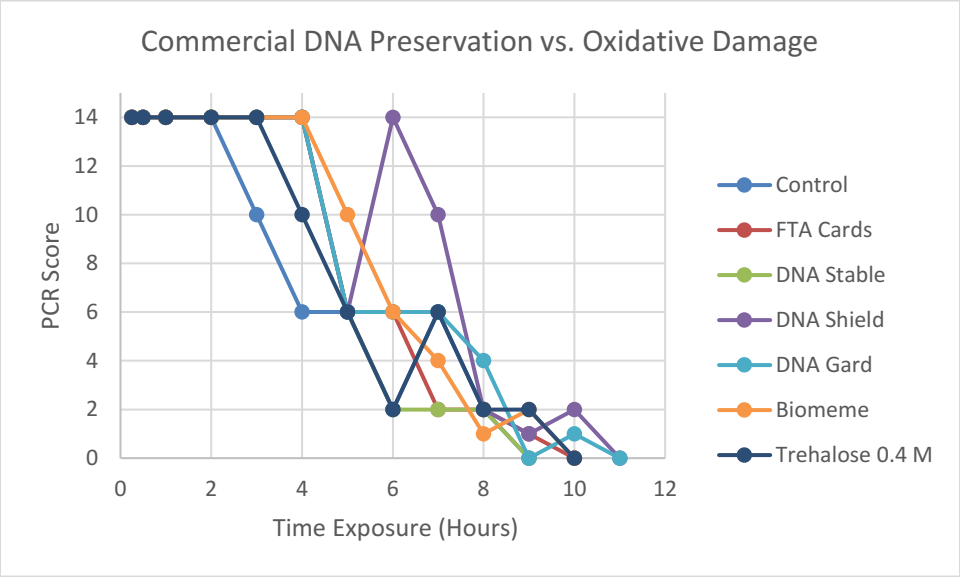

Figure 27: Oxidative Damage Results of Commercial DNA Preservatives.
The PCR amplification score of DNA samples—stored using a range of commercial methods (FTA Elute Card, DNAstable, DNA Shield, DNAgard, Biomeme's solution), and 0.4 M trehalose—after oxidative damage exposure over a 12 h period.

In oxidative damage experiments, DNA Shield again showed the best ability to protect against damage than the other methods tested. A larger amplicon (800 bp) was recovered at the 6 h time point than for any of the other preservatives, but all preservation methods displayed a continual step-down pattern in amplicon size and recoverability that sat within a narrow range (Figure 27). Specifically, Figure 27 shows that: the control sample had full amplicon recovery until 2 h of exposure, declining to complete PCR failure at 9 h; the FTA Elute Card retained large amplicon recovery for 4 h with PCR failure occurring at 10 h; DNAstable showed large amplicon recovery up until 4 h of exposure and PCR failure at 9 h; DNA Shield showed large

amplicon recovery at 6 h and PCR failure at 11 h; DNAgard displayed large amplicon recovery up until 4 h and variable performance until eventual PCR failure at 11 h; Biomeme's preservative solution was able to retain large amplicon up until the 4 h time point with PCR failure after 10 h; and, finally, 0.4 M trehalose showed large amplicon recovery at 3 h, with PCR failure occurring after exposure for 10 h.

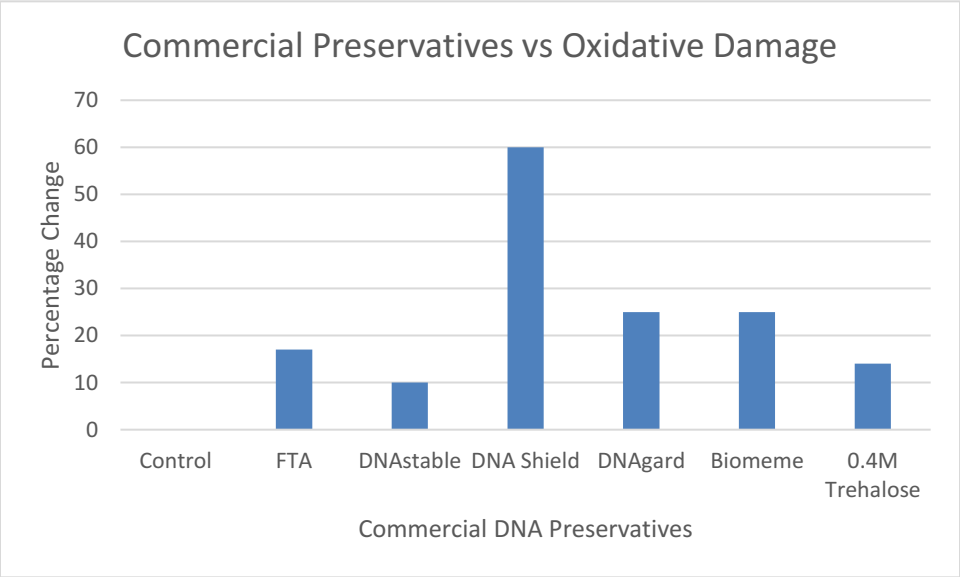

Figure 28: Commercial Preservatives vs Oxidative Damage
Efficiency of commercial preservative concentrations against control samples. PCR scores of commercial preservative concentrations divided by PCR control score expressed as percentage change

As shown in Figure 28, DNA Shield showed approximately a threefold increase in protection against oxidative damage in comparison to all the other preservatives. DNAstable, which performed relatively well in the hydrolytic and enzymatic damage experiments, was only slightly better than the untreated control in this case, and fell significantly short of the performance of all the other commercial products in protecting the DNA against oxidative damage.

4.4.3 Acid/Heat

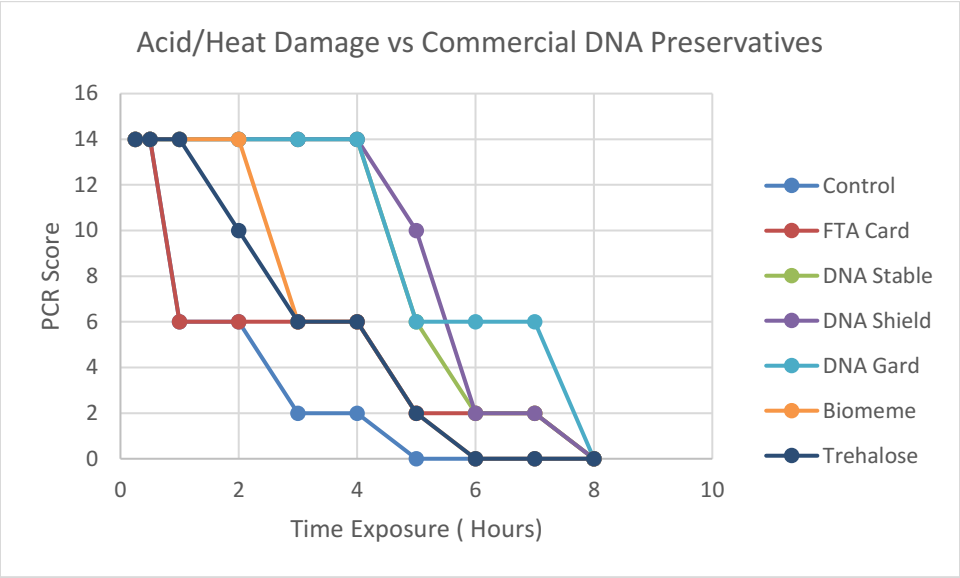

Figure 29: Acid/Heat Results of Commercial DNA Preservatives.

PCR amplification scores of DNA samples stored in a range of commercial methods (FTA Elute Card, DNAstable, DNA Shield, DNAgard, Biomeme's solution) and 0.4 M trehalose, with acid/heat exposure to induce hydrolytic damage over a 10 h period.

In the acid/heat experiments (Figure 29), DNAgard performed slightly better than DNA Shield and DNAstable but all three of these products showed a relatively similar protective capacity against the acid/heat treatment's ability to damage the DNA. Compared to the control, DNA Shield and DNAstable showed approximately 2× greater ability to mitigate this damage over time. FTA Elute Card punches and 0.4 M trehalose both showed notable damage inhibition, but to a much lesser extent than the top three commercial products (DNA Shield, DNAstable, and DNAgard). The FTA Elute Cards continued to suffer from lower size recoverable amplicons, almost from the outset, but offered some resistance to damage over significant exposure times, with complete PCR failure not occurring until 8 h. The Biomeme DNA preservation buffer offered the least protection among the commercial preservative solutions, performing little better than the FTA Elute Cards.

Specifically, Figure 29 shows that the control samples rapidly declined in DNA quality, with large amplicon recovery only retained for 1 h and PCR failure at 5 h. The FTA Elute Cards also showed large amplicon recovery at after 30 minutes but dropped after 1 hour, with PCR failure after exposure for 8 h. DNAstable, DNA Shield and DNAgard all permitted large amplicon recovery at the 4 h time point, with subsequent decline in DNA quality and PCR failure at 8 h. The Biomeme solution displayed large amplicon recovery at 2 h, and PCR failure at 6 h. Trehalose (0.4 M) was only able to maintain large amplicon recovery for 1 h, after which there was an essentially linear decline in DNA recoverability with complete PCR failure at 6 h.

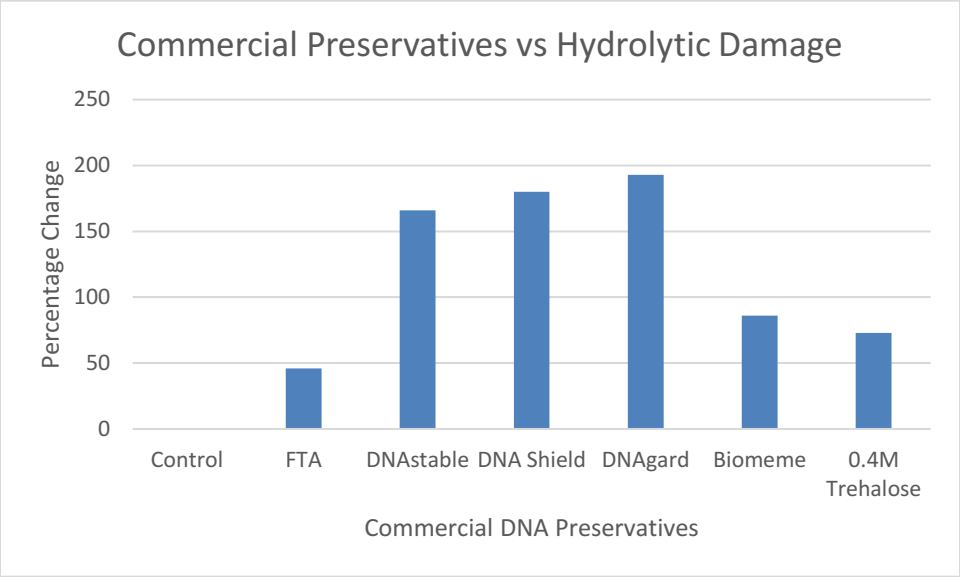

Figure 30: Commercial Preservatives vs Hydrolytic Damage
Efficiency of commercial preservative concentrations against control samples. PCR scores of commercial preservative concentrations divided by PCR control score expressed as percentage change

The overall effectiveness of the commercial DNA preservatives against experimentally induced hydrolytic damage is shown in Figure 30. All of the commercial products showed a substantial ability to protect the DNA from damage under these experimental conditions. DNAstable, DNA Shield, and DNAgard all showed approximately double the protection of the Biomeme preservative solution or 0.4M trehalose, and 3× more than the FTA Elute Cards.

Overall, whereas all of the commercial DNA preservation products demonstrated relatively poor protective capacity against oxidative damage, relative to control, they showed rather substantial increases in protective ability against acid/heat and enzymatic damage. The only exception was Biomeme's DNA preservation buffer, which performed poorly in the heat/acid experiment.

4.5 Discussion

The commercial preservatives all performed a protective/inhibitory role in all three damage experiments, with even the worst performer—the Biomeme product—able to double the exposure times over which viable DNA was retrievable in comparison with the control. These protective abilities were not distributed equally among damage types, and some variation was observed in the different products' ability to handle individual damage-inducing conditions. There were significant protective qualities and shielding from enzymatic damage, as well as significant protection overall from the heat/acid treatments, which induced hydrolytic damage. All of the products showed lower efficiency in protecting against oxidatively induced damage. Even the best performer, DNA Shield, was only slightly better than both the common trehalose additive in water or the TE buffer control.

Overall, DNA Shield had the greatest ability with regard to both consistently protecting the size of amplicons and recovering amplifiable DNA, across all three damage types. DNAgard was able to produce larger amplicons in the hydrolytic damage assay than DNA Shield, but underperformed against the other two damage categories. DNAstable and DNAgard both performed comparably, and proved only slightly inferior to DNA Shield overall. The FTA Elute Card showed consistent results; however, a significant problem was encountered with fully removing the DNA from the card (Siegel et al., 2017), and there was an initial loss in the DNA quantity recovered from the punches throughout all the experiments. Because of this initial drop, the product scored poorly even though its performance was consistent across all three experiments. The initial deposition of sample DNA, and therefore its recovery from individual punches, may have also been uneven. This, combined with the problematic elution step, most likely affected the quantity of DNA recovered, precluding an accurate assessment of the product's protection/preservation efficiency (Dentinger et al., 2010). These two factors make the

results for the FTA Elute Cards unreliable, and therefore this product cannot be accurately ranked for DNA preservation ability. One possible contributing factor is that the DNA became stuck in the fiber matrix of the card, as has previously been reported to be an issue (McClure et al., 2009).

The Biomeme preservative solution did confer some protection in all three damage experiments; however, it only fared slightly better than the control, which performed the worst overall. Trehalose actually performed the best overall relative to commercial products at high molarities in the enzymatic damage experiment but was overall was only moderately effective in relation to the other commercial preservatives. The addition of a suitable chelator to a trehalose solution would be expected to increase its efficiency (Brogna et al., 2021; Restrepo et al., 2019) in the enzymatic damage experiment, likely increasing its effectiveness against the commercial preservatives

4.6 Conclusions

The ability to inhibit enzymatic and hydrolytic damage to DNA, for room temperature shipping and short-term storage, is illustrated in the experimental data from this study and the results are consistent with current literature. In the long term, DNA stored in any of these formats will still show degradation since hydrolytic, oxidative, and enzymatic forms of damage will continue to accumulate over time. Of these damage types, oxidative damage could be a significant challenge for all the commercial preservatives examined as all samples displayed a relatively steady rate of accumulating damage, regardless of the commercial additive, under oxidizing conditions.

Dehydrating the DNA into a lyophilized state may offer similar preservative value to the commercial additives, in slowing or inhibiting damage mechanisms. The commercial preservatives often contain a mixture of a proprietary buffer, a chelator, and a polysaccharide-type substance, in an optimized ratio. Such preparations offer a convenient option, but an in-house blend could potentially achieve the same results with some trial, error, and optimization.

The poor performance of the FTA Elute Cards in this study is in large part due to the initial DNA drop that was experienced in recoverable DNA quantity, most likely due to the DNA being tightly bound within the card matrix and perhaps requiring more than one elution to release it

fully (Mas et al., 2007). The performance of the FTA cards, if the initial drop is allowed for, seems comparable to the other commercial methods, ranking in the middle of these methods overall (Table 10). It is therefore recommended that these cards be investigated further with different extraction methods, as experimental design flaws contributed to its poor overall performance in this study. Nonetheless, it still failed to provide superior protection over time against all three types of experimentally induced damage, compared to the other methods tested. Table 9 shows the overall ranking of the commercial preservatives, together with trehalose. Additionally, special acknowledgment is given to the manufacturers who graciously supplied free samples of their products for evaluation.

Table 9: Ranking of Commercial DNA Preservatives[a]

DNA Product	Enzymatic Damage	Oxidative Damage	Hydrolytic Damage	Overall Performance
FTA Card[b]	6	6	6	*
DNAstable	2	3	3	Third
DNA Shield	1	1	2	Best Overall
DNAgard	3	2	1	Second
Biomeme's DNA Preservation Buffer	5	5	4	Fifth
Trehalose 0.4 M	4	4	5	Fourth

[a]Ranking of commercial DNA products and buffers against three damage-inducing experimental conditions. DNA Shield performed the best overall.

[b]The FTA Card performed the worst in these experiments due to the initial DNA concentration loss in extraction, but overall, it did not have superior preservation qualities compared with the other methods tested.

Chapter 5: Dps as a DNA preservation medium

5.1 Abstract

Preservation of DNA over the long term presents significant challenges that have yet to be overcome. The prevalent methods—storing samples dry or at low temperature—still incur accumulating damage of various types over the long term. In this study, we propose a potentially new method of DNA storage using a prokaryotic Dps protein to form protein–DNA biocrystals that show significant protection from various damaging agents. DNA samples were incubated with different Dps concentrations and subjected to experimental damaging conditions to induce oxidative, enzymatic, and hydrolytic damage. The Dps–DNA complexes showed significant protection against all three damage mechanisms. This approach may therefore provide a useful addition to current methodology, or potentially form the basis of a new long-term DNA storage method.

5.2 Introduction

The ferritin family of proteins incorporates well-known and ubiquitous proteins that are found in all forms of life and are vital for the sequestration and regulation of iron. Using iron in an oxygenic environment requires organisms to precisely control intracellular availability of Fe(II) and Fe(III), the two most common oxidation states of iron (Gao et al., 2019). Ferritin proteins store iron in its Fe(III) form within their hollow core to regulate the amount of biologically available iron. Ferritin, and many ferritin superfamily proteins, also protect the cell from ROS, which can damage many cellular components. These proteins have a noncovalent bonded structure that is very stable under a wide range of pH and temperature conditions. Members of the ferritin superfamily have also shown to offer protection and chaperone abilities under environmental stress. Ferritin-like proteins have shown protective abilities as heat and cold shock proteins (Hébraud et al., 2000), and as multiple stress proteins under a range of cellular stresses. In addition, some ferritin-like proteins can bind to cellular components or form larger complexes themselves. The active form of ferritin for iron storage is a multimer containing

24 subunits, arranged in a cage-like structure to enclose the contents stored in the core. The larger complexes are highly ordered and take on a crystal-like structure.

Crystalline structures, in most cases, are considered incompatible with biological systems, but this kind of biocrystalline structure can form in living systems to protect them from extreme environmental conditions or to contain excess toxic substrates (Rampelotto, 2010). These structures form to sequester and protect the vital components of a cell including, and probably most importantly, its nucleic acids; specifically, DNA (Wolf et al., 1999).

DNA protection during starvation protein (Dps) belongs to the subtype of ferritin-like proteins and was first discovered in *E. coli* (Almiron et al., 1992). It is considered a histone-like protein that can bind DNA without any sequence specificity and condense it into highly-ordered crystalline structures (Dadinova et al. 2019; Grant et al., 1998). Its ability to protect the cell from oxidative stress has been well documented and investigated within *E. coli* and other prokaryotes (Azam et al., 1999). Even in the absence of significant binding or crystallization—as shown in studies involving some homologues in other prokaryotes that do not have the ability to crystallize DNA)—Dps still has significant ability to mitigate oxidative stress (Calhoun & Kwon, 2011; Karas et al., 2015). In addition to oxidative stress, the crystalline protein–DNA complexes have also been shown to protect cells from heat shock, UV exposure, acid hydrolysis, and physical damage by acting as a protective shield (Almiron et al., 1992; Chen & Helmann, 1995; Gupta & Chatterji, 2003; Martinez & Kolter, 1997; Prenkiel-Krispin et al., 2006; Ren et al., 2003).

The structure of the Dps protein has been thoroughly investigated, despite the binding and protective mechanisms remaining under debate. The overall charge of the protein surface is negative, so it should be repelled from the negatively charged DNA molecule. There are several theories regarding how the negatively charged protein surface can bind to a negatively charged DNA molecule, but the most experimentally supported thesis is that of the positively-charged residues on the Dps protein interacting with the DNA molecule. The negative charge on the DNA backbone is thought to be attracted to the extended lysine-containing N-terminal regions of Dps subunits. Mutant studies where N-terminal regions are deleted have shown inhibited DNA binding, but crystalline structures were still able to form (Cieci et al., 2004; Karas et al., 2015; Roy et al., 2007). Studies have also shown that the presence of Mg^{2+} and other divalent cations

can increase or decrease binding and crystal formation (Lee et al., 2016). This ion-dependant mechanism is thought to be a salt bridge helping to stabilize the structure (Roy et al., 2008). When the concentration dependence was tested, a small amount of Mg^{2+} was found to increase DNA binding and helped biocrystals form, but at higher concentrations both processes were completely inhibited (Ghatak et al., 2011). Unexpectedly, the crystalline structures could still form with N-terminal mutants at low divalent ion concentrations (Minato et al., 2020). This suggests that formation of these biocrystalline structures occurs through a combination of several distinct mechanisms acting interdependently (Williams et al., 2021).

The concentrations of NaCl can negatively affect the binding ability of Dps to DNA, similarly to the addition of Mg^{2+} or other ions. Where ion concentrations are too high or too low, they can inhibit formation of the salt bridges and disrupt hydrogen bonding of the charged residues that are thought to be the main binding mechanisms driving formation of Dps–DNA complexes. There is reduced DNA binding at high salt concentrations, and over a large pH range, and these observations further supporting the multiple binding mechanisms argument (Soshinskayaet al., 2020).

Dps has highly conserved structures across its many homologues. Its monomeric form contains 167 amino acids and has a molecular weight of approximately 18.7 kDa. It oligomerizes to form a dodecameric structure consisting of 12 identical subunits assembled with crystallographic point group 23 (tetrahedral) symmetry (Grant et al., 1998).

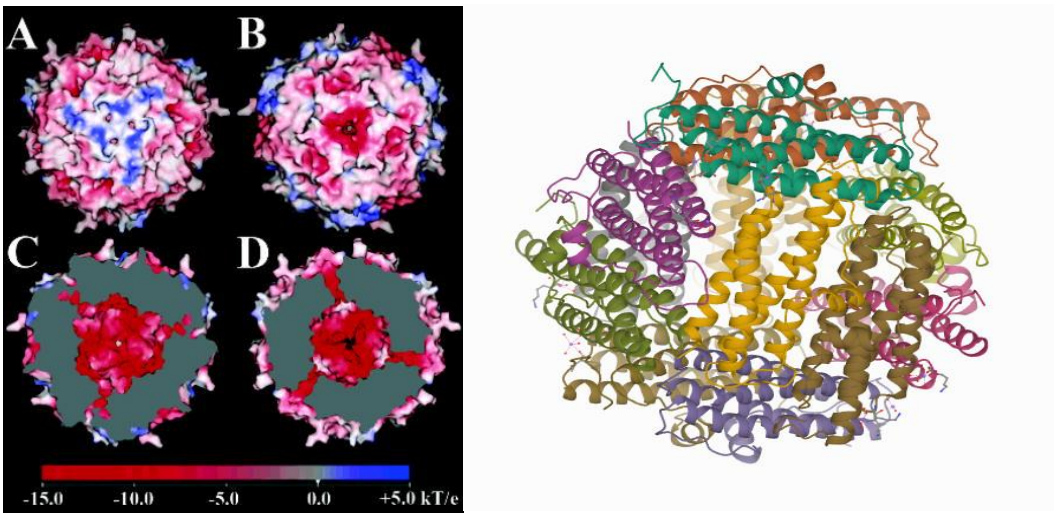

http://www.rcsb.org/pdb/explore/explore.do?structureId=1QGH

Figure 31: The surface electrostatic potential of the Dps dodecamer structure.

(A) The surface surrounding the N-terminal 3-fold interface; (B) exterior surface surrounding the C-terminal 3-fold pore. The surrounding surface is acidic, with strong negative electrostatic potential (red); (C) interior surface surrounding the N-terminal pore (center); (D) interior surface surrounding the C-terminal pore. The ribbon structure of the Dps protein oligomer is shown on the right (Gauss et al., 2006).

One of the main functions of Dps in the cell is to sequester iron. Its cage-like conformation has a hollow ferroxidase center that, analogously to ferritin, allows the Dps structure to oxidize Fe(II) with hydrogen peroxide, preventing free radical production via the Fenton reaction (Calhoun & Kwon, 2011; Papinutto et al., 2002).

The ability of Dps to sequester iron, and its ability to bind DNA and form biocrystalline structures, are not related. The protection afforded to DNA, against a variety of damaging agents, by forming a complex crystalline structure with Dps does not inhibit the protein's oxidative protective qualities (Pesek et al., 2011). In fact, the dodecameric structure that is integral to the sequestration of iron does not need to be present for the DNA binding and subsequent protection to occur (Karas et al., 2015).

Dps can also exist *in vitro* and *in vivo* in monomeric, dimeric, and trimeric forms (Soshinskaya et al., 2020). The monomeric and dimeric forms cannot bind DNA. The trimeric form is able to bind DNA but lacks iron sequestering ability. It is, however, unable to form the

large crystalline structures (Dadinova et al., 2019), but instead forms more of a “bead on a string” type structure than a large solid crystal, when complexed to DNA. This formation nonetheless provides a physical barrier for the DNA similar to the biocrystalline formation, and offers protection from multiple damage agents (Antipov et al., 2017; Selvaraj et al., 2012). Gupta et al. (2003) showed that incubating the trimeric form at 37°C causes it to associate into dodecameric structure (Gupta & Chatterji et al., 2003), but this ferritin-like association of Dps monomers into a larger structure actually appears to be stabilized only when the monomers are in closer proximity due to crowding, meaning that formation of the trimeric forms and assembly into the dodecameric structure are dependent on concentration (Selvaraj et al., 2012).

It is thought that Dps does not form the large crystalline structures with short DNA fragments as the DNA must be of sufficient length for the process to occur, approximately 4,000 bp; but it does not matter if it is linear, coiled, circular, or condensed (Dadinova et al., 2019). The Dps–DNA biocrystal formation occurs through dodecameric Dps units associating with one another to create a highly ordered lattice of varying size, with the DNA embedded within the overall structure. The DNA is not oriented in any particular direction or plane within the crystal matrix (Evgeniy et al., 2021).

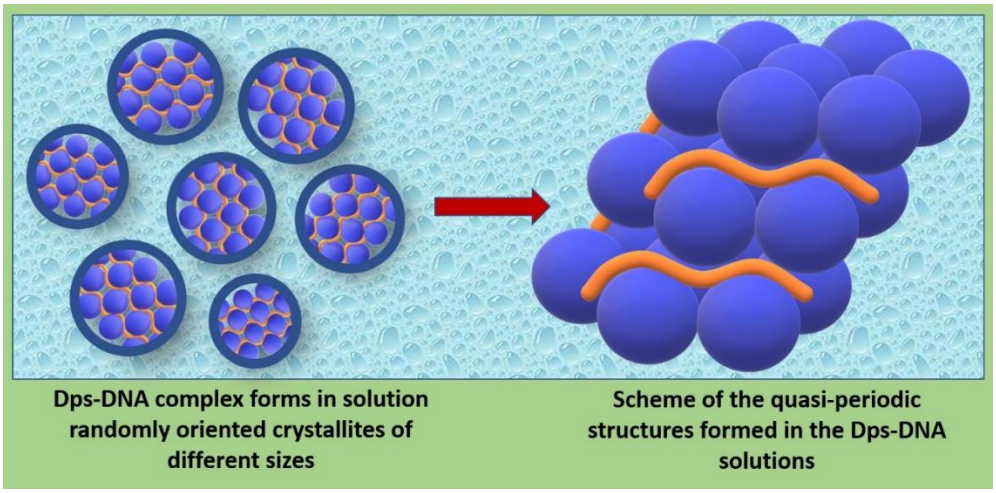

https://febs.onlinelibrary.wiley.com/doi/full/10.1002/1873-3468.13439

Figure 32: Dps–DNA Crystal Formation in Solution
Dps in its dodecameric form can aggregate to form large crystalline structures in solution. The process leads to highly ordered crystalline structures, but within the overall structure, the DNA is oriented in a random fashion. The crystals can also vary in size.

The presence of Dps homologues in many distantly-related bacteria indicate that DNA biocrystallization may be a widespread tool used by prokaryotes to protect their DNA in high-stress environments (Facey et al., 2013). Exploiting this highly effective *in vivo* DNA biocrystallization mechanism as an *in vitro* storage medium might prove useful, since it fulfills many of the requirements for a long-term DNA storage solution. These include a physical matrix which supports the fragile backbone of the DNA structure, effective exclusion of water molecules, an effective blocking agent for oxidation, and the ability to withstand physical damage. Dps in this experiment will be evaluated by concentration what its potential ability to provide DNA protective qualities against the three most common damage types enzymatic, oxidative and hydrolytic damage. The degree of protection foreach specific damage type will help evaluate the potential of Dps as a DNA preservative and long term storage medium. B

5.3Materials and Methods

5.3.2 Extraction and PCR

Samples were extracted in a 2 mL microcentrifuge tube with 400 µl of extraction buffer—comprising 290 µL TNE (10 mM Tris, 100 mM NaCl, 1.0 mM EDTA, pH 8), 40 µL 20% SDS (Fluka, catalogue # 05030), 0.39 M DTT (Fisher Scientific, catalogue # BP17225), 5 µL Proteinase K (20 mg/mL, EN ISO 9001/07/94, Qiagen, catalogue # 19131), and 25 µL water (ultrapure RNase/DNase-free water, Invitrogen, catalogue # 10977-23)—followed by a 3 h incubation at 56°C on a thermomixer (Eppendorf Thermomixer R 5355 Mixer Shaker) with agitation at 350 rpm.

At the end of the incubation step, samples were centrifuged 12,000 *g* speed for 1 min and the supernatant was transferred to a sterile 1.5 mL microcentrifuge tube (crosslinked/autoclaved). Then, 4 M guanidine thiocyanate (1 µL, Sigma, Catalogue # G9277) and 15 µL of silica beads (Sigma, Catalogue # 119H0212) were added to the tube and the sample was mixed, using a vortex mixer, for 30 seconds. The tubes were placed on ice for 6 h, following which they were centrifuged at high speed for 1 min then the supernatant carefully removed and discarded. Each sample was then resuspended in 500 µL of wash buffer (50 mM Tris–HCl pH 7.5, 50 mM NaCl, 1 mM EDTA in EtOH–H_2O (1:1); prepared using ultrapure, DNase/RNase-free distilled water, Invitrogen, catalogue # 10977-23), then vortexed until the silica beads were resuspended, centrifuged on high speed for 1 min and the supernatant removed. To remove any residual salts, 500 µl of ice cold 75% EtOH was added and the sample vortexed again until the silica beads were resuspended, then centrifuged on high speed for 1 min and the supernatant removed and discarded. An additional wash step was carried out using 200 µL of cold 100% EtOH, with vortexing, centrifugation and aspiration steps as before.

Samples were then dried overnight in a forensic drying cabinet (DrySafe forensic evidence drying cabinet, AirClean Systems, model 300) at 28°C. After 24 h, 50 µL of ultrapure water (Invitrogen) was added and the sample was vortexed. The tubes were incubated for 1 h, with 350 rpm agitation, at 56°C, then the purified extracts were pooled and diluted to a concentration of 10 ng/µL in 50 µL of ultrapure water.

As in previous experiments, various sized target areas were amplified to assess DNA preservation or protection. A set of three amplicons of 230 bp, 425 bp, and 800 bp, was amplified by PCR. Thermostable DNA polymerase from *Thermus aquaticus* (*Taq* polymerase)

was used to amplify DNA samples after extraction and following storage at various temperatures over the appropriate time intervals. Standard reactions were performed in 20 μL volume in 0.2 mL tubes, and used the mitochondrial DNA primers listed (Table 3) to generate three amplicons with sizes 800, 425, and 230 bp. All reaction mixtures were prepared on ice. The PCR reaction, after optimization, contained: 200 μM dNTPs, 0.2 μM of each primer, 1.0 mM $MgCl_2$, 1× PCR buffer (750 mM Tris–HCl pH 8.8, 200 mM $(NH_4)_2SO_4$, 0.1% Tween-20), 0.5 U *Taq* DNA polymerase, and 10 ng of DNA template. The remaining volume was made up to 20 μL using ddH_2O. Tubes were vortexed, spun down, and placed in a 96-well Gradient Mastercycler (Eppendorf).

The cycling parameters included an initial denaturation at 94°C for 2 min followed by 30 cycles of 94°C for 30 sec, 60°C for 1 min, and 72°C for 2 min. On completion, the reaction was placed at 4°C on hold. This PCR protocol was adapted and optimized from Lorenz (2012).

For agarose gel electrophoresis (AGE), PCR products were applied to a 2% agarose gel containing ethidium bromide (EtBr, ~1% in H_2O, Sigma–Aldrich, catalogue # 46067) for detection, and viewed with a transilluminator under UV light. One well was loaded with a molecular marker (5 μL) and the remaining wells with 3 μL of 6× loading buffer (Invitrogen) and 5 μL of sample (10ng/μL). Gels were run for 30 minutes at 110 V in 1× TBE buffer, then removed from the running buffer and subsequently viewed on the transilluminator (UVB wavelength) and photographed.

5.3.3 Purification

QIAquick columns (Qiagen, QIAquick PCR Purification Kit (50), catalogue # 28104) were used to purify DNA PCR product after amplification before Dps incubation and initial agarose gel identification. QIAquick columns were then again used to purify the samples after damage treatments to remove solutions and impurities before PCR except for the acid buffer solution samples that were purified with ethanol precipitation after damage experiments. The necessary buffer solutions were supplied with the columns. Five volumes of PB Buffer were added to the sample to be purified, which was briefly vortexed before being transferred by

pipette to the center of the column membrane. The column was then centrifuged for 1 min at 17,900 g. The eluate was discarded. A volume of 750 µL of PE Buffer was pipetted into the column, which was again centrifuged for 1 min at 17,900 *g*, and the eluate again discarded. The column was transferred to a sterile 1.5 mL microcentrifuge tube and 50 µL of sterile ddH_2O was added to center of the column membrane. The column was then incubated for 1 min at room temperature (18°C) and centrifuged at 17,900 *g* for 1 min to elute the DNA.

5.3.3 DPS

Dps protein was initially purified in-house but due to pandemic related issues the production had to be outsourced. The target DNA sequence of Dps was optimized and synthesized (GenScript). The synthesized sequence was cloned into vector pET-30a(+) with a His-tag for recombinant protein expression. *E. coli* strain BL21(DE3) was transformed with the plasmid. A single colony was inoculated into TB medium containing kanamycin. The culture was incubated at 37°C. When the OD_{600} reached approximately 1.2, the culture was induced with IPTG at and incubated at 37°C for a further 4 h. Cells were harvested by centrifugation. Cell pellets were resuspended in lysis buffer followed by sonication and centrifugation. The supernatant was kept for future purification. The target protein was obtained by one-step purification using Ni–NTA resin and sterilized by 0.22 µm filter before storage in aliquots.

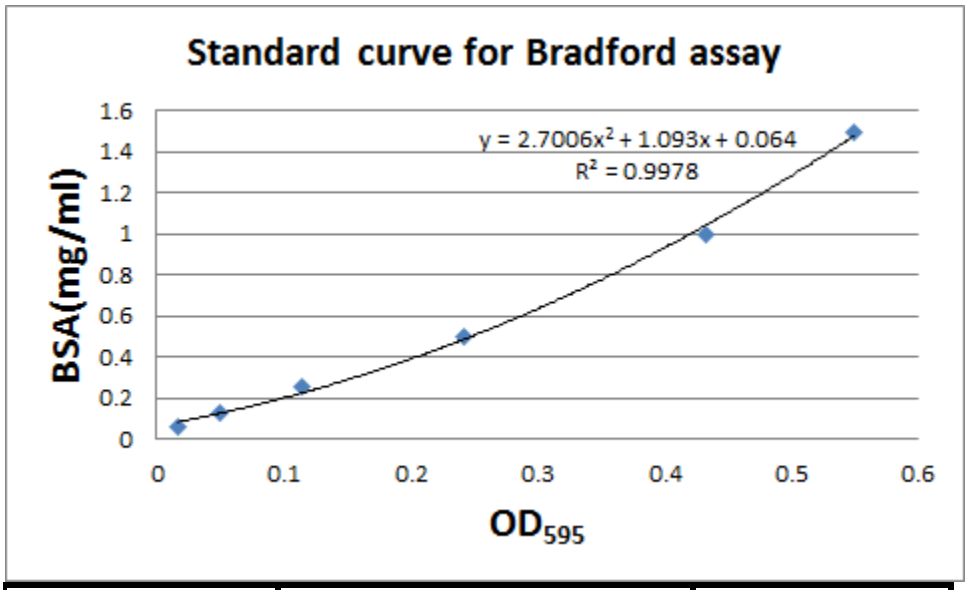

Sample	OD595	Concentration
DPS protein	0.455	1.12 mg/ml

Figure 33: Standard Curve and Result for Bradford Assay

The concentration was determined by Bradford protein assay (Figure 33) with BSA as standard. The protein purity and molecular weight were determined by standard SDS-PAGE along with Western blot confirmation. There was some protein precipitation from a solution in 1× PBS (pH 7.4) after purification. A second batch was stored in 50 mM Tris, 500 mM NaCl, pH 8.0; however, the protein continued to precipitate. After trying several different buffers, addition of arginine proved successful at keeping the Dps protein in solution. Full results are listed in Table 10.

Table 10: Dps Solubility within a Range of Buffered Solutions

Buffer	Result
1× PBS, pH 7.4	Precipitation
50 mM Tris, 500 mM NaCl, pH 8.0	Precipitation
50 mM Tris, 500 mM NaCl, pH 8.5	Precipitation
50 mM Tris, 500 mM NaCl, pH 9.0	Precipitation
50 mM Tris, 500 mM NaCl, pH 8.0, 0.1 M L-Arginine	Success

50 mM Tris, 500 mM NaCl, pH 8.0, 0.2 M L-Arginine	Success
50 mM Tris, 500 mM NaCl, pH 8.0, 0.3 M L-Arginine	Success
50 mM Tris, 500 mM NaCl, pH 8.0, 0.4 M L-Arginine	Success

Overall, the Dps produced in house was either not of sufficient purity or quantity to complete all the planned experiments. Therefore, DPS was therefore purchased commercially from GenScript to perform the experiments (Appendix C).

5.3.1 Cloning Strategy

Construct for expression of full-length protein:

> U9698EC110-1 (Dps protein)

NdeI--ATG--His tag--TEV protease site-- dps protein --Stop codon--HindIII

Protein Length=180 MW=20369.9 Predicted pI=6.59 vector: pET30a

MHHHHHHENLYFQG**STAKLVKSKATNLLYTRNDVSDSEKKATVELLNRQVIQFIDLSLITKQAHWNMRGANFIAVHEMLDGFRTA**
LIDHLDTMAERAVQLGGVALGTTQVINSKTPLKSYPLDIHNVQDHLKELADRYAIVANDVRKAIGEAKDDDTADILTAASRDLDK
FLWFIESNIE..

DNA sequence: 555bp

CATATGCATCACCACCACCACCACGAAAACCTATACTTCCAAGGATCAAC**AGCGAAGCTGGTTAAGAGCAAGGCGACCAATCTGC**
TGTATACCCGTAACGATGTGAGCGACAGCGAGAAGAAAGCGACCGTGGAACTGCTGAACCGTCAGGTTATCCAATTCATTGATCT
GAGCCTGATCACCAAGCAGGCGCACTGGAACATGCGTGGTGCGAACTTCATTGCGGTTCACGAGATGCTGGACGGCTTTCGTACC
GCGCTGATCGATCACCTGGACACCATGGCGGAACGTGCGGTGCAGCTGGGTGGCGTTGCGCTGGGTACCACCCAAGTGATCAACA
GCAAGACCCCGCTGAAAAGCTACCCGCTGGATATTCACAACGTTCAAGACCACCTGAAAGAGCTGGCGGATCGTTATGCGATCGT
GGCGAACGACGTTCGTAAGGCGATTGGCGAAGCGAAAGACGATGACACCGCGGATATTCTGACCGCGGCGAGCCGTGACCTGGAC
AAGTTCCTGTGGTTTATTGAAAGCAACATTGAATAATGAAAGCTT

5.3.4 Incubation

Dps and the DNA PCR products were added together into 1.5 µL microcentrifuge tubes and incubated for 12 hours at 37°C to convert the trimeric forms of the Dps present into the dodecameric form which binds DNA and assembles into large crystal structures (Gupta &

Chatterji et al. 2003). A volume of 2 µL Mg^{2+} was added from stock to a final concentration of 10 mM to each tube which has shown to promote DNA binding (Ghatak et al., 2011).

500 ng of DNA PCR product of each of the amplicons 800, 425, and 230 bp product after QIAquick purification and Qubit quantification was added each tube. Concentrations of Dps were added to each amplicon tube at concentration of 0 as a control, 1.12 µg, 5.6 µg, 11.2 µg, 16.8 µg, 22.4 µg, 28.0 µg, 33.6 µg. for each damage experiment time interval. Tubes were brought to a volume of 50uL with DNase/RNase-free distilled water (Invitrogen, catalogue # 10977-23).

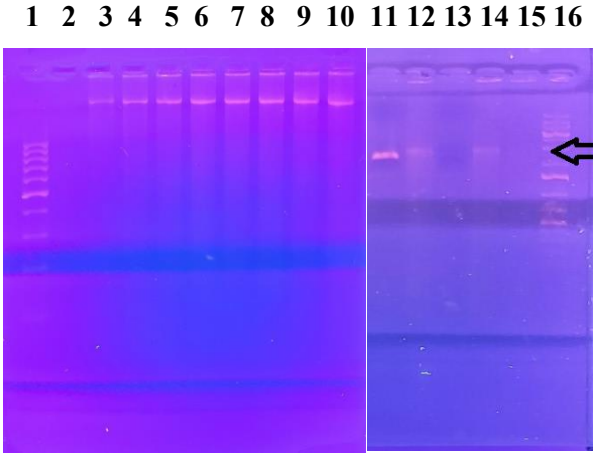

Figure 34: DNA Mobility Retardation Gel, 800 bp Amplicon

Lane 1: 100 bp ladder; Lane 2: 2.24 µg Dps no DNA; Lane 3: 800 bp (50ng), 1.12 µg Dps; Lane 4: 800 bp (50ng), 1.68 µg Dps; Lane 5: 800 bp (50ng) 2.24 µg Dps; Lane 6: 800 bp (50ng), 2.24 µg Dps; Lane 7: 800 bp 3.36 µg Dps; Lane 8: 800 bp (50ng), 1.12 µg Dps and 10 mM Mg^{2+}; Lane 9: 800 bp (50ng), 1.68 µg Dps, Mg^{2+} 10 mM; Lane 10: 800 bp (50ng), 2.24 µg Dps and 10 mM Mg^{2+}; Lane 11: 800 bp (50ng) no Dps; Lane 12: 800bp (25ng), 1.12 µg Dps, Lane 13: 800bp (20ng) 1.12 µg Dps; Lane 14: 800bp (15ng) 1.12 µg Dps; Lane15: 800bp (10ng) 1.12 µg Dps. Lane 16 100 bp Ladder arrow at 800bp.

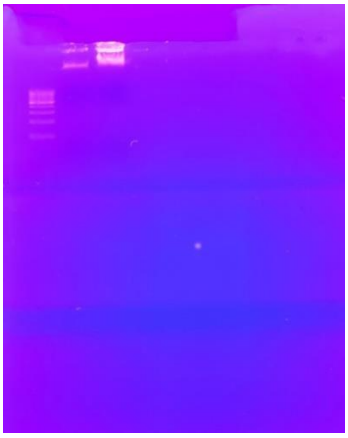

Figure 35: DNA Mobility Retardation, 800 bp Amplicon, Gel 2

Lane 1: 100 bp ladder; Lane 2: 800 bp (50ng), 2.8 µg Dps and Mg^{2+} 10 mM, Lane 3: 800 bp (50ng), 3.36 µg Dps, Mg^{2+} 10 mM.

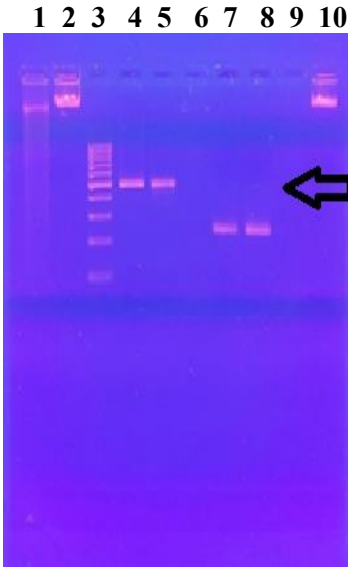

Figure 36: DNA Mobility Retardation Gel, 425 bp and 230 bp amplicons.
Lane 1: 425 bp (50ng), 3.36 µg Dps; Lane 2: 425 bp (50ng), 3.36 µg Dps and Mg^{2+} 10 mM; Lane 3:100 bp ladder; Lane 4: 425 bp (50ng) without Dps; Lane 5: 425 bp (50ng) no Dps; Lane 6: 3.36 µg Dps only; Lane 7: 230 bp (50ng)) without Dps; Lane 8: 230 bp (50ng)) without Dps ; Lane 9: 3.36 µg Dps, Mg^{2+} 10 mM (control); Lane 10: 230 bp (50ng), 3.36 µg Dps, Mg^{2+} 10 mM. Arrow indicates 400bp on ladder 400bp.

The PCR amplicons were greatly retarded in a 2% agarose gel after incubation of the DNA with Dps, when compared against the same untreated DNA amplicons as seen in figures

34,35,36. The Dps binds to the 425 bp amplicon and slows the amplicon's migration through the agarose gel by greatly increasing its effective size and altering its electrophoretic mobility compared to the DNA al one (compare lanes 1 and 2 with lanes 4 and 5 in Figure 36). The addition of 10 mM Mg^{2+} in lane 2, compared to lane 1, increased the retardation with more DNA stuck in the well, resulting in a stronger band and indicating additional stabilization of the Dps–DNA complex. The result for the 230 bp amplicon with the Dps and Mg^{2+} again showed that the DNA was bound up with the Dps, and its movement through the gel was being retarded due to its size in the Dps–DNA complex (compare lane 10 with lanes 7 and 8 in Figure 36).

5.3.5 DNase Treatments

Solutions of 100 µL, with a final concentration of 5 ng/µL DNA and increasing concentrations of Dps, were made by combining 50 µL of 10 ng/µL DNA acid buffer solution and increasing volumes of Dps solution with ultrapure water to attain the final assay volume (Table 12).

Table 11: Dps Concentration in DNase Treatments

DNA Solution, 500 ng total	Dps Concentration 1.12 mg/ml	$MgCl_2$ 10 mM	Ultrapure Water	DNase, 100 U/mL.in buffer
50 µL	0	2 µL	43 µL	5 µL
50 µL	1.12 µg	2 µL	41 µL	5 µL
50 µL	5.6 µg	2 µL	38µL	5 µL
50 µL	11.2 µg	2 µL	33 µL	5 µL
50 µL	16.8 µg,	2 µL	28 µL	5 µL
50 µL	22.4 µg	2 µL	23 µL	5 µL
50 µL	28.0 µg	2 µL	18 µL	5 µL
50 µL	33.6 µg	2 µL	13 µL	5µL

5.3.6 Oxidative Damage

Solutions of 100 µL, with a final concentration of 5 ng/µL DNA and increasing concentrations of Dps, were made by combining 50 µL of 10 ng/µL DNA solution, 10 µL of 6% hydrogen

peroxide solution (~1.8 M), and increasing volumes of Dps solution as indicated, with ultrapure water to attain the final assay volume (Table 12).

Table 12: Dps Concentrations in Oxidative Damage Treatments

DNA Solution, 500ng	Dps Concentration 1.12 mg/ml	$MgCl_2$ 10 mM	Ultrapure Water	H_2O_2 (1.80M)
50 µL	0	2 µL	38 µL	10 µL
50 µL	1.12 µg	2 µL	37 µL	10 µL
50 µL	5.6 µg	2 µL	33 µL	10 µL
50 µL	11.2 µg	2 µL	28 µL	10 µL
50 µL	16.8 µg,	2 µL	23 µL	10 µL
50 µL	22.4 µg	2 µL	18 µL	10 µL
50 µL	28.0 µg	2 µL	13 µL	10 µL
50 µL	33.6 µg	2 µL	8 µL	10 µL

5.3.7 Heat/Acid Damage

Solutions of 100 µL, with a final concentration of 500 ng/µL DNA and increasing concentrations of Dps, were made by combining 50 µL of 10 ng/µL DNA in acid buffer with increasing volumes of Dps solution, and ultrapure water to attain the final assay volume (Table 13).

Table 13: Dps Concentrations in Heat/Acid Damage Treatments

500ng DNA in Acid Buffer Solution	Dps Concentration 1.12 mg/ml	$MgCl_2$ 10 mM	Ultrapure Water
50 µL	0	2 µL	48 µL
50 µL	1.12 µg	2 µL	47 µL
50 µL	5.6 µg	2 µL	43 µL
50 µL	11.2 µg	2 µL	38 µL
50 µL	16.8 µg,	2 µL	33 µL
50 µL	22.4 µg	2 µL	28 µL
50 µL	28.0 µg	2 µL	23 µL

50 µL	33.6 µg	2 µL	18 µL

5.4 Results

5.4.1 DNase Treatments

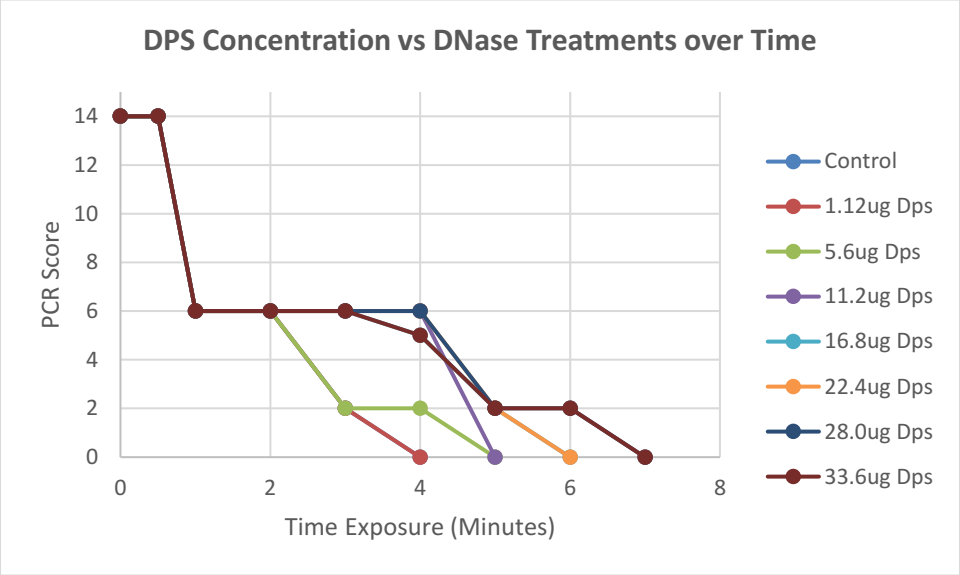

Figure 37: Dps Concentration vs DNase Damage Treatments.

Various concentrations of Dps exposed to DNase over time periods to induce enzymatic damage. The Dps had protective qualities at the 5.6ug concentration with significant increasing protection at the 33.6ug concentration which enabled successful PCR at 6 Minutes.

Figure 37 shows the PCR amplification scores of DNA samples treated with DNase solution, in the presence of increasing concentrations of Dps, to induce enzymatic damage over 8 min. The control sample lost recoverability of the largest amplicon after 30 s, with complete PCR failure at 4 min. With 1 µL Dps, the results were the same as for the control. At the 5 µL Dps concentration, the largest amplicon was again lost at time points beyond 30 s with PCR failure at 5 min. For the remaining Dps concentrations, recoverability of the large amplicon was again only apparent at the 30 s time point. Complete PCR failure occurred after 5 min for the 11.2 µg Dps sample, after 6 min with 16.8 µg or 22.4 µg Dps, and after 7 min for the 28.0 µg Dps and 33.6 µg Dps samples.

There was an approximately 33% increase in the recovery of amplifiable DNA associated with the highest concentration (33.6 µg) of Dps in comparison to the control samples. At above 11.2 µg Dps concentration, protective ability for amplifiable DNA became apparent over the exposure times used. Below that concentration (at the 1.12 µg and 5.6 µg, and 11.2 µg Dps concentrations), there was little apparent difference between the various treatments and the control. The 16.8 µg and 22.4 µg Dps concentrations extended the PCR recovery range up to the 6 min mark, compared to 4 min for the control, although this was for the smaller amplicons. The 28.0 µg and 33.6 µg Dps concentrations did not exhibit and greater ability to maintain recovery of the larger amplicons, but they did further increase the PCR recovery time for the smallest 230 bp amplicon to 7 min.

5.4.2 Oxidative Damage

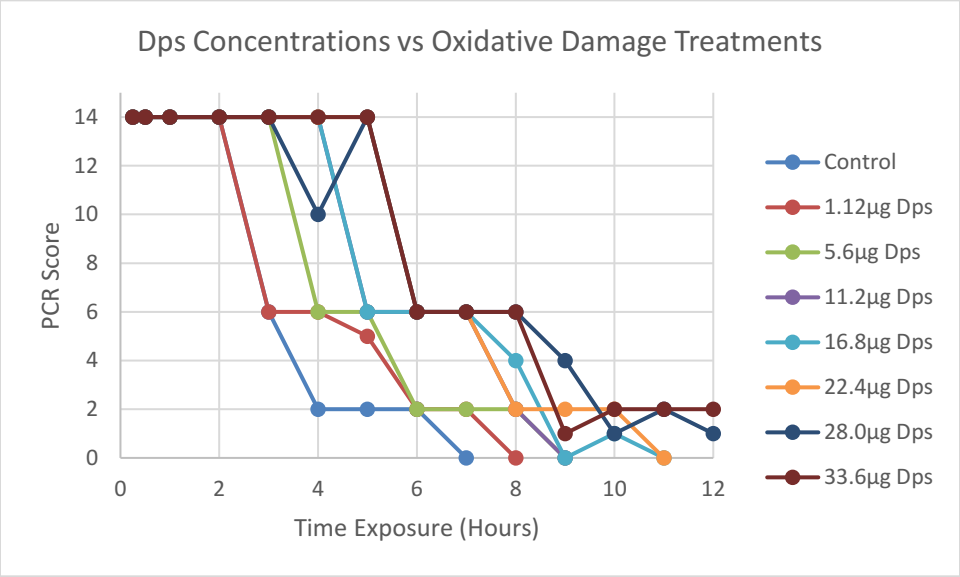

Figure 38: Dps Concentrations with Oxidative Damage Treatments over Time

The PCR amplification scores of DNA samples treated with hydrogen peroxide, in the presence of increasing concentrations of Dps, to induce oxidative damage over 12 h. These conditions were used to determine the ability of Dps to protect the sample DNA against oxidative damage.

The control sample showed large amplicon recovery for up to 2 h and PCR failure at 7 h. The sample with 1.12 µg Dps also showed large amplicon recovery up until the 2 h time point,

with PCR failure at 8 h. With 5.6 µg Dps the large amplification was recoverable for up to 3 h, with PCR failure at 9 h. The 11.2 µg and 16.8 µg Dps concentrations displayed large amplicon recovery for up to 4 h, with complete PCR failure occurring at 9 h and 11 h, respectively. The 22.4 µg Dps concentration allowed for large amplicon up until the 5 h time point, with PCR failure at 11 h. For the highest concentrations of Dps, 28.0 µg and 33.6 µg, the largest 800 bp amplicon could be recovered for the first 5 h of exposure, with at least some successful amplification of the 225 bp fragment remaining for the full duration of the experiment.

The sample with the highest concentration of Dps (33.6 µg) was able to fully recover the 230 bp amplicon even after 12 h of oxidatively-induced damage. The control sample without Dps failed PCR completely at 7 h, indicating that the Dps was able to almost double the efficiency in recovering amplicons under these conditions of induced oxidative damage. The overall trend showed a direct correlation between the amount of Dps in solution and the rate and length of time that viable DNA could be recovered and amplified.

5.4.3 Heat/Acid Treatment

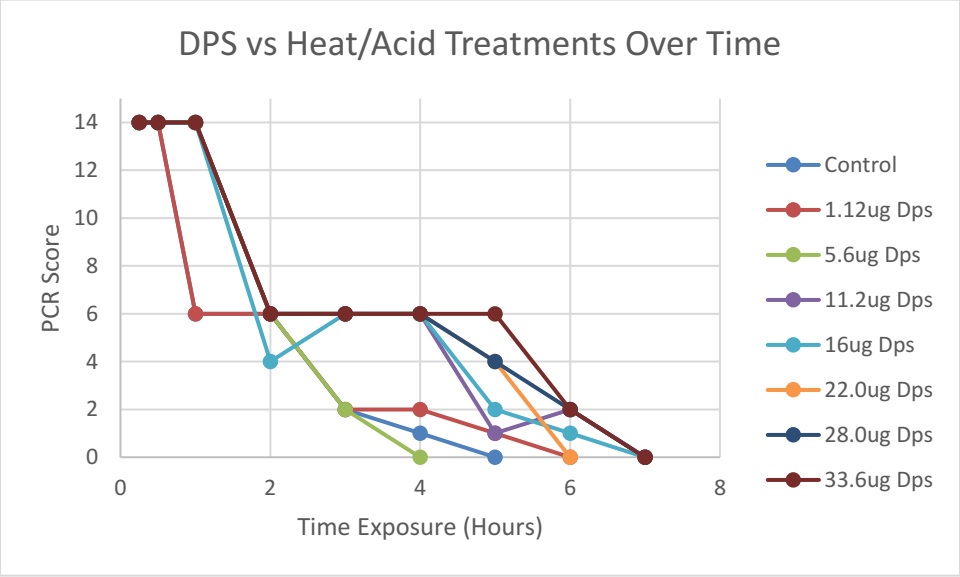

Figure 39: Dps Protection of DNA Against Heat/Acid Treatments over Time.
The PCR amplification scores of DNA samples after heat/acid treatments in solution, with increasing concentrations of Dps, to induce hydrolytic damage over a period of 8 h.

The control sample lost large amplicon recoverability beyond 30 min of exposure and experienced PCR failure at 5 h. The 1.12 µg Dps concentration performed similarly, except that complete PCR failure did not occur until 6 h. The remaining Dps concentrations all permitted successful PCR recoverability of the largest amplicon for the first 1 h of exposure, with a decline in PCR score beyond that point. For the 5.6 µg Dps sample, the point of complete PCR failure was reached after 4 h of exposure, whereas the remaining concentrations showed a somewhat inconsistent pattern. With 11.2, 16.8, 22.4, 28, and 33.6 µg Dps, PCR failure occurred at 7 h, 9 h, 6 h, 7 h, and 7 h, respectively.

For the 11.2–33.6 µg Dps concentrations, higher concentrations had a greater effect of protecting the recoverable amplicon size against the heat/acid treatment, which induces hydrolytic damage. A direct concentration-dependent trend was seen in preservation and protection against the damaging conditions by Dps, in terms of DNA quality and the ability to recover amplicons for longer; an effect which is especially apparent for preservation of PCR viability of the 425 bp amplicon. For each additional 5.6 µg of Dps that was added, there was a corresponding ability to recover a larger amplicon over a longer time period, up to a maximum of 6 h. From 4–6 h, the results show that the higher the amount of Dps present, the larger the amplicons recovered. There was variability after 6–7 h of exposure, with the 16.8 µg concentration of Dps scoring higher in the final hour than the 22.4 µg concentration. However, the overall trend showed that higher Dps concentrations were associated with a greater protective effect on the DNA against the hydrolytic damage-inducing heat/acid treatment.

5.5 Discussion

When Dps–DNA solutions were subjected to the induced experimental damage, direct concentration-dependent correlations were observed with regard to the ability of the solution to preserve larger amplicons and extend the time over which DNA of sufficient quality for PCR was recoverable. The gel shift experiments showed that there was Dps binding to the DNA, retarding migration of the DNA through the agarose gel and, for smaller amplicons, greatly affecting its mobility. It was unclear if any larger crystalline protein–DNA structures actually formed even at high concentrations of Dps relative to DNA. However, the Dps-treated DNA

showed significant protection against, or inhibition of, all three experimentally induced damage types and particularly in the oxidative damage category, as was expected given that this is a well-known attribute of the Dps protein. We were unable to detect any physical crystals in our solutions after drying or filtration through the 0.2 micron filter.

The ability of the Dps proteins to bind the DNA and protect it from damage is a physical process that involves shielding of the DNA structure, blocking access to the susceptible locations on the DNA backbone and to the bases themselves. This Dps–DNA complex is very thermally stable at lower pH and protects the DNA from heat.

The process through which Dps binds to DNA is still not fully understood. The working model is that several independent mechanisms are involved: a salt bridge, electrostatic interaction of positively-charged amino acid residues with the phosphodiester backbone, and the Dps subunits binding to each other. Together, these aspects work to form a highly ordered stable structure (Antipov et al., 2017; Facey et al., 2013; Jacinto et al., 2021; Tereshkin et al., 2019). The more optimal factors that are present, the larger and more ordered the biocrystalline structures will be.

This physical shielding of DNA is unrelated to the iron sequestering process usually associated with protection against oxidative stress, which also protects the DNA in hydrated conditions. Without forming the Dps–DNA biocrystalline structure, the bound DNA remains highly resistant to oxidative damage even with the protein in its non-dodecameric form (Chiancone, 2008). The DNA is also highly resistant to enzymatic attack, and hydrolytic damage caused by low pH, in the non-crystalline structure (Jeong et al., 2008). These observations were verified in our experimental damage assays where significant protective effects of Dps were evident, but we assume large biocrystalline structures were not formed.

All protective mechanisms involved incorporate a reversible physical attachment to the DNA which blocks the damaging agent from attacking the bonds along the DNA backbone and keeps the DNA in a stable conformation that prevents fragmentation. It has also been shown that the Dps–DNA complexes are highly resistant to UV-induced damage (Nair et al., 2004). The use of Dps or some other protein to form biocrystals is therefore a potential long-term storage method for DNA. Viruses use a biocrystalline to protect themselves from environmental damage

and lie dormant in a biocrystalline state until ingested by the host. After ingestion, the pH change in the gut leads to dissolution of the biocrystal, releasing the virus to infect the host indicating a simple reversible state that is pH dependent (Minsky et al., 2002).

The robustness and efficiency associated with Dps satisfy all the conditions for an effective long-term DNA storage method. Such components of an ideal solution include stabilizing the structure in a physical matrix; protecting the molecule from water without destabilizing the negatively charged backbone of the DNA due to lost interactions; preventing highly reactive oxygen molecules from modifying nucleotides or attacking susceptible bonds; physically blocking UV radiation to prevent intra- and inter-strand crosslinking or protein–DNA crosslinking; and effectively blocking nucleases that degrade DNA by providing a robust physical coating, preventing binding. There is also the possibility to add Dps to other storage buffers to increase their efficiency, but solubility and pH would need to be considered. Importantly, the biocrystals are dissolvable and reversible, and the protein can also be easily removed by purification using differential solubility, proteolysis, and routine purification methods (Zeth et al. 2012). The effects of pH on crystal formation and attachment are major issues. Efficient protein–DNA binding occurs only within specific pH range, and the protein tends to precipitate out without binding the DNA when the pH is too low. It also will not bind to DNA when the pH is too high. More research is needed in this area, but overall, biocrystallization could be a viable way to greatly slow the degradation of genetic material, as well as store it in a biologically relevant state. Using Dps as a template protein cage and using protein engineering, formations could be designed with higher affinity for DNA and suitable modifications on the surface and interior to increase oxidative damage protection, as well as protection from hydrolytic and enzymatic damage.

Chapter 6: Conclusions and Future Work

Throughout the course of these studies, the robustness of the DNA molecule was investigated to understand if current damage models can correctly predict the viability of DNA in long-term storage. The DNA molecule by itself is very stable when left in a static stable environment protected from oxygen, UV radiation, and free water molecules. The factors which affect long-term storage and preservation of DNA are more complex than originally considered. Readable DNA has been recovered from increasingly ancient specimens because of advances in sequencing technology and improved methodology. Protection from UV radiation—involving the physical shielding of the DNA grooves through a protective shield or conformational variation, such an A-form or Z-form shift, which may also prevent nucleases from attaching—can help prevent degradation over time. The removal of surrounding water as a medium for damaging agents to be able to initiate chemical reactions is important, but the backbone of the negatively-charged DNA needs some sort of ionic support to balance out the negative charge and help stabilize the overall structure. This can be achieved in various ways such crystallization, dehydration, a physical barrier, or possibly some kind of embedding.

Physical protection of the DNA could be achieved effectively in many ways, allowing long-term viable storage. A greater challenge is efficient recovery of the DNA from these protectants. The DNA molecule becomes very fragile and susceptible to fragmentation in a dry state, or when bonded to a substrate. The hydration shell supplied by water also increases the flexibility of the DNA, but simultaneously provides multiple damaging agents with a medium. Replacing the water solvation shell with other hydrogen bonding molecules helps to prevent fragmentation of the DNA—by retaining more of it in the B-form, which is less susceptible to fragmentation—while denying damaging agents a ready solvent. Locally, the DNA molecule is quite rigid by itself with some sequence specificity and needs packaging protein interactions and hydration to increase its flexibility.

In a dried state, the DNA strand can be compared to a strand of dry pasta where, if forces are applied, it will break easily, but after hydration it can readily be bent and twisted. The form of the DNA then takes on a larger role, since by analogy, spaghettini—which is tiny—breaks very easily compared to, say, more compact linguini, where breakage would require more force.

This analogy relates to the Z-form of elongated DNA (spaghettini) being easier to break than the A-form (linguini). Condensing and packaging the DNA together, as in chromatin, increases its strength, just as a bundle of dry pasta is more difficult to break than a few strands. Likewise, embedding or supporting the dry molecule in a physical matrix becomes very important to maintain its structural integrity over the long term. All the storage methods tested, and currently available, can inhibit or slow the degradation process but there remains no way to entirely halt it. Biocrystallization is a promising new way to store DNA in the future. It is already employed by many organisms that can preserve their functioning genome under a wide variety of harsh conditions over decades and, potentially, centuries (Loiko et al 2017). The ability to preserve DNA in a bioactive state, along with the associated proteins and conformations, may provide significant opportunities for improved DNA storage and biotechnology in the future. There is currently much research around artificial ferritin and ferritin-like protein cages as delivery mechanisms for drugs (Palombarini et al., 2020). These might also be applied in efforts to develop an artificial Dps-like cage that has higher affinity for DNA, and the hollow core could also potentially be loaded with other DNA preservatives and stabilizing components.

With currently available methods, efforts should focus on preventing base modifications, and using preservatives that will exclude or inhibit oxidative damage or other agents that can cause base modifications which can lead to blocking lesions and a corruption of the base code. High molecular weight, large DNA strands could be sacrificed in favor of a larger number of higher-quality, shorter fragments. Fragmentation can increasingly be dealt with via repair protocols and the use of new sequencing technology that is compatible with shorter fragments for analysis, so this should not be a primary concern. The best opportunity to preserve DNA for long-term storage might be provided by combining: (i) a sugar, like trehalose, that can coat the DNA and remove or displace as much of the solvating water as possible; (ii) a chelator to bind divalent metal ions; and (iii) storage in a hermetically-sealed container that excludes oxygen and also has some kind of physical matrix. These conditions would not only provide the best chance of preserving the information encoded in the DNA but would still be cost-effective and maintain the DNA in an easily recoverable state with minimal processing, thereby reducing the risk of damage events during handling.

Further experimentation is required to continue investigation of the biocrystals. Combining protein, and possibly mineral, structures may increase the ability to preserve DNA in a biological-like state. Due to the pandemic challenges with labor and low yield of the Dps protein we could obtain in our time frame, we were unable to fully investigate the storage properties associated with its crystallization, but there are other biocrystalline structures that should be further researched as potentially effective storage agents for DNA over the long term. At this time, all current methods, additives, and environmental controls can only slow accumulation of the various damage types that occur to DNA over time. Each available strategy to mitigate different forms of damage during long-term DNA storage represents a trade-off. Taking advantage of new sequencing technology (Der Sarkissian et al., 2015), that can use smaller fragments of DNA at lower concentrations may allow DNA to be stored under more robust conditions that, despite increasing fragmentation, can prevent some of the more damaging lesions like crosslinking or oxidative damage, which can lead to DNA polymerase blocks. Even with the ability to recover, amplify, and analyze smaller fragments of DNA (which has allowed sequence information to be recovered from a lot of older and lower quality DNA samples), further work is needed to quantify the amount of code alterations that occur by damage modification, and the degree of mispairing of bases. Sequencing samples after periods of storage in various preservatives will assist in evaluating the amount of base modifications occurring over time under these conditions.

Further research is needed to fully understand, characterize, and improve DNA stability in the context of sample preservation during storage. Long-term studies over multiple decades, combined with frequent short-term analysis work, will increase our understanding of the subtle and multifactorial degradation processes. A major challenge will continue to be access to the DNA, as the most robust storage methods render the DNA not easily recoverable without significant secondary processing. This comes with its own challenges and may prove cost- and time-prohibitive in real-life situations. There will always be trade-offs in efficiencies with respect to cost and convenience but optimizing a combination of known preservatives in a DNA damage-specific protective formulation is seemingly the best option currently available.

References

Aboul-ela, F. M. (1987) Sequence dependant structure and thermodynamics of DNA oligonucleotides and polynucleotides: uv meltingand NMR (nuclear magnetic resonance) studies. No. LBL-24830. Lawrence Berkeley Lab., CA (USA). https://doi.org/10.2172/5211306

Aladdini, R., Walsh, S. J., & Abbas, A. (2010). Forensic implications of genetic analyses from degraded DNA—A review. *Forensic Science International: Genetics, 4*(3), 148–157. doi:10.1016/j.fsigen.2009.09.00

Almiron, M., Link, A. J., Furlong, D., & Kolter, R. (1992). A novel DNA-binding protein with regulatory and protective roles in starved Escherichia coli. *Genes & development*, *6*(12b), 2646-2654. doi:10.1101/gad.6.12b.2646

Anchordoquy, T. J., & Molina, M. C. (2007). Preservation of DNA. *Cell Preservation Technology, 5*(4), 180–188. https://doi.org/10.1089/CPT.2007.0511

Ånensen, H., Provan, F., Lian, A. T., Reinertsen, S. H. H. S., Ueno, Y., Matsuda, A., Seeberg, E., & Bjelland, S. (2001). Mutations induced by 5-formyl-2′-deoxyuridine in Escherichia coli include base substitutions that can arise from mispairs of 5-formyluracil with guanine, cytosine and thymine. *Mutation Research/Fundamental and Molecular Mechanisms of Mutagenesis*, *476*(1–2), 99–107. https://doi.org/10.1016/S0027-5107(01)00086-0

Antipov, S. S., Tutukina, M. N., Preobrazhenskaya, E. V., Kondrashov, F. A., Patrushev, M. V., Toshchakov, S. V., Dominova, I., Shvyreva, U.S., Vrublevskaya, V.V., Morenkov, O.S., Sukharicheva, N.A., Panyukov, V.V. & Ozoline, O. N. (2017). The nucleoid protein Dps binds genomic DNA of Escherichia coli in a non-random manner. *PLoS One*, *12*(8), e0182800. https://doi.org/10.1371/journal.pone.0182800

Arriola, L. A., Cooper, A., & Weyrich, L. S. (2020). Palaeomicrobiology: Application of Ancient DNA Sequencing to Better Understand Bacterial Genome Evolution and Adaptation. *Frontiers in Ecology and Evolution*, *0*, 40. https://doi.org/10.3389/FEVO.2020.00040

Aust, A. E., & Eveleigh, J. F. (1999). Mechanisms of DNA Oxidation. *Proceedings of the Society for Experimental Biology and Medicine*, *222*(3), 246–252. https://doi.org/https://doi.org/10.1046/j.1525-1373.1999.d01-141.x

Azam, T. A., & Ishihama, A. (1999). Twelve species of the nucleoid-associated protein from Escherichia coli. Sequence recognition specificity and DNA binding affinity. *Journal of Biological Chemistry*, *274*(46), 33105–33113. https://doi.org/10.1074/jbc.274.46.33105

Baker, E. S., & Bowers, M. T. (2007). B-DNA Helix Stability in a Solvent-Free Environment. *Journal of the American Society for Mass Spectrometry*, *18*(7), 1188–1195. https://doi.org/10.1016/J.JASMS.2007.03.001

Ball, Rebecca & Bajaj, Palak & Whitehead, Kathryn. (2016). Achieving long-term stability of lipid nanoparticles: Examining the effect of pH, temperature, and lyophilization. International Journal of Nanomedicine. Volume 12. 305-315. 10.2147/IJN.S123062.

Baltz, R. H., Bingham, P. M., & Drake, J. W. (1976). Heat mutagenesis in bacteriophage T4: the transition pathway. *Proceedings of the National Academy of Sciences*, *73*(4), 1269–1273. https://doi.org/10.1073/pnas.73.4.1269

De Barba, M., Miquel, C., Lobréaux, S., Quenette, P. Y., Swenson, J. E., & Taberlet, P. (2016). High-throughput microsatellite genotyping in ecology: improved accuracy, efficiency, standardization and success with low-quantity and degraded DNA. *Molecular Ecology Resources, 17*(3), 492–507. doi:10.1111/1755-0998.12594

Bailleul, A. M., & Li, Z. (2021). DNA staining in fossil cells beyond the Quaternary: Reassessment of the evidence and prospects for an improved understanding of DNA preservation in deep time. *Earth-Science Reviews, 216*, 103600. doi:10.1016/j.earscirev.2021.103600

Barker, S., Weinfeld, M., & Murray, D. (2005). DNA–protein crosslinks: their induction, repair, and biological consequences. *Mutation Research/Reviews in Mutation Research*, *589*(2), 111–135. https://doi.org/10.1016/J.MRREV.2004.11.003

Barra, G. B., Santa Rita, T. H., Vasques, J. de A., Chianca, C. F., Nery, L. F. A., & Costa, S. S. S. (2015). EDTA-mediated inhibition of DNases protects circulating cell-free DNA from ex vivo degradation in blood samples. *Clinical Biochemistry*, *48*(15), 976–981. https://doi.org/10.1016/j.clinbiochem.2015.02.014

Barth, H., Morel, A., Mougin, C., Averous, G., Legrain, M., Fender, M., Risch, S., Fafi-Kremer, S., Velten, M., Oudet, P., Baldauf, J. J., & Stoll-Keller, F. (2016). Long-term storage and safe retrieval of human papillomavirus DNA using FTA elute cards. *Journal of Virological Methods*, *229*, 60–65. https://doi.org/10.1016/j.jviromet.2015.12.010

Basu, A. K., Loechler, E. L., Leadon, S. A., & Essigmann, J. M. (1989). Genetic effects of thymine glycol: site-specific mutagenesis and molecular modeling studies. *Proceedings of the National Academy of Sciences*, *86*(20), 7677-7681. https://doi.org/10.1073/pnas.86.20.7677

Becker, M. M., & Wang, Z. (1989). Origin of ultraviolet damage in DNA. *Journal of Molecular Biology*, *210*(3), 429–438. https://doi.org/10.1016/0022-2836(89)90120-4

Berg, J. M., Tymoczko, J. L., & Stryer, L. (2002). *DNA Can Assume a Variety of Structural Forms*. In W. Freeman (Ed.), *Biochemistry* (5th ed.). W H Freeman. https://www.ncbi.nlm.nih.gov/books/NBK22585/

Beyerle, E. R. Dinpajooh, M., Ji, H., von Hippel, P. H., Marcus, A. H., & Guenza, M. G. (2021). Dinucleotides as simple models of the base stacking-unstacking component of DNA 'breathing'mechanisms. *Nucleic acids research, 49*(4), 1872-1885. https://doi.org/10.1093/nar/gkab015

Boiteux S., & Guillet, M. (2004). Abasic sites in DNA: repair and biological consequences in Saccharomyces cerevisiae. *DNA repair*, *3*(1), 1-12. https://doi.org/10.1016/j.dnarep.2003.10.002.

Bonner, G., & Klibanov, A. M. (2000). Structural stability of DNA in nonaqueous solvents. *Biotechnology and Bioengineering*, *68*(3), 339–344.

Boom, R. C. J. A., Sol, C. J., Salimans, M. M., Jansen, C. L., Wertheim-van Dillen, P. M., & Van der Noordaa, J. P. M. E. (1990). Rapid and simple method for purification of nucleic acids. *Journal of clinical microbiology, 28*(3), 495-503. https://doi.org/10.1128/jcm.28.3.495-503.1990

Borde, Y. M., Tonnany, M. B., & Champod, C. (2008). A Study on the Effects of Immersion in River Water and Seawater on Blood, Saliva, and Sperm Placed on Objects Mimicking Crime Scene Exhibits. *Canadian Society of Forensic Science Journal*, *41*(3), 149–163. https://doi.org/10.1080/00085030.2008.10757172

Brogna, R., Fan, J., Sieme, H., Wolkers, W. F., & Oldenhof, H. (2021). Drying and temperature induced conformational changes of nucleic acids and stallion sperm chromatin in trehalose preservation formulations. *Scientific Reports, 11*(1), 1-13. https://doi.org/10.1038/s41598-021-93569-y

Bundgaard-Nielsen, C., Hagstrøm, S., & Sørensen, S. (2018). Interpersonal Variations in Gut Microbiota Profiles Supersedes the Effects of Differing Fecal Storage Conditions. *Scientific Reports*, *8*(1), 17367. https://doi.org/10.1038/s41598-018-35843-0

Burgos, G., Flores-Espinoza, R., Ruiz-Pozo, V. A., & Villacrés Granda, I. (2019). Efficient preservation of DNA extracted from blood in FTA cards by Chelex method. *Forensic Science International: Genetics Supplement Series*, *7*(1), 539–541. https://doi.org/10.1016/j.fsigss.2019.10.082

Cadet, J., & Davies, K. J. A. (2017). Oxidative DNA damage & repair: An introduction. *Free Radical Biology and Medicine*, *107*, 2–12. https://doi.org/https://doi.org/10.1016/j.freeradbiomed.2017.03.030

Cadet, J., Delatour, T., Douki, T., Gasparutto, D., Pouget, J.-P., Ravanat, J.-L., & Sauvaigo, S. (1999). Hydroxyl radicals and DNA base damage. *Mutation Research/Fundamental and Molecular Mechanisms of Mutagenesis*, *424*(1), 9–21. https://doi.org/https://doi.org/10.1016/S0027-5107(99)00004-4

Calhoun, L. N., & Kwon, Y. M. (2011). Structure, function and regulation of the DNA-binding protein Dps and its role in acid and oxidative stress resistance in Escherichia coli: A review. In *Journal of Applied Microbiology*, 110(2), 375–386. https://doi.org/10.1111/j.1365-2672.2010.04890.x

Calsou, P., Frit, P., & Salles, B. (1996). Double Strand Breaks in DNA Inhibit Nucleotide Excision Repair in Vitro. *Journal of Biological Chemistry*, *271*(44), 27601–27607. https://doi.org/10.1074/jbc.271.44.27601

Camacho-Sanchez, M., Burraco, P., Gomez-Mestre, I., & Leonard, J. A. (2013). Preservation of RNA and DNA from mammal samples under field conditions. *Molecular Ecology Resources*, *13*(4), 663–673. https://doi.org/https://doi.org/10.1111/1755-0998.12108

Cannan, W. J., & Pederson, D. S. (2016). Mechanisms and Consequences of Double-Strand DNA Break Formation in Chromatin. *Journal of cellular physiology*, *231*(1), 3–14. https://doi.org/10.1002/jcp.25048

Cannon-Carlson, S. V, Gokhale, H., & Teebor, G. W. (1989). Purification and Characterization of 5-Hydroxymethyluracil-DNA Glycosylase from Calf Thymus: Its possible role in the maintenance of methylated cytosine residues. *Journal of Biological Chemistry*, *264*(22), 13306–13312. https://doi.org/https://doi.org/10.1016/S0021-9258(18)51629-X

Cano, R. J. (1996). Analysing ancient DNA. *Endeavour*, *20*(4), 162–167. https://doi.org/https://doi.org/10.1016/S0160-9327(96)10031-4

Ceci, P., Cellai, S., Falvo, E., Rivetti, C., Rossi, G.L., Chiancone, E. (2004). DNA condensation and self-aggregation of Escherichia coli Dps are coupled phenomena related to the properties of the N-terminus. *Nucleic Acids Research 32*(19), 5935–5944. doi:10.1093/nar/gkh915

Chen, Y., Geng, A., Zhang, W., Qian, Z., Wan, X., Jiang, Y., & Mao, Z. (2020). Fight to the bitter end: DNA repair and aging. *Ageing Research Reviews*, *64*, 101154. https://doi.org/https://doi.org/10.1016/j.arr.2020.101154

Cheng, K. C., Cahill, D. S., Kasai, H., Nishimura, S., & Loeb, L. A. (1992). 8-Hydroxyguanine, an abundant form of oxidative DNA damage, causes G-T and A-C substitutions. *Journal of Biological Chemistry*, *267*(1), 166–172. https://doi.org/https://doi.org/10.1016/S0021-9258(18)48474-8

Chiancone, E. (2008). Dps proteins, an efficient detoxification and DNA protection machinery in the bacterial response to oxidative stress. *Rendiconto Lincei 19*(3), 261 https://doi.org/10.1007/s12210-008-0018-4

Choo, J. M., Leong, L. E. X., & Rogers, G. B. (2015). Sample storage conditions significantly influence faecal microbiome profiles. *Scientific Reports*, *5*(1), 1-10. https://doi.org/10.1038/srep16350

Chowdhury, R. P., Vijayabaskar, M. S., Vishveshwara, S., & Chatterji, D. (2008). Molecular mechanism of in vitro oligomerization of Dps from Mycobacterium smegmatis: Mutations of the residues identified by "interface cluster" analysis. *Biochemistry*, *47*(42), 11110–11117. https://doi.org/10.1021/bi801158e

Colotte, M., Coudy, D., Tuffet, S., & Bonnet, J. (2011). Adverse Effect of Air Exposure on the Stability of DNA Stored at Room Temperature. *Biopreservation and Biobanking*, *9*(1), 47–50. https://doi.org/10.1089/bio.2010.0028

Cooke, M. S., Evans, M. D., Dizdaroglu, M., & Lunec, J. (2003). Oxidative DNA damage: mechanisms, mutation, and disease. *The FASEB Journal*, *17*(10), 1195–1214. https://doi.org/https://doi.org/10.1096/fj.02-0752rev

Coolen, M. J. L., Orsi, W. D., Balkema, C., Quince, C., Harris, K., Sylva, S. P., Filipova-Marinova, M., & Giosan, L. (2013). Evolution of the plankton paleome in the Black Sea from the Deglacial to Anthropocene. *Proceedings of the National Academy of Sciences*, *110*(21), 8609-8614. https://doi.org/10.1073/pnas.1219283110

Cooper, V. R., Thonhauser, T., Puzder, A., Schröder, E., Lundqvist, B. I., & Langreth, D. C. (2008). Stacking interactions and the twist of DNA. *Journal of the American Chemical Society*, *130*(4), 1304–1308. https://doi.org/10.1021/ja0761941

Coppola, L., Cianflone, A., Grimaldi, A. M., Incoronato, M., Bevilacqua, P., Messina, F., Baselice, S., Soricelli, A., Mirabelli, P., & Salvatore, M. (2019). Biobanking in health care: evolution and future directions. *Journal of translational medicine*, *17*(1), 172. https://doi.org/10.1186/s12967-019-1922-3

Corradini, B., Alù, M., Magnanini, E., Galinier, M. E., & Silingardi, E. (2019). The importance of forensic storage support: DNA quality from 11-year-old saliva on FTA cards. *International Journal of Legal Medicine*, *133*(6), 1743–1750. https://doi.org/10.1007/s00414-019-02146-6

Coulibaly, F., Chiu, E., Ikeda, K., Gutmann, S., Haebel, P. W., Schulze-Briese, C., Mori, H., & Metcalf, P. (2007). The molecular organization of cypovirus polyhedra. *Nature*, *446* (7131), 97–101. https://doi.org/10.1038/nature05628

da Cunha Santos, G. (2018). FTA Cards for Preservation of Nucleic Acids for Molecular Assays: A Review on the Use of Cytologic/Tissue Samples. *Archives of Pathology & Laboratory Medicine*, *142*(3), 308–312. https://doi.org/10.5858/arpa.2017-0303-RA

Dąbkowska, I., Gonzalez, H. V., Jurečka, P., & Hobza, P. (2005). Stabilization Energies of the Hydrogen-Bonded and Stacked Structures of Nucleic Acid Base Pairs in the Crystal Geometries of CG, AT, and AC DNA Steps and in the NMR Geometry of the 5‘-d(GCGAAGC)-3‘ Hairpin: Complete Basis Set Calculations at the MP2 and CCSD (T) levels. *The Journal of Physical Chemistry A*, *109*(6), 1131–1136. https://doi.org/10.1021/jp046738a

Dabrowska, N., & Wiczkowski, A. (2017). Analytics of oxidative stress markers in the early diagnosis of oxygen DNA damage. *Advances in Clinical and Experimental Medicine, 26*(1), 155-166. https://doi.org/10.17219/acem/43272

Dadinova, L. A., Chesnokov, Y. M., Kamyshinsky, R. A., Orlov, I. A., Petoukhov, M. V., Mozhaev, A. A., Soshinskaya, E. Y., Lazarev, V. N., Manuvera, V. A., Orekhov, A. S., Vasiliev, A. L., & Shtykova, E. V. (2019). Protective Dps–DNA co-crystallization in stressed cells: an in vitro structural study by small-angle X-ray scattering and cryo-electron tomography. *FEBS Letters*, *593*(12), 1360–1371. https://doi.org/10.1002/1873-3468.13439

Davis, D. L., O’Brie, E. P., & Bentzley, C. M. (2000). Analysis of the Degradation of Oligonucleotide Strands During the Freezing/Thawing Processes Using MALDI-MS. *Analytical Chemistry*, *72*(20), 5092–5096. https://doi.org/10.1021/ac000225s

da Cunha Santos, G. (2018). FTA cards for preservation of nucleic acids for molecular assays a review on the use of cytologic/tissue samples. *Archives of Pathology and Laboratory Medicine, (3),* 308–312. https://doi.org/10.5858/arpa.2017-0303-RA

Deagle, B.E., Eveson, J.P. & Jarman, S.N. (2006). Quantification of damage in DNA recovered from highly degraded samples – a case study on DNA in faeces. *Frontiers Zoology 3*(1)**,** 1-10. https://doi.org/10.1186/1742-9994-3-11

Dentinger Bryn T.M. ; Margaritescu Simona ; Moncalvo Jean-Marc (2010). Rapid and reliable high- throughput methods of DNA extraction for use in barcoding and molecular systematics of mushrooms. , 10(4), 628–633. doi:10.1111/j.1755-0998.2009.02825.x Der Sarkissian, C., Allentoft, M. E., Ávila-Arcos, M. C., Barnett, R., Campos, P. F., Cappellini, E., Ermini, L., Fernández, R., da Fonseca, R., Ginolhac, A., Hansen, A. J., Jónsson, H., Korneliussen, T., Margaryan, A., Martin, M. D., Moreno-Mayar, J. V., Raghavan, M., Rasmussen, M., Velasco, M. S., Schroeder, H., … Orlando, L. (2015). Ancient genomics. *Philosophical transactions of the Royal Society of London. Series B, Biological sciences*, *370*(1660), 20130387. https://doi.org/10.1098/rstb.2013.0387

de Rosa, M., de Sanctis, D., Rosario, A. L., Archer, M., Rich, A., Athanasiadis, A., & Carrondo, M. A. (2010). Crystal structure of a junction between two Z-DNA helices. *Proceedings of the National Academy of Sciences*, *107*(20), 9088-9092. https://doi.org/10.1073/pnas.1003182107

de Vargas Wolfgramm, E., de Carvalho, F. M., da Costa Aguiar, V. R., de Nadai Sartori, M. P., Hirschfeld-Campolongo, G. C. R., Tsutsumida, W. M., & Louro, I. D. (2009). Simplified buccal DNA extraction with FTA® Elute Cards. *Forensic Science International: Genetics*, *3*(2), 125–127. https://doi.org/10.1016/j.fsigen.2008.11.008

deWaard, J. R., Ivanova, N. V., Hajibabaei, M., & Hebert, P. D. N. (2008). Assembling DNA Barcodes. *Methods in Molecular Biology (Clifton, N.J.)*, *410*, 275–294. https://doi.org/10.1007/978-1-59745-548-0_15

Dizdaroglu, M., Kirkali, G., & Jaruga, P. (2008). Formamidopyrimidines in DNA: Mechanisms of formation, repair, and biological effects. *Free Radical Biology and Medicine*, *45*(12), 1610–1621. https://doi.org/10.1016/J.FREERADBIOMED.2008.07.004

Dizdaroglu, M., Von Sonntag, C., & Schulte-Frohlinde, D. (1975). Strand breaks and sugar release by .gamma.-irradiation of DNA in aqueous solution. *Journal of the American Chemical Society*, *97*(8), 2277–2278. https://doi.org/10.1021/ja00841a051

Do, H., & Dobrovic, A. (2015). Sequence artifacts in DNA from formalin-fixed tissues: Causes and strategies for minimization. *Clinical Chemistry*, *61*(1), 64-71 .https://doi.org/10.1373/clinchem.2014.223040

Dobbs, T. A., Palmer, P., Maniou, Z., Lomax, M. E., & O'Neill, P. (2008). Interplay of two major repair pathways in the processing of complex double-strand DNA breaks. *DNA Repair*, *7*(8), 1372–1383. https://doi.org/10.1016/J.DNAREP.2008.05.001

Dong, Y., Sun, F., Ping, Z., Ouyang, Q., & Qian, L. (2020). DNA storage: research landscape and future prospects. *National Science Review*, *7*(6), 1092–1107. https://doi.org/10.1093/nsr/nwaa007

Driessen RP, Sitters G, Laurens N, et al. Effect of temperature on the intrinsic flexibility of DNA and its interaction with architectural proteins. *Biochemistry*. 2014;53(41):6430-6438. doi:10.1021/bi500344j

Dubrovin, E. V., Dadinova, L. A., Petoukhov, M. V., Soshinskaya, E. Y., Mozhaev, A. A., Klinov, D. V., Schaffer, E., Shtykova, E. & Batishchev, O. V. (2021). Spatial organization of Dps and DNA–Dps complexes. *Journal of Molecular Biology*, *433*(10), 166930. https://doi.org/10.1016/j.jmb.2021.166930

Durmaz, R., Otlu, B., & Direkel, S. (2002). Effect of multiple freezing and thawing of serum on TT virus and hepatitis B virus DNA positivity. *Archives of Virology*, *147*(3), 515–518. https://doi.org/10.1007/s007050200003

Elkins, K., Kadunc, R. E., Mann, G. R., & McLaughlin, S. (2009). Comparison Of Quantity And Quality Of DNA Recovered From Burn Samples In Which Burn Temperatures And Conditions Were Varied. *Internet J. Forensic Sci.,* 4.

Evans, M. D., Dizdaroglu, M., & Cooke, M. S. (2004). Oxidative DNA damage and disease: induction, repair and significance. *Mutation Research/Reviews in Mutation Research*, *567*(1), 1–61. https://doi.org/10.1016/j.mrrev.2003.11.001

Evans, R. K., Xu, Z., Bohannon, K. E., Wang, B., Bruner, M. W., & Volkin, D. B. (2000). Evaluation of Degradation Pathways for Plasmid DNA in Pharmaceutical Formulations via Accelerated Stability Studies. *Journal of Pharmaceutical Sciences*, *89*(1), 76–87. https://doi.org/10.1002/(SICI)1520-6017(200001)89:1<76::AID-JPS8>3.0.CO;2-U

Extance, A. (2016). How DNA could store all the world's data. *Nature News 537* (7618), 22.

Facey, P. D., Hitchings, M. D., Williams, J. S., Skibinski, D. O., Dyson, P. J., & Del Sol, R. (2013). The evolution of an osmotically inducible Dps in the genus Streptomyces. *PloS one*, *8*(4), e60772. https://doi.org/10.1371/journal.pone.0060772

Frantzen, M. A. J., Silk, J. B., Ferguson, J. W. H., Wayne, R. K., & Kohn, M. H. (1998). Empirical evaluation of preservation methods for faecal DNA. *Molecular Ecology, 7(10),* 1423-1428. https://doi.org/10.1046/j.1365-294x.1998.00449.x

Frenkiel-Krispin, D., & Minsky, A. (2006). Nucleoid organization and the maintenance of DNA integrity in E. coli, B. subtilis and D. radiodurans. *Journal of Structural Biology, 156*(2), 311-319 https://doi.org/10.1016/j.jsb.2006.05.014

Figueroa-González, G., & Figueroa-González, G. (2017). Strategies for the evaluation of DNA damage and repair mechanisms in cancer. *Oncology Letters, 13*(6) 3982-3988. https://doi.org/10.3892/ol.2017.6002

Frippiat, C., Zorbo, S., Leonard, D., Marcotte, A., Chaput, M., Aelbrecht, C., & Noel, F. (2011). Evaluation of novel forensic DNA storage methodologies. *Forensic Science International: Genetics*, *5*(5), 386–392. https://doi.org/10.1016/j.fsigen.2010.08.007

Fu, Xuebing. (2008). How trehalose protects DNA in the dry state: A molecular dynamics simulation. Doctoral dissertation. Texas A&M University. https://hdl.handle.net/1969.1/86002

Gao G., Li J., Zhang Y., Chang YZ. (2019) Cellular Iron Metabolism and Regulation. In: Chang YZ. (eds) Brain Iron Metabolism and CNS Diseases. Advances in Experimental Medicine and Biology, vol 1173. Springer, Singapore. https://doi.org/10.1007/978-981-13-9589-5_2

García-Valverde, M., & Torroba, T. (2005). Sulfur-Nitrogen Heterocycles. *Molecules, 10*(2). https://doi.org/10.3390/10020318

Gauss, G. H., Benas, P., Wiedenheft, B., Young, M., Douglas, T., & Lawrence, C. M. (2006). Structure of the Dps-like protein from Sulfolobus solfataricus reveals a bacterioferritin-like dimetal binding site within a Dps-like dodecameric assembly. *Biochemistry*, *45*(36), 10815–10827. https://doi.org/10.1021/bi060782u

GE Health Care (2013) Nucleic Acid Sample Preparation for Downstream Analyses

Ghatak, P., Karmakar, K., Kasetty, S., & Chatterji, D. (2011). Unveiling the Role of Dps in the Organization of Mycobacterial Nucleoid. *PLoS ONE*, *6*(1), 16019. https://doi.org/10.1371/journal.pone.0016019

Goldberg, I. H. (1987). Free radical mechanisms in neocarzinostatin-induced DNA damage. *Free Radical Biology and Medicine*, *3*(1), 41–54. https://doi.org/10.1016/0891-5849(87)90038-4

Grant, R. A., Filman, D. J., Finkel, S. E., Kolter, R., & Hogle, J. M. (1998). The crystal structure of Dps, a ferritin homolog that binds and protects DNA. *Nature Structural Biology*, *5*(4), 294–303.

Gray, M. A., Pratte, Z. A., & Kellogg, C. A. (2013). Comparison of DNA preservation methods for environmental bacterial community samples. *FEMS Microbiology Ecology*, *83*(2), 468–477. https://doi.org/10.1111/1574-6941.12008

Green, H., Tillmar, A., Pettersson, G., & Montelius, K. (2019). The use of FTA cards to acquire DNA profiles from postmortem cases. *International Journal of Legal Medicine*, *133*(6), 1651–1657. https://doi.org/10.1007/s00414-019-02015-2

Gupta, S., & Chatterji, D. (2003). Bimodal protection of DNA by Mycobacterium smegmatis DNA-binding protein from stationary phase cells. *Journal of Biological Chemistry*, *278*(7), 5235–5241. https://doi.org/10.1074/jbc.M208825200

Gutaker, R. M., & Burbano, H. A. (2017). Reinforcing plant evolutionary genomics using ancient DNA. *Current Opinion in Plant Biology*, *36*, 38–45. https://doi.org/10.1016/J.PBI.2017.01.002

Gyuri Park, Byunghwa Kang, Soyeon V Park, Donghwa Lee, Seung Soo Oh, A unified computational view of DNA duplex, triplex, quadruplex and their donor–acceptor interactions, *Nucleic Acids Research*, Volume 49, Issue 9, 21 May 2021, Pages 4919–4933 https://doi.org/10.1093/nar/gkab285

Hailemariam, Z., Ahmed, J. S., Clausen, P. H., & Nijhof, A. M. (2017). A comparison of DNA extraction protocols from blood spotted on FTA cards for the detection of tick-borne pathogens by Reverse Line Blot hybridization. *Ticks and Tick-Borne Diseases*, *8*(1), 185–189. https://doi.org/10.1016/J.TTBDIS.2016.10.016

Hajibabaei, M., deWaard, J. R., Ivanova, N. V, Ratnasingham, S., Dooh, R. T., Kirk, S. L., Mackie, P. M., & Hebert, P. D. N. (2005). Critical factors for assembling a high volume of DNA barcodes. *Philosophical Transactions of the Royal Society B: Biological Sciences*, *360*(1462), 1959–1967. https://doi.org/10.1098/rstb.2005.1727

Hallmaier-Wacker, L. K., Lueert, S., Roos, C., & Knauf, S. (2018). The impact of storage buffer, DNA extraction method, and polymerase on microbial analysis. *Scientific Reports*, *8*(1), 6292. https://doi.org/10.1038/s41598-018-24573-y

Hansen, A. J., Mitchell, D. L., Wiuf, C., Paniker, L., Brand, T. B., Binladen, J., Gilichinsky, D. A., Rønn, R., & Willerslev, E. (2006). Crosslinks Rather Than Strand Breaks Determine Access to Ancient DNA Sequences From Frozen Sediments. *Genetics*, *173*(2), 1175–1179. https://doi.org/10.1534/genetics.106.057349

Hara, J., Tottori, J., Anders, M., Dadhwal, S., Asuri, P., & Mobed-Miremadi, M. (2017). Trehalose effectiveness as a cryoprotectant in 2D and 3D cell cultures of human embryonic kidney cells. *Artificial Cells, Nanomedicine and Biotechnology*, *45*(3), 609–616. https://doi.org/10.3109/21691401.2016.1167698

Harrel Michelle, Mayes Carrie, Houston Rachel, Holmes Amy S., Gutierrez Ryan, Hughes Sheree (2021) The performance of quality controls in the Investigator® Quantiplex® Pro RGQ and Investigator® 24plex STR kits with a variety of forensic samples. *Forensic Science International: Genetics*, *55*,102586. https://doi.org/10.1016/j.fsigen.2021.102586

Hashimoto, S., Anai, H. & Hanada, K. (2016) Mechanisms of interstrand DNA crosslink repair and human disorders. *Genes and Environment 38*(1), 1-8. https://doi.org/10.1186/s41021-016-0037-9

Hedges, R. E. M., & Millard, A. R. (1995). Bones and Groundwater: Towards the Modelling of Diagenetic Processes. *Journal of Archaeological Science*, *22*(2), 155–164. https://doi.org/10.1006/JASC.1995.0017

Hébraud Michel; Guzzo Jean (2000). The main cold shock protein of Listeria monocytogenes belongs to the family of ferritin-like proteins. ,190(1), 29–34. doi:10.1111/j.1574-

Herbert A. (2019). A Genetic Instruction Code Based on DNA Conformation. *Trends in Genetics*, *35*(12), 887–890. https://doi.org/10.1016/j.tig.2019.09.007

Herbert, A., Karapetyan, S., Poptsova, M., Vasquez, K. M., Vicens, Q., & Vögeli, B. (2021). Special Issue: A, B and Z: The Structure, Function and Genetics of Z-DNA and Z-RNA. *International journal of molecular sciences*, *22*(14), 7686. https://doi.org/10.3390/ijms22147686

Hewitt, S. M., Lewis, F. A., Cao, Y., Conrad, R. C., Cronin, M., Danenberg, K. D., Goralski, T. J., Langmore, J. P., Raja, R. G., Williams, P. Mickey, Palma, J. F., & Warrington, J. A. (2008). Tissue Handling and Specimen Preparation in Surgical Pathology Issues Concerning the Recovery of Nucleic Acids From Formalin-Fixed, Paraffin-Embedded Tissue. *Archives of Pathology & Laboratory Medicine, 132*(12), 1929-1935 https://doi.org/10.1043/1543-2165-132.12.1929

Hofreiter, M., Jaenicke, V., Serre, D., Haeseler, A. von, & Pääbo, S. (2001). DNA sequences from multiple amplifications reveal artifacts induced by cytosine deamination in ancient DNA. *Nucleic Acids Research*, *29*(23), 4793. https://doi.org/10.1093/NAR/29.23.4793

Holmes, A. S., Roman, M. G., & Hughes-Stamm, S. (2018). In-field collection and preservation of decomposing human tissues to facilitate rapid purification and STR typing. *Forensic Science International: Genetics*, *36*, 124–129. https://doi.org/10.1016/J.FSIGEN.2018.06.015

Hori, M., Yonei, S., Sugiyama, H., Kino, K., Yamamoto, K., & Zhang, Q. (2003). Identification of high excision capacity for 5-hydroxymethyluracil mispaired with guanine in DNA of Escherichia coli MutM, Nei and Nth DNA glycosylases . *Nucleic Acids Research*, *31*(4), 1191–1196. https://doi.org/10.1093/nar/gkg223

Hormeño, S., Ibarra, B., Valpuesta, J. M., Carrascosa, J. L., & Arias-Gonzalez, J. R. (2012). Mechanical stability of low-humidity single DNA molecules. *Biopolymers*, *97*(4), 199–208. https://doi.org/10.1002/BIP.21728

Hormeño, S., Moreno-Herrero, F., Ibarra, B., Carrascosa, J. L., Valpuesta, J. M., & Arias-Gonzalez, J. R. (2011). Condensation Prevails over B-A Transition in the Structure of DNA at Low Humidity. *Biophysical Journal*, *100*(8), 2006. https://doi.org/10.1016/J.BPJ.2011.02.049

Horst, J. P., & Fritz, H. J. (1996). Counteracting the mutagenic effect of hydrolytic deamination of DNA 5-methylcytosine residues at high temperature: DNA mismatch N-glycosylase

Mig.Mth of the thermophilic archaeon Methanobacterium thermoautotrophicum THF. *The EMBO Journal*, *15*(19), 5459–5469. https://doi.org/https://doi.org/10.1002/j.1460-2075.1996.tb00929.x

Howlett, S. E., Castillo, H. S., Gioeni, L. J., Robertson, J. M., & Donfack, J. (2014). Evaluation of DNAstable™ for DNA storage at ambient temperature. *Forensic Science International: Genetics*, *8*(1), 170–178. https://doi.org/10.1016/J.FSIGEN.2013.09.003

Huang, R., Zhou, PK. (2021). DNA damage repair: historical perspectives, mechanistic pathways and clinical translation for targeted cancer therapy. *Signal Transduction Targeted Therapy, 6*(1), 1-35 https://doi.org/10.1038/s41392-021-00648-7

Hubel, A., Spindler, R., & Skubitz, A. P. N. (2014). Storage of human biospecimens: Selection of the optimal storage temperature. *Biopreservation and Biobanking, 12*(3), 165-175 https://doi.org/10.1089/bio.2013.0084

Hussain, S. O., Shahad, H. K., & Al-Badry, K. I. (2016). Effect of dilution, cooling and freezing on physical and biochemical properties of semen for holstein bull Born in Iraq. *Advances in Animal and Veterinary Sciences*, *4*(11), 575–579. https://doi.org/10.14737/JOURNAL.AAVS/2016/4.11.575.579

Hyde, E. R., Lozano, H., & Cox, S. (2020). BIOME-Preserve: A Novel Storage and Transport Medium for Preserving Anaerobic Microbiota Samples for Culture Recovery. *bioRxiv* https://doi.org/10.1101/2020.12.07.415638

Khimji, I., Shin, J., & Liu, J. (2013). DNA duplex stabilization in crowded polyanion solutions. *Chemical Communications*, *49*(13), 1306-1308. https://doi.org/10.1039/C2CC38627E

Immel, A., Le Cabec, A., Bonazzi, M., Herbig, A., Temming, H., Schuenemann, V. J., ... & Krause, J. (2016). Effect of X-ray irradiation on ancient DNA in sub-fossil bones–Guidelines for safe X-ray imaging. *Scientific reports*, *6*(1), 1-14. https://doi.org/10.1038/srep32969

Ivanova, N. v., & Kuzmina, M. L. (2013). Protocols for dry DNA storage and shipment at room temperature. *Molecular Ecology Resources*, *13*(5), 890–898. https://doi.org/10.1111/1755-0998.12134

Iturriaga, G., Suárez, R., & Nova-Franco, B. (2009). Trehalose metabolism: from osmoprotection to signaling. *International journal of molecular sciences*, *10*(9), 3793-3810. https://doi.org/10.3390/ijms10093793

Jacinto, J. P., Penas, D., Guerra, J. P., Almeida, A. V., Jones, N. C., Hoffmann, S. V., Tavares, P., & Pereira, A. S. (2021). Dps–DNA interaction in Marinobacter hydrocarbonoclasticus

protein: effect of a single-charge alteration. *European Biophysics Journal*, 1-9. https://doi.org/10.1007/s00249-021-01538-0

Jeong, K. C., Hung, K. F., Baumler, D. J., Byrd, J. J., & Kaspar, C. W. (2008). Acid stress damage of DNA is prevented by Dps binding in Escherichia coli O157: H7. *BMC microbiology*, *8*(1), 1-13. https://doi.org/10.1186/1471-2180-8-181

Jayaram, B., Sprous, D., Young, M. A., & Beveridge, D. L. (1998). Free Energy Analysis of the Conformational Preferences of A and B Forms of DNA in Solution. *Journal of the American Chemical Society, 120*(41), 10629–10633. doi:10.1021/ja981307p

Kaczmarek, Roszkowska, M., Fontaneto, D., Jezierska, M., Pietrzak, B., Wieczorek, R., Poprawa, I., Kosicki, J. Z., Karachitos, A., & Kmita, H. (2019). Staying young and fit? Ontogenetic and phylogenetic consequences of animal anhydrobiosis. *Journal of Zoology, 309*(1), 1-11. https://doi.org/10.1111/jzo.12677

Kamiya, H. (2004). Mutagenicities of 8-Hydroxyguanine and 2-Hydroxyadenine Produced by Reactive Oxygen Species. *Biological and Pharmaceutical Bulletin*, *27*(4), 475–479. https://doi.org/10.1248/bpb.27.475

Kaplan, M. (2012). DNA has a 521-year half-life. *Nature News, 10*. https://doi.org/10.1038/nature.2012.11555

Karas, V. O., Westerlaken, I., & Meyer, A. S. (2015). The DNA-binding protein from starved cells (Dps) utilizes dual functions to defend cells against multiple stresses. *Journal of Bacteriology*, *197*(19), 3206–3215. https://doi.org/10.1128/JB.00475-15

Karimi-Busheri, F., Lee, J., Tomkinson, A. E., & Weinfeld, M. (1998). Repair of DNA strand gaps and nicks containing 3'-phosphate and 5'-hydroxyl termini by purified mammalian enzymes. *Nucleic Acids Research*, *26*(19), 4395. https://doi.org/10.1093/NAR/26.19.4395

Karino, N., Ueno, Y., & Matsuda, A. (2001). Synthesis and properties of oligonucleotides containing 5-formyl-2′-deoxycytidine: in vitro DNA polymerase reactions on DNA templates containing 5-formyl-2′-deoxycytidine. *Nucleic Acids Research*, *29*(12), 2456–2463. https://doi.org/10.1093/nar/29.12.2456

Karni, M., Zidon, D., Polak, P., Zalevsky, Z., & Shefi, O. (2013). Thermal Degradation of DNA. *DNA and Cell Biology*, *32*(6), 298–301. https://doi.org/10.1089/dna.2013.2056

Kasprzak, K. S., Jaruga, P., Zastawny, T. H., North, S. L., Riggs, C. W., Olinski, R., & Dizdaroglu, M. (1997). Oxidative DNA base damage and its repair in kidneys and livers of nickel(II)-treated male F344 rats. *Carcinogenesis*, *18*(2), 271–277. https://doi.org/10.1093/carcin/18.2.271

Kowalska, M., Piekut, T., Prendecki, M., Sodel, A., Kozubski, W., & Dorszewska, J. (2020). Mitochondrial and nuclear DNA oxidative damage in physiological and pathological aging. *DNA and cell biology, 39*(8), 1410-1420. https://doi.org/10.1089/dna.2019.5347

Kerfeld, C. A., & Erbilgin, O. (2015). Bacterial microcompartments and the modular construction of microbial metabolism. *Trends in Microbiology*, *23*(1), 22–34. https://doi.org/10.1016/J.TIM.2014.10.003

Kim, Chun. (2020). How Z-DNA/RNA binding proteins shape homeostasis, inflammation, and immunity. *BMB Reports*, *53*(9), 453–457. https://doi.org/10.5483/BMBREP.2020.53.9.141

Kim, Y., Li, H., He, Y., Chen, X., Ma, X., & Lee, M. (2017). Collective helicity switching of a DNA-coat assembly. *Nature Nanotechnology*, *12*(6), 551–556. https://doi.org/10.1038/nnano.2017.42

Klingström, T., Bongcam-Rudloff, E., & Pettersson, O. V. (2018). A comprehensive model of DNA fragmentation for the preservation of High Molecular Weight DNA. *BioRxiv*, 254276. https://doi.org/10.1101/254276

Knebelsberger, T., & Stöger, I. (2012). DNA extraction, preservation, and amplification. *Methods in Molecular Biology*, *858*, 311–338. https://doi.org/10.1007/978-1-61779-591-6_14

Kool, Eric T. (2001) Hydrogen Bonding, Base Stacking, and Steric Effects in DNA Replication, Annual Review of Biophysics and Biomolecular Structure, P 1-22,30. 30, 10.1146/annurev.biophys.30.1.1

Kool, Eric T.; Morales C. Juan; Guckian Kevin M (2000). *Mimicking the Structure and Function of DNA: Insights into DNA Stability and Replication, 39*(6), 990–1009. doi:10.1002/(sici)1521-3773(20000317)39:6<990::aid-anie990>3.0.co;2-0

Kosar, F., Akram, N. A., Sadiq, M., Al-Qurainy, F., & Ashraf, M. (2019). Trehalose: a key organic osmolyte effectively involved in plant abiotic stress tolerance. *Journal of Plant Growth Regulation*, *38*(2), 606-618. https://doi.org/10.1007/s00344-018-9876-x

Kreutzer, D. A., & Essigmann, J. M. (1998). Oxidized, deaminated cytosines are a source of C→ T transitions in vivo. *Proceedings of the National Academy of Sciences*, *95*(7), 3578-3582. https://doi.org/10.1073/pnas.95.7.3578

Kulstein, G., Schacker, U., & Wiegand, P. (2018). Old meets new: Comparative examination of conventional and innovative RNA-based methods for body fluid identification of laundered seminal fluid stains after modular extraction of DNA and RNA. *Forensic Science International: Genetics*, *36*, 130–140. https://doi.org/10.1016/J.FSIGEN.2018.06.017

Laage, D., Elsaesser, T., & Hynes, J. T. (2017). Water Dynamics in the Hydration Shells of Biomolecules. *Chemical Reviews*, *117*(16), 10694–10725. https://doi.org/10.1021/acs.chemrev.6b00765

Lamers, R., Hayter, S., & Matheson, C. D. (2009). Postmortem miscoding lesions in sequence analysis of human ancient mitochondrial DNA. *Journal of molecular evolution*, *68*(1), 40-55. doi:10.1007/s00239-008-9184-3

Latham, K. E., & Madonna, M. E. (2013). DNA survivability in skeletal remains. *Manual of forensic taphonomy*, 385-407. Retrieved July 20, 2021, from https://books.google.ca/books?hl=en&lr=&id=dQfSBQAAQBAJ&oi=fnd&pg=PA403&ots=-Jg8wwjoPp&sig=MLQPZ1tQvFsVrdX_uFuDfXJNiBk

Latham, K. E., & Miller, J. J. (2018). DNA recovery and analysis from skeletal material in modern forensic contexts. *Forensic Sciences Research*, *4*(1), 51–59. https://doi.org/10.1080/20961790.2018.1515594

Lee, S. B., Clabaugh, K. C., Silva, B., Odigie, K. O., Coble, M. D., Loreille, O., Scheible, M., Fourney, R. M., Stevens, J., Carmody, G. R., Parsons, T. J., Pozder, A., Eisenberg, A. J., Budowle, B., Ahmad, T., Miller, R. W., & Crouse, C. A. (2012). Assessing a novel room temperature DNA storage medium for forensic biological samples. *Forensic Science International: Genetics*, *6*(1), 31–40. https://doi.org/10.1016/j.fsigen.2011.01.008

Leprince, O., Buitink, J. (2015). Introduction to desiccation biology: from old borders to new frontiers. *Planta 242***,** 369–378. https://doi.org/10.1007/s00425-015-2357-6

Liang, R., Li, Z., Lau Vetter, M. C. Y., Vishnivetskaya, T. A., Zanina, O. G., Lloyd, K. G., Pfiffner, S. M., Rivkina, E. M., Wang, W., Wiggins, J., Miller, J., Hettich, R. L., & Onstott, T. C. (2021). Genomic reconstruction of fossil and living microorganisms in ancient Siberian permafrost. *Microbiome*, *9*(1). https://doi.org/10.1186/s40168-021-01057-2

Lindahl, T. (1993). Instability and decay of the primary structure of DNA. *Nature, 362*(6422), 709–715. https://doi.org/10.1038/362709a0

Lindahl, T., & Andersson, A. (2002). Rate of chain breakage at apurinic sites in double-stranded deoxyribonucleic acid. *Biochemistry*, *11*(19), 3618–3623. https://doi.org/10.1021/BI00769A019

Lindahl, T., & Wood, R. D. (1999). Quality Control by DNA Repair. *Science*, *286*(5446), 1897–1905. https://doi.org/10.1126/SCIENCE.286.5446.1897

Liu, J. (2019). Freezing DNA for Controlling Bio/nano Interfaces and Catalysis. *General Chemistry*, *5*(4).

Liu, T., Zhu, L., Zhang, Z., Huang, H., Zhang, Z., & Jiang, L. (2017). Protective role of trehalose during radiation and heavy metal stress in Aureobasidium subglaciale F134. *Scientific Reports*, *7*(1), 1–9. https://doi.org/10.1038/s41598-017-15489-0

Lodish H, Berk A, Zipursky SL, et al. Molecular Cell Biology. 4th edition. New York: W. H. Freeman; 2000. Section 4.1, Structure of Nucleic Acids. Available from: https://www.ncbi.nlm.nih.gov/books/NBK21514/

Loiko, N.G., Suzina, N.E., Soina, V.S. *et al.* Biocrystalline structures in the nucleoids of the stationary and dormant prokaryotic cells. *Microbiology* **86,** 714–727 (2017). https://doi.org/10.1134/S002626171706011X

Lorenz T. C. (2012). Polymerase chain reaction: basic protocol plus troubleshooting and optimization strategies. *Journal of visualized experiments : JoVE*, (63), e3998. https://doi.org/10.3791/3998

Lou, J. J., Mirsadraei, L., Sanchez, D.E, Wilson, R.W., Shabihkhani, M., Lucey, G.M., Wei, B., Singer, E.J., Mareninov, S., & Yong, W.H. (2014). A review of room temperature storage of biospecimen tissue and nucleic acids for anatomic pathology laboratories and biorepositories. *Clinical Biochemistry, 47*(4-5), 267-273. doi:10.1016/j.clinbiochem.2013.12.011

Luijsterburg, M. S., Noom, M. C., Wuite, G. J. L., & Dame, R. T. (2006). The architectural role of nucleoid-associated proteins in the organization of bacterial chromatin: A molecular perspective. *Journal of Structural Biology*, *156*(2), 262–272. https://doi.org/10.1016/J.JSB.2006.05.006

Luo, Y., Li, W. M., & Wang, W. (2008). Trehalose: Protector of antioxidant enzymes or reactive oxygen species scavenger under heat stress? *Environmental and Experimental Botany*, *63*(1–3), 378–384. https://doi.org/10.1016/J.ENVEXPBOT.2007.11.016

Mak, C. H. (2016). Unraveling base stacking driving forces in DNA. *The Journal of Physical Chemistry B, 120*(26), 6010-6020. doi:10.1021/acs.jpcb.6b01934

Matange, K., Tuck, J. M., & Keung, A. J. (2021). DNA stability: a central design consideration for DNA data storage systems. *Nature communications*, *12*(1), 1-9. https://doi.org/10.1038/s41467-021-21587-5

Malsagova, K., Kopylov, A., Stepanov, A., Butkova, T., Sinitsyna, A., Izotov, A., & Kaysheva, A. (2020). Biobanks—A Platform for Scientific and Biomedical Research. *Diagnostics*, *10*(7), 485. https://doi.org/10.3390/diagnostics10070485

Mas, S, Crescenti, A., Gassó, P., Vidal-Taboada, J. M., & Lafuente, A. (2007). DNA cards: determinants of DNA yield and quality in collecting genetic samples for pharmacogenetic studies. *Basic & clinical pharmacology & toxicology*, *101*(2), 132–137. https://doi.org/10.1111/j.1742-7843.2007.00089.x

Matange, K., Tuck, J. M., & Keung, A. J. (2021). DNA stability: a central design consideration for DNA data storage systems. *Nature communications, 12*(1), 1-9. https://doi.org/10.1038/s41467-021-21587-5

Matros, A., Peshev, D., Peukert, M., Mock, H. P., & van den Ende, W. (2015). Sugars as hydroxyl radical scavengers: Proof-of-concept by studying the fate of sucralose in Arabidopsis. *Plant Journal*, *82*(5), 822–839. https://doi.org/10.1111/tpj.12853

Mayr, E., & Provine, W. B. (1980). *The evolutionary synthesis* (Vol. 231). Cambridge, MA: Harvard University Press. https://doi.org/10.4159/harvard.9780674865389

McClure, M. C., McKay, S. D., Schnabel, R. D., & Taylor, J. F. (2009). Assessment of DNA extracted from FTA® cards for use on the Illumina iSelect BeadChip. *BMC Research Notes*, *2*(1), 1-4. https://doi.org/10.1186/1756-0500-2-107

Minato, T., Teramoto, T., Kakuta, Y., Ogo, S., & Yoon, K. S. (2020). Biochemical and structural characterization of a thermostable Dps protein with His-type ferroxidase centers and outer metal-binding sites. *FEBS open bio*, *10*(7), 1219-1229. https://doi.org/10.1002/2211-5463.12837

Mimitou, E. P., & Symington, L. S. (2009). DNA end resection: Many nucleases make light work. In *DNA Repair*, *8*(9), 983-995 https://doi.org/10.1016/j.dnarep.2009.04.017

Minsky, A., Shimoni, E., & Frenkiel-Krispin, D. (2002). Stress, order and survival. *Nature Reviews Molecular Cell Biology*, *3*(1), 50-60. https://doi.org/10.1038/nrm700

Mitchell, D., Willerslev, E., & Hansen, A. (2005). Damage and repair of ancient DNA. *Mutation Research/Fundamental and Molecular Mechanisms of Mutagenesis, 571*(1-2), 265–276. doi:10.1016/j.mrfmmm.2004.06.060

Miyabe, I., Zhang, Q.-M., Sugiyama, H., Kino, K., & Yonei, S. (2001). Mutagenic effects of 5-formyluracil on a plasmid vector during replication in Escherichia coli. *International Journal of Radiation Biology*, *77*(1), 53–58. https://doi.org/10.1080/095530001453113

MM, G. (2005). DNA interstrand cross-links from modified nucleotides: mechanism and application. *Nucleic Acids Symposium Series, 2004* (49), 57–58. https://doi.org/10.1093/NASS/49.1.57

Mohan, S Yathindra, N. (1991). Studies On The Cross Strand Hydrogen Bonds In DNA Double Helices. Journal of Biomolecular Structure and Dynamics, 9(1), 113–126. doi:10.1080/07391102.1991.10507897

Mol, C. D., Parikh, S. S., Putnam, C. D., Lo, T. P., & Tainer, J. A. (1999). DNA Repair Mechanisms for the Recognition and Removal of Damaged DNA Bases. *Annual Review of Biophysics and Biomolecular Structure*, *28*(1), 101–128. https://doi.org/10.1146/annurev.biophys.28.1.101

Morano, K. A. (2014). Anhydrobiosis: Drying out with sugar. *Current Biology, 24(*23), R1121-R1123 https://doi.org/10.1016/j.cub.2014.10.022

Nair, S., & Finkel, S. E. (2004). Dps protects cells against multiple stresses during stationary phase. *Journal of bacteriology*, *186*(13), 4192–4198. https://doi.org/10.1128/JB.186.13.4192-4198.2004

Nakahama, N., Isagi, Y., & Ito, M. (2019). Methods for retaining well-preserved DNA with dried specimens of insects. *European Journal of Entomology*, *116*, 486-491.

Nakamura, J., & Swenberg, J. A. (1999). Endogenous Apurinic/Apyrimidinic Sites in Genomic DNA of Mammalian Tissues. *Cancer Research*, *59*(11), 2522-2526. http://cancerres.aacrjournals.org/content/59/11/2522.abstract

Nakayama, Y., Yamaguchi, H., Einaga, N., Esumi,M., & Fujii, H. (2016). Pitfalls of DNA Quantification Using DNA-Binding Fluorescent Dyes and Suggested Solutions. *PLOS ONE, 11*(3), e0150528–. doi:10.1371/journal.pone.0150528

Nam, S. K., Im, J., Kwak, Y., Han, N., Nam, K. H., Seo, A. N., & Lee, H. S. (2014). Effects of fixation and storage of human tissue samples on nucleic acid preservation. *Korean Journal of Pathology*, *48*(1), 36–42. https://doi.org/10.4132/KoreanJPathol.2014.48.1.36

Nataliya Kitsera, Marta Rodriguez-Alvarez, Steffen Emmert, Thomas Carell, Andriy Khobta, (2019) Nucleotide excision repair of abasic DNA lesions, *Nucleic Acids Research, 47*(16), 8537-8547 https://doi.org/10.1093/nar/gkz558

Nishino, T., & Morikawa, K. (2002). Structure and function of nucleases in DNA repair: shape, grip and blade of the DNA scissors. *Oncogene, 21*(58), 9022–9032. https://doi.org/10.1038/sj.onc.1206135

O., K. V., Ilja, W., S., M. A., & L., G. R. (2015). The DNA-Binding Protein from Starved Cells (Dps) Utilizes Dual Functions to Defend Cells against Multiple Stresses. *Journal of Bacteriology*, *197*(19), 3206–3215. https://doi.org/10.1128/JB.00475-15

O'Connor, T. R., Boiteux, S., & Laval, J. (1988). Ring-opened 7-methylguanine residues in DNA are a block to in vitro DNA synthesis. *Nucleic Acids Research*, *16*(13), 5879–5894. https://doi.org/10.1093/NAR/16.13.5879

Oh, J., & Symington, L. S. (2018). Role of the Mre11 complex in preserving genome integrity. *Genes, 9*(12), 589. https://doi.org/10.3390/genes9120589

Olgenblum, G. I., Sapir, L., & Harries, D. (2020). Properties of Aqueous Trehalose Mixtures: Glass Transition and Hydrogen Bonding. *Journal of Chemical Theory and Computation*, *16*(2), 1249–1262. https://doi.org/10.1021/ACS.JCTC.9B01071

O'Neill. (1983). Pulse radiolytic study of the interaction of thiols and ascorbate with OH adducts of dGMP and dG: implications for DNA repair processes. *Radiation Research*, *96*(1), 198–210. https://doi.org/10.2307/3576178

Organick, L., Nguyen, B. H., McAmis, R., Chen, W. D., Kohll, A. X., Ang, S. D., Grass, R. N., Ceze, L., & Strauss, K. (2021). An Empirical Comparison of Preservation Methods for Synthetic DNA Data Storage. *Small Methods*, *5*(5). https://doi.org/10.1002/smtd.202001094

Paleček, E. (1991). Local supercoil-stabilized DNA structure. *Critical reviews in biochemistry and molecular biology*, *26*(2), 151-226. http://doi.org/10.3109.10409239109081126

Palombarini, F., Di Fabio, E., Boffi, A., Macone, A., & Bonamore, A. (2020). Ferritin Nanocages for Protein Delivery to Tumor Cells. *Molecules (Basel, Switzerland)*, *25*(4), 825. https://doi.org/10.3390/molecules25040825

Pang, B. C., & Cheung, B. K. (2006). One-step generation of degraded DNA by UV irradiation. *Analytical biochemistry*, *360*(1), 163-165. DOI: 10.1016/j.ab.2006.10.004

Payne, C. C., & Mertens, P. P. C. (1983). Cytoplasmic Polyhedrosis Viruses. *The Reoviridae*, 425–504. https://doi.org/10.1007/978-1-4899-0580-2_9

Peluso, A. L., Cascone, A. M., Lucchese, L., Cozzolino, I., Ieni, A., Mignogna, C., Pepe, S., & Zeppa, P. (2015). Use of FTA cards for the storage of breast carcinoma nucleic acid on fine-needle aspiration samples. *Cancer Cytopathology*, *123*(10), 582–592. https://doi.org/10.1002/CNCY.21577

Peris D, Janssen K, Barthel HJ, Bierbaum G, Delclòs X, Peñalver E, et al. (2020) DNA from resin-embedded organisms: Past, present, and future. PLoS ONE 15(9): e0239521. https://doi.org/10.1371/journal.pone.0239521

Pesek, J., Büchler, R., Albrecht, R., Boland, W., & Zeth, K. (2011). Structure and mechanism of iron translocation by a Dps protein from Microbacterium arborescens. *The Journal of biological chemistry*, *286*(40), 34872–34882. https://doi.org/10.1074/jbc.M111.246108

Poetsch, A. R. (2020). The genomics of oxidative DNA damage, repair, and resulting mutagenesis. *Computational and structural biotechnology journal*, *18*, 207-219. https://doi.org/10.1016/j.csbj.2019.12.013

Ponti. G., Maccaferri, M., Manfredini, M., Kaleci, S., Mandrioli, M., Pellacani, G., Ozben, T Depenni, R., Bianchi, G., Pirola, G., Tomasi, A. (2018). The value of fluorimetry(Qubit) and spectrophotometry (NanoDrop) in the quantification of cell-free DNA(cfDNA) in malignant melanoma and prostate cancer patients. *Clinica Chimica Acta, 479(), 14–19.* doi:10.1016/j.cca.2018.01.007

Potaman, V. N., & Sinden, R. R. (2005). DNA. In *DNA conformation and transcription* (pp. 3-17). Springer, Boston, MA. https://www.ncbi.nlm.nih.gov/books/NBK6545/

Protozanova, E., Yakovchuk, P., & Frank-Kamenetskii, M. D. (2004). Stacked–unstacked equilibrium at the nick site of DNA. *Journal of molecular biology, 342*(3), 775-785. https://doi.org/10.1016/j.jmb.2004.07.075

Pusch, C. M., Broghammer, M., & Blin, N. (2003). Molecular phylogenetics employing modern and ancient DNA. *Journal of applied genetics*, *44*(3), 269-290.

Qiagen (2021). Indicating FTA Cards. [Manufacturer's Instructions]. Retrieved from: https://www.qiagen.com/us/products/human-id-and-forensics/sample-collection/indicating-fta-cards/indicating-fta-cards/

Rahikainen, A. L., Palo, J. U., de Leeuw, W., Budowle, B., & Sajantila, A. (2016). DNA quality and quantity from up to 16 years old post-mortem blood stored on FTA cards. *Forensic Science International*, *261*, 148–153. https://doi.org/10.1016/J.FORSCIINT.2016.02.014

Rapoport Alexander, Rusakova Anna, Khroustalyova Galina, Walker Graeme (2014). Thermotolerance in Saccharomyces cerevisiae is linked to resistance to anhydrobiosis, Process Biochemistry, Volume 49, Issue 11,Pages 1889-1892,ISSN 1359-5113,https://doi.org/10.1016/j. procbio.2014.07.006.

Rajendram, D., Ayenza, R., Holder, F. M., Moran, B., Long, T., & Shah, H. N. (2006). Long-term storage and safe retrieval of DNA from microorganisms for molecular analysis using FTA matrix cards. *Journal of Microbiological Methods*, *67*(3), 582–592. https://doi.org/10.1016/J.MIMET.2006.05.010

Rao. T. R. (2018). Anhydrobiosis Drying Without Dying. *Resonance, 23*(5), 545-553. https://doi.org/10.1007/s12045-018-0648-5

Rampelotto, P.H. (2010) Resistance of Microorganisms to Extreme Environmental Conditions and Its Contribution to Astrobiology. *Sustainability*, *2*(6), 1602-1623 doi:10.3390/su2061602

Razin, A., & Riggs, A. (1980). DNA methylation and gene function. *Science*, *210*(4470), 604–610. https://doi.org/10.1126/SCIENCE.6254144

Reid, K. M., Maistry, S., Ramesar, R., & Heathfield, L. J. (2017). A review of the optimization of the use of formalin fixed paraffin embedded tissue for molecular analysis in a forensic post-mortem setting. *Forensic science international*, *280*, 181-187. https://doi.org/10.1016/j.forsciint.2017.09.020

Restrepo Giovanni, Varela Elizabeth , Duque Juan Esteban, Gómez Jorge Enrique, Rojas (2019) Freezing, Vitrification, and Freeze-Drying of Equine Spermatozoa: Impact on Mitochondrial Membrane Potential, Lipid Peroxidation, and DNA Journal of Equine Veterinary Science,Volume 72,Pages 8-15,ISSN0737-0806,https://doi.org/10.1016/j.jevs. 2018.10.006.

Röder, B., Frühwirth, K., Vogl, C., Wagner, M., & Rossmanith, P. (2010). Impact of Long-Term Storage on Stability of Standard DNA for Nucleic Acid-Based Methods. *Journal of Clinical Microbiology*, *48*(11), 4260. https://doi.org/10.1128/JCM.01230-10

Rohland, N., Glocke, I., Aximu-Petri, A., & Meyer, M. (2018). Extraction of highly degraded DNA from ancient bones, teeth and sediments for high-throughput sequencing. *Nature Protocols, 13*(11), 2447-2461. https://doi.org/10.1038/s41596-018-0050-5

Rothfuss. A., & Grompe, M. (2004). Repair Kinetics of Genomic Interstrand DNA Cross-Links: Evidence for DNA Double-Strand Break-Dependent Activation of the Fanconi Anemia/BRCA Pathway. *Molecular and Cellular Biology*, *24*(1), 123. https://doi.org/10.1128/MCB.24.1.123-134.2004

Roy, R., Chakraborty, P., Chatterjee, A., & Sarkar, J. (2021). Comparative review on left-handed Z-DNA. *Frontiers in bioscience (Landmark edition)*, *26*(5), 29–35. https://doi.org/10.52586/4922

Roy, S., Saraswathi, R., Gupta, S., Sekar, K., Chatterji, D., & Vijayan, M. (2007). Role of N and C-terminal tails in DNA binding and assembly in Dps: structural studies of Mycobacterium smegmatis Dps deletion mutants. *Journal of molecular biology*, *370*(4), 752-767. https://doi.org/10.1016/j.jmb.2007.05.004

Roy, S., Saraswathi, R., Chatterji, D., & Vijayan, M. (2008). Structural studies on the second Mycobacterium smegmatis Dps: invariant and variable features of structure, assembly and function. *Journal of molecular biology*, *375*(4), 948-959. https://doi.org/10.1016/j.jmb.2007.10.023Ruhal R, Kataria R, Choudhury B. Trends in bacterial trehalose metabolism and significant nodes of metabolic pathway in the direction of trehalose accumulation. *Microb Biotechnol*. 2013;6(5):493-502. doi:10.1111/1751-7915.12029

Sinha Kaustubh, Sangani Sahil S., Kehr Andrew D., Rule Gordon S., and Jen-Jacobson Linda (2016).Metal Ion Binding at the Catalytic Site Induces Widely Distributed Changes in a Sequence Specific Protein–DNA Complex*Biochemistry* 2016 *55* (44), 6115-6132DOI: 10.1021/acs.biochem.6b00919

Saieg, M. A., Geddie, W. R., Boerner, S. L., Liu, N., Tsao, M., Zhang, T., Kamel-Reid, S., & Santos, G. da C. (2012). The use of FTA cards for preserving unfixed cytological material for high-throughput molecular analysis. *Cancer Cytopathology*, *120*(3), 206–214. https://doi.org/10.1002/CNCY.20205

Sambrook, J., & Russell, D. W. (2001). Protocol 5: DNA transfection by electroporation. *Molecular Cloning: A Laboratory Manual*, 16.33-16.36, 16.54.

Santos, J. H., Mandavilli, B. S., & van Houten, B. (2002). Measuring oxidative mtDNA damage and repair using quantitative PCR. *Methods in Molecular Biology (Clifton, N.J.)*, *197*, 159–176. https://doi.org/10.1385/1-59259-284-8:159

Sargsyan, K. (2017). Logistic Steps of Tissue Sample Processing in a Clinical Biobank - A Short Overview. *Advances in Cytology & Pathology*, *2*(4). https://doi.org/10.15406/acp.2017.02.00033Schlaak, C., Hoffmann, P., May, K., & Weimann, A. (2005). Desalting minimal amounts of DNA for electroporation in E. coli: a comparison of different physical methods. *Biotechnology letters*, *27*(14), 1003–1005. https://doi.org/10.1007/s10529-005-7867-z

Selvaraj, M., Ahmad, R., Varshney, U., & Vijayan, M. (2012). Crowding, molecular volume and plasticity: An assessment involving crystallography, NMR and simulations. *Journal of Biosciences*, *37*(1), 953–963. https://doi.org/10.1007/s12038-012-9276-5

Sedlackova, T., Repiska, G., Celec, P., Szemes, T., & Minarik, G. (2013). Fragmentation of DNA affects the accuracy of the DNA quantitation by the commonly used methods. *Biological Procedures Online*, *15*(1), 1-8. https://doi.org/10.1186/1480-9222-15-5

Shabihkhani, M., Lucey, G. M., Wei, B., Mareninov, S., Lou, J. J., Vinters, H. v., Singer, E. J., Cloughesy, T. F., & Yong, W. H. (2014). The procurement, storage, and quality assurance

of frozen blood and tissue biospecimens in pathology, biorepository, and biobank settings. *Clinical Biochemistry*, *47*(4–5), 258–266. https://doi.org/10.1016/j.clinbiochem.2014.01.002

Shapiro, R. (1981). Damage to DNA Caused by Hydrolysis. *Chromosome Damage and Repair*, 3–18. https://doi.org/10.1007/978-1-4684-7956-0_1

Sharpe, A., Barrios, S., Gayer, S., Allan-Perkins, E., Stein, D., Appiah-Madson, H. J., ... & Distel, D. L. (2020). DESS deconstructed: Is EDTA solely responsible for protection of high molecular weight DNA in this common tissue preservative?. *PloS one*, *15*(8), e0237356.https://doi.org/10.1371/journal.pone.0237356

Shen Li; Cooper, Valentino R.; Thonhauser, T.; Lundqvist, Bengt I.; Langreth, David C. (2009). Stacking Interactions and DNA Intercalation. The Journal of Physical Chemistry B, 113(32), 11166–11172. doi:10.1021/jp905765c

Shiraga, K., Adachi, A., & Ogawa, Y. (2017). Characterization of the hydrogen-bond network of water around sucrose and trehalose: HOH bending analysis. *Chemical Physics Letters, 678*, 59-64. DOI: 10.1016/j.cplett.2017.04.023

Siegel, C. S., Stevenson, F. O., & Zimmer, E. A. (2017). Evaluation and comparison of FTA card and CTAB DNA extraction methods for non-agricultural taxa. *Applications in Plant Sciences*, *5*(2), 1600109. https://doi.org/10.3732/APPS.1600109

Sigma Aldrich (2021). DNAgard® Protocol [Manufacturers Instructions]. Retrieved from: https://www.sigmaaldrich.com/CA/en/technical-documents/protocol/genomics/dna-and-rna-purification/dnagard-tissue

Sigma Aldrich (2021). DNAstable® Protocol [Manufacturers Instructions]. Retrieved from: https://www.sigmaaldrich.com/CA/en/technical-documents/protocol/genomics/dna-and-rna-purification/dnastable

Silva, L. C. F., Lopes, D. R. G., Lima, H. S., Quartaroli, L., de Sousa, M. P., Waldow, V. de A., Akamine, R. N., de Paula, S. O., & Silva, C. C. da. (2021). Comparison of methods for preservation of activated sludge samples for high-throughput nucleic acid sequencing and bacterial diversity analysis. *International Biodeterioration and Biodegradation*, *157*. https://doi.org/10.1016/j.ibiod.2020.105139

Singh, A., & Singh, N. (2015). Effect of salt concentration on the stability of heterogeneous DNA. Physica A: Statistical Mechanics and its Applications, 419, 328-334. https://doi.org/10.1016/j.physa.2014.10.029

Singh, S. K. (2018). Sucrose and trehalose in therapeutic protein formulations. In *Challenges in Protein Product Development* (pp. 63-95). Springer, Cham. https://doi.org/10.1007/978-3-319-90603-4_3

Smith, S., & Morin, P. A. (2005). Optimal storage conditions for highly dilute DNA samples: a role for trehalose as a preserving agent. Journal of Forensic Science, 50(5), 10.1520/JFS2004411

Soshinskaya, E. Y., Dadinova, L. A., Mozhaev, A. A., & Shtykova, E. V. (2020). Effect of buffer composition on conformational flexibility of N-terminal fragments of Dps and the nature of interactions with DNA. Small-angle X-ray scattering study. *Crystallography Reports, 65*(6), 891-899.https://doi.org/10.1134/S1063774520060334

Spiess, A.-N., Mueller, N., & Ivell, R. (2004). Trehalose Is a Potent PCR Enhancer: Lowering of DNA Melting Temperature and Thermal Stabilization of Taq Polymerase by the Disaccharide Trehalose. *Clinical Chemistry*, *50*(7), 1256–1259. https://doi.org/10.1373/CLINCHEM.2004.031336

Stangegaard, M., Ferrero-Miliani, L., Børsting, C., Frank-Hansen, R., Hansen, A. J., & Morling, N. (2011). Repeated extraction of DNA from FTA cards. *Forensic Science International: Genetics Supplement Series*, *3*(1), e345–e346. https://doi.org/10.1016/J.FSIGSS.2011.09.035

Stella, S., Cascio, D., & Johnson, R. C. (2010). The shape of the DNA minor groove directs binding by the DNA-bending protein Fis. *Genes & Development*, *24*(8), 814. https://doi.org/10.1101/GAD.1900610

Stiller, M., Green, R.E, Ronan, M., Simons, J.F., Du, L., He, W., Egholm, M., Rothberg, J.M., Keates, S.G., Ovodov, N.D., Antipina, E.E., Baryshnikov, G.F., Kuzmin, Y.V., Vasilevski, A.A., Wuenschell, G.E., Termini, J., Hofreiter, M., Jaenicke-Despres, V., & Pääbo, S. (2006). Patterns of nucleotide misincorporations during enzymatic amplification and direct large-scale sequencing of ancient DNA. *Proceedings of the National Academy of Sciences*, *103*(37), 13578-13584. https://doi.org/10.1073/pnas.0605327103

Stutzer, A., Welp, L. M., Raabe, M., Sachsenberg, T., Kappert, C., Wulf, A., ... & Urlaub, H. (2020). Analysis of protein-DNA interactions in chromatin by UV induced cross-linking and mass spectrometry. *Nature communications*, *11*(1), 1-12.doi:10.1038/s41467-020-19047

Svozil, D., Kalina, J., Omelka, M., & Schneider, B. (2008). DNA conformations and their sequence preferences. *Nucleic Acids Research*, *36*(11), 3690–3706. https://doi.org/10.1093/nar/gkn260

Tan, X., Grollman, A. P., & Shibutani, S. (1999). Comparison of the mutagenic properties of 8-oxo-7,8-dihydro-2′-deoxyadenosine and 8-oxo-7,8-dihydro-2′-deoxyguanosine DNA lesions in mammalian cells. *Carcinogenesis*, *20*(12), 2287–2292. https://doi.org/10.1093/CARCIN/20.12.2287

Teoule, R. (1987). Radiation-induced DNA damage and its repair. *International Journal of Radiation Biology and Related Studies in Physics, Chemistry and Medicine*, *51*(4), 573-589. https://doi.org/10.1080/09553008414552111

Tereshkin, E. V., Tereshkina, K. B., Kovalenko, V. V., Loiko, N. G., & Krupyanskii, Y. F. (2019). Structure of Dps Protein Complexes with DNA. *Russian Journal of Physical Chemistry B*, *13*(5), 769-777. https://doi.org/10.1134/S199079311905021X

Thorp, H. H. (2000). The importance of being r: greater oxidative stability of RNA compared with DNA. *Chemistry & Biology*, 7(2), R33–R36. doi:10.1016/s1074-5521(00)00080-6

Tuo, J., Jaruga, P., Rodriguez, H., Bohr, V. A., & Dizdaroglu, M. (2003). Primary fibroblasts of Cockayne syndrome patients are defective in cellular repair of 8-hydroxyguanine and 8-hydroxyadenine resulting from oxidative stress. *The FASEB Journal*, *17*(6), 668–674. https://doi.org/10.1096/FJ.02-0851COM

Twin, J., Jensen, J. S., Bradshaw, C. S., Garland, S. M., Fairley, C. K., Min, L. Y., & Tabrizi, S. N. (2012). Transmission and selection of macrolide resistant mycoplasma genitalium infections detected by rapid high resolution melt analysis. *PLoS ONE*, *7*(4). https://doi.org/10.1371/journal.pone.0035593

Ussery, D.W. (2002). DNA Structure: A-, B- and Z-DNA Helix Families. *Encyclopedia of life sciences*, 1-7. https://doi.org/10.1038/npg.els.0003122

van der Valk, T., Pečnerová, P., Díez-del-Molino, D., Bergström, A., Oppenheimer, J., Hartmann, S., Xenikoudakis, G., Thomas, J. A., Dehasque, M., Sağlıcan, E., Fidan, F. R., Barnes, I., Liu, S., Somel, M., Heintzman, P. D., Nikolskiy, P., Shapiro, B., Skoglund, P., Hofreiter, M., & Dalén, L. (2021). Million-year-old DNA sheds light on the genomic history of mammoths. *Nature, 591*(7849), 265-269. https://doi.org/10.1038/s41586-021-03224-9

Vanapalli, S. A., Ceccio, S. L., & Solomon, M. J. (2006). Universal scaling for polymer chain scission in turbulence. *Proceedings of the National Academy of Sciences*, *103*(45), 16660–16665. https://doi.org/10.1073/PNAS.0607933103

Vanaporn, M., & Titball, R. W. (2020). Trehalose and bacterial virulence. *Virulence, 11*(1), 1192-1202. https://doi.org/10.1080/21505594.2020.1809326

Vayssié, L., Skouri, F., Sperling, L., & Cohen, J. (2000). Molecular genetics of regulated secretion in Paramecium. *Biochimie*, *82*(4), 269–288. https://doi.org/10.1016/S0300-9084(00)00201-7

Victoria Hartmen, Lise Matke, and Peter H. Watson. (2019). Biopreservation and Biobanking.264-270. http://doi.org/10.1089/bio.2018.0120

Vider, J., Croaker, A., Cox, A. J., Raymond, E., Rogers, R., Adamson, S., Doyle, M., O'Brien, B., Cripps, A. W., & West, N. P. (2020). Comparison of skin biopsy sample processing and storage methods on high dimensional immune gene expression using the Nanostring nCounter system. *Diagnostic Pathology*, *15*(1), 57. https://doi.org/10.1186/s13000-020-00974-4

Villanueva, A. V., Podzorski, R. P., & Reyes, M. P. (1998). Effects of various handling and storage conditions on stability of Treponema pallidum DNA in cerebrospinal fluid. *Journal of Clinical Microbiology*, *36*(7), 2117–2119. https://doi.org/10.1128/JCM.36.7.2117-2119.1998

Villarrubia, C. W. N., Tumas, K. C., Chauhan, R., MacDonald, T., Dattelbaum, A. M., Omberg, K., & Gupta, G. (2021). Long-term stabilization of DNA at room temperature using a one-step microwave assisted process. *Emergent Materials*, 1. https://doi.org/10.1007/S42247-021-00208-3

Vinayykumarr·, M., Burrittt, D. J., Pirjo, M., & Mäkelä, S. A. (2019). Proline, glycinebetaine, and trehalose uptake and interorgan transport in plants under stress. *Osmoprotectant-Mediated Abiotic Stress Tolerance in Plants Recent Advances and Future Perspectives*. 201-223. doi: 10.1007/978-3-030-27423-8

Wan, E., Akana, M., Pons, J., Chen, J., Musone, S., Kwok, P.-Y., & Liao, W. (n.d.). *Green Technologies for Room Temperature Nucleic Acid Storage*. http://www.cimb.org

Wang, S., Lee, PC., Elsayed, A. *et al.* Preserving the Female Genome in Trehalose Glass at Supra-Zero Temperatures: The Relationship Between Moisture Content and DNA Damage in Feline Germinal Vesicles. *Cel. Mol. Bioeng.* **14,** 101–112 (2021). https://doi.org/10.1007/s12195-020-00635-y

Wang, C., Grohme, M. A., Mali, B., Schil, R. O., & Frohme, M. (2014). Towards decrypting cryptobiosis - Analyzing anhydrobiosis in the tardigrade Milnesium tardigradum using transcriptome sequencing. *PLoS ONE*, *9*(3). https://doi.org/10.1371/journal.pone.0092663

Wang, C., Pi, L., Jiang, S., Yang, M., Shu, C., & Zhou, E. (2018). ROS and trehalose regulate sclerotial development in Rhizoctonia solani AG-1 IA. *Fungal Biology*, *122*(5), 322–332. https://doi.org/10.1016/J.FUNBIO.2018.02.003

Waters, T. R., & Swann, P. F. (2000). Thymine-DNA glycosylase and G to A transition mutations at CpG sites. *Mutation Research/Reviews in Mutation Research*, *462*(2–3), 137–147. https://doi.org/10.1016/S1383-5742(00)00031-4

Waters, J. T., Lu, X. J., Galindo-Murillo, R., Gumbart, J. C., Kim, H. D., Cheatham, T. E., & Harvey, S. C. (2016). Transitions of Double-Stranded DNA between the A- and B-Forms. *Journal of Physical Chemistry B*, *120*(33), 8449–8456. https://doi.org/10.1021/acs.jpcb.6b02155

Watson, J. D., & Crick, F. H. C. (1953). Molecular Structure of Nucleic Acids: A Structure for Deoxyribose Nucleic Acid. *Nature 1953 171:4356*, *171*(4356), 737–738. https://doi.org/10.1038/171737a0

Watson, T. (2017). Archaeology: Mummy DNA unravels ancestry of ancient Egyptians. *Nature*, *546*(7656), 17. https://doi.org/10.1038/546017A

Weber, G., Haslam, N., Essex, J. W., & Neylon, C. (2008). Thermal equivalence of DNA duplexes for probe design. *Journal of Physics: Condensed Matter*, *21*(3), 034106. https://doi.org/10.1088/0953-8984/21/3/034106

Williams, S. M., & Chatterji, D. (2021). An Overview of Dps: Dual Acting Nanovehicles in Prokaryotes with DNA Binding and Ferroxidation Properties. *Sub-cellular biochemistry*, *96*, 177–216. https://doi.org/10.1007/978-3-030-58971-4_3

Williams, S. T. (2007). Safe and legal shipment of tissue samples: Does it affect DNA quality? *Journal of Molluscan Studies*, *73*(4), 416–418. https://doi.org/10.1093/mollus/eym039

Wolf, S.G. Frenkiel, D., Arad, T., Finkel, S. E., Kolter, R., & Minsky, A. (1999). DNA protection by stress-induced biocrystallization. *Nature*, *400*(6739), 83-85.

Wolfe, L.M Thiagarajan, R. D., Boscolo, F., Taché, V., Coleman, R. L., Kim, J., Kwan, W. K, Loring, J. F., Parast, M., & Laurent, L. C. (2014). Banking placental tissue: An optimized collection procedure for genome-wide analysis of nucleic acids HHS Public Access. *Placenta*, *35*(8), 645–654. https://doi.org/10.1016/j.placenta

Wolfenden, R., Lu, X., & Young, G. (1998). Spontaneous Hydrolysis of Glycosides. *Journal of the American Chemical Society*, *120*(27), 6814–6815. https://doi.org/10.1021/ja9813055

Wong, P. B. Y., Wiley, E. O., Johnson, W. E., Ryder, O. A., O'Brien, S. J., Haussler, D., Koepfli, K. P., Houck, M. L., Perelman, P., Mastromonaco, G., Bentley, A. C., Venkatesh, B., Zhang, Y. P., & Murphy, R. W. (2012). Tissue sampling methods and standards for vertebrate genomics. *GigaScience, 1*(1). https://doi.org/10.1186/2047-217X-1-8https://doi.org/10.1186/2047-217X-1-8

Woo, Joshua and Lee Jeoung Soo, (2021), Effects of lyoprotectants on long-term stability and, transfection efficacy of lyophilized poly(lactide-co-glycolide)-graft-polyethylenimine/plasmid DNA polyplexes, Nanomedicine, 16,15, 1269-1280,10.2217/nnm-2021-0065

Wood, B. R. (2016). The importance of hydration and DNA conformation in interpreting infrared spectra of cells and tissues. *Chemical Society Reviews, 45*(7), 1980–1998. doi:10.1039/c5cs00511f

Wowk, B. (2010). Thermodynamic aspects of vitrification. Cryobiology, *60*(1), 11–22. doi: 10.1016/j.cryobiol.2009.05.007

Xavier, C., Eduardoff, M., Bertoglio, B., Amory, C., Berger, C., Casas-Vargas, A., Pallua, J., & Parson, W. (2021). Evaluation of DNA extraction methods developed for forensic and ancient DNA applications using bone samples of different age. *Genes*, *12*(2), 1–15. https://doi.org/10.3390/GENES12020146

Yakovchuk P, Protozanova E, Maxim D. Frank-Kamenetskii, Base-stacking and base-pairing contributions into thermal stability of the DNA double helix, *Nucleic Acids Research*, Volume 34, Issue 2, 1 January 2006, Pages 564–74, https://doi.org/10.1093/nar/gkj454

Yang, L., Zhao, X., Zhu, H., Paul, M., Zu, Y., & Tang, Z. (2014). Exogenous trehalose largely alleviates ionic unbalance, ROS burst, and PCD occurrence induced by high salinity in arabidopsis seedlings. *Frontiers in Plant Science*, *5*(October). https://doi.org/10.3389/fpls.2014.00570

Yuan, M. L., Wogan, G. O. U., & Wang, I. J. (2018). Trehalose improves PCR amplification of vertebrate nuclear DNA from historical allozymes. *Conservation Genetics Resources*, *10*(3), 313–315. https://doi.org/10.1007/s12686-017-0811-4

Zacharias, Martin (2020). Base-Pairing and Base-Stacking Contributions to Double-Stranded DNA Formation. The Journal of Physical Chemistry B, acs. jpcb.0c07670–. doi: 10.1021/acs.jpcb.0c0767

Zanotto, E. D., & Mauro, J. C. (2017). The glassy state of matter: Its definition and ultimate fate. *Journal of Non-Crystalline Solids*, *471*, 490–495. https://doi.org/10.1016/j.jnoncrysol.2017.05.019

Zayed, G., & Roos, Y. H. (2004). Influence of trehalose and moisture content on survival of Lactobacillus salivarius subjected to freeze-drying and storage. *Process Biochemistry*, *39*(9), 1081–1086. https://doi.org/10.1016/S0032-9592(03)00222-X

Zeth, Kornelius(2012)). *Dps biomineralizing proteins: multifunctional architects of nature. Biochemical Journal,445(3), 297-311* doi:10.1042/BJ20120514

Zhang, B., Cao, H. juan, Lin, H. min, Deng, S. gui, & Wu, H. (2019). Insights into ice-growth inhibition by trehalose and alginate oligosaccharides in peeled Pacific white shrimp (Litopenaeus vannamei) during frozen storage. *Food Chemistry*, *278*, 482–490. https://doi.org/10.1016/J.FOODCHEM.2018.11.087

Zhang, M., Oldenhof, H., Sydykov, B., Bigalk, J., Sieme, H., & Wolkers, W. F. (2017). Freeze-drying of mammalian cells using trehalose: preservation of DNA integrity. *Scientific Reports 2017 7:1*, *7*(1), 1–10. https://doi.org/10.1038/s41598-017-06542-z

Zhang, Q.-M. (2001). Role of the Escherichia coli and Human DNA Glycosylases That Remove 5-Formyluracil from DNA in the Prevention of Mutations. *J. RADIAT. RES*, *42*, 11–19. https://academic.oup.com/jrr/article/42/1/11/937660

Zhang, X., Rosenstein, B. S., Wang, Y., Lebwohl, M., & Wei, H. (1997). Identification of Possible Reactive Oxygen Species Involved in Ultraviolet Radiation-Induced Oxidative DNA Damage. *Free Radical Biology and Medicine*, *23*(7), 980–985. https://doi.org/10.1016/S0891-5849(97)00126-3

Zhao, J., Bacolla, A., Wang, G., & Vasquez, K. M. (2010). Non-B DNA structure-induced genetic instability and evolution. *Cellular and molecular life sciences : CMLS*, *67*(1), 43–62. https://doi.org/10.1007/s00018-009-0131-2

Zupanič Pajnič, I., Marrubini, G., Pogorelc, B. G., Zupanc, T., Previderè, C., & Fattorini, P. (2019). On the long-term storage of forensic DNA in water. *Forensic Science International*, *305*. https://doi.org/10.1016/j.forsciint.2019.110031

Zymo Research (2021). DNA/RNA Shield™ [Manufacturers Instructions]. Retrieved from: https://files.zymoresearch.com/protocols/_r1100-50_r1100-250_r1200-25_r1100-125_dna_rna_shield.pdf

Appendix A

Data tables DNA PCR and Quantification over 5-year study

		Quantification		Quantification		Quantification		Quantification		Quantification		Quantification		Quantifica
Time	DNA H2O	Alkaline PH	DNA H2O	Acidic PH 5	DNA H2O	Neutral (ult	DNA TE		DRY		Ethanol		Filter Paper	
Room Temperature														
1	14	10	14	10	14	10	14	10	14	10	14	10	14	10
2	14	9.2	14	9.1	14	9.4	14	7.4	14	6.7	14	6.6	14	5.2
3	14	9.2	14	9.3	14	9.5	14	7	14	6.8	14	6.6	14	4.9
4	14	9.1	14	8.7	14	9.1	14	6.9	14	7	14	6.3	14	4.8
5	14	9.2	14	8.2	14	9.3	14	7.2	14	7.1	14	7.2	14	5.5
6	14	8.7	14	7.7	14	9.4	14	7.3	14	7.3	14	6.9	14	5.1
7	14	8.8	10	7.5	14	9.2	14	7.3	14	6.9	14	6.9	14	5
8	14	9	14	6.8	14	9.1	14	7.2	14	7.1	14	7.2	14	4.7
9	14	8.9	10	7	14	9.6	14	7.3	14	6.9	14	7.4	14	5.8
10	14	8.5	10	5.5	14	9	14	7	14	6.2	14	7.3	14	6
11	14	8.1	6	5.2	14	8.7	14	6.8	14	7.4	14	7.7	14	5
12	14	8	6	5.1	14	9.2	14	7.4	14	7.5	14	7.9	14	5.8
13	14	7.4	6	5.8	14	9.1	14	7	14	7.5	10	7.7	14	4.7
14	14	8.7	6	4	14	9.1	14	6.7	14	7.5	14	7.7	14	5.2
21	14	8.2	6	4.2	14	9	14	7.3	14	7.4	14	7.6	14	5.6
28	14	7.3	6	4.5	14	9.3	14	7.1	14	7.5	14	7.7	14	4.7
35	14	7.7	4	4	14	8.9	14	6.8	14	7.2	14	7.3	14	5.6
42	14	8.1	4	3.9	14	9.4	14	6.7	14	7.1	14	7.3	14	5.5
49	14	7.2	4	3.7	14	8.7	14	7	14	7.7	14	7.6	14	5.5
56	14	6.8	2	3	14	9.1	14	6.6	14	7.4	14	7.7	14	5
63	14	7.2	1	2.8	14	9	14	6.6	14	7.6	14	7.4	14	5.7
70	14	6	1	1.3	14	8.9	14	7	6	7.7	14	7.6	14	4.8
77	14	6	2	1.5	14	9.3	14	8	14	7.1	14	7.8	14	5.2
84	14	4	2	1.8	14	8.8	14	7.1	14	7.8	10	7.7	14	5.4
120	10	3.2	1	0.8	10	7.2	14	6	14	7.7	6	7.8	14	4.7
150	6	3.3	0	0.5	10	6.1	14	6.7	6	7.7	14	7.8	14	4.8
180	6	3.4			6	6	14	6.2	14	7	14	7.8	14	5
210	4	3			6	5.3	14	6.7	14	7.2	14	7.2	14	5.3
240	4	3.4			6	5	14	6.9	14	7.3	6	7.7	14	5.1
270	4	3.5			6	5.2	14	6.1	10	7.2	14	7.8	14	5.2
300	4	2.9			6	4	14	6.2	14	7.1	6	7.1	14	5.1
330	4	3.3			2	3.9	6	6.4	6	7	4	6.4	14	5.1
360	4	3.4			2	3.3	10	5.8	14	6.8	14	6.7	14	4.7
390	4	3			2	2.1	6	5.9	6	6.7	6	6.9	14	4.7
420	2	2.8			0	2	6	5.8	14	6.8	10	7.1	14	5.2
450	2	2.9					6	5.4	10	7	4	6.7	14	5.4
480	2	2.2					6	5.9	6	6.7	4	7.1	14	5.1
510	1	2.1					6	5.2	14	6.5	4	6.9	14	5.2
540	2	2					6	5.1	6	6.9	4	6.7	14	4.9
570	0	1.3					6	5.5	14	6.5	2	7.2	14	4.4
600							6	5.5	10	6.3	2	7	14	5.6
630							6	5	6	6.6	4	6.9	14	5.5
660							6	4.9	2	6.5	2	7.2	14	5.1
690							6	5.3	6	6	2	7	14	5.3
720							6	4.8	10	6.2	2	6.8	6	5.2
810							6	5.1	6	6.4	2	6.7	10	4.5
900							6	5.3	6	6	2	6.7	14	4.7
990							2	4.9	1	6.4	2	6.6	6	4.5
1080							2	4.7	10	6.4	2	7	14	4.7
1170							2	4.9	2	6.1	2	6.5	6	4.4
1260							2	5	2	6	1	6.8	14	4.5
1440							2	5.3	2	6.2	0	6.8	6	4.6
1530							0	4.9	2	6.4			6	4.6
1620									2	5.9			6	4.4
1800									2	6.2			2	4.3

tion		Quantification		Quantification		Quantification		Quantification		Quantification		Quantification		Quantifica
Time	DNA H2O Alkaline		DNA H2O Acidic		DNA H2O Neutral (ult		DNA TE		DRY		Ethanol		Filter Paper	
4 Degrees	Celsius													
1	14	10	14	10	14	10	14	10	14	10	14	10	14	10
2	14	9.2	14	8	14	9.5	14	9.1	14	7	14	8	14	5
3	14	9.2	14	8.4	14	9.3	14	9	14	7.1	14	8.2	14	5.3
4	14	9.1	14	8.2	14	9.1	14	9.2	14	7	14	8	14	5.5
5	14	9.2	14	8.4	14	9.1	14	9	14	7	14	7.8	14	5.6
6	14	8.7	14	8	14	9.2	14	9	14	7	14	8.2	14	5.6
7	14	8.8	10	7.5	14	9.2	14	9.2	14	6.9	14	8.3	14	5.5
8	14	9	14	7.6	14	9.1	14	9.3	14	7.1	14	8	14	5.4
9	14	8.9	10	7.7	14	9.2	14	9.4	14	6.9	14	8.1	14	5.8
10	14	8.5	10	7.4	14	9	14	9.2	14	6.8	14	8.3	14	5.7
11	14	8.1	6	6	14	8.8	14	9.3	14	7.1	14	8.2	14	5.6
12	14	8	6	5.1	14	9.2	14	9	14	7.2	14	8	14	5.8
13	14	8.2	6	4.7	14	9.1	14	9.1	14	7.4	14	7.8	14	5.7
14	14	8.7	6	4	14	9.1	14	9.3	14	7	14	7.9	14	5.5
21	14	8.2	6	3.3	14	9	14	9.4	14	7.3	14	8	14	5.8
28	14	8.3	6	4.5	14	8.9	14	8.9	14	7.6	14	7.7	14	5.3
35	14	8.4	6	4	14	9.2	14	9.5	6	7.4	14	8.3	6	5
42	14	8.1	6	3.9	14	9.1	14	9.2	14	7.5	14	8.1	14	5.7
49	14	7.2	4	3.7	14	9	14	9	14	7.3	14	8.3	14	5.6
56	14	7.8	2	2.4	14	8.8	14	9	6	7.2	14	8	6	5.2
63	14	7.2	2	2.3	14	9	14	9	6	7.4	14	7.9	14	5.5
70	14	7.6	1	1.9	14	9.2	14	9.2	10	7.3	14	7.9	10	5.5
77	14	7.7	2	1.8	14	9	14	9.2	6	7.2	14	8	6	5.5
84	14	7.5	2	1.4	14	9.5	14	9.3	10	7.5	6	7.7	10	5.4
120	14	7.8	1	0.8	14	9.4	14	9.4	14	7.2	14	8.3	14	5.5
150	14	7.9	0	LTB	14	9.3	14	9.5	2	7.1	14	8	2	5.2
180	6	7.6			14	6	14	9.6	14	7	14	8.1	14	5.7
210	6	4.9			14	5.3	14	9.7	14	7.2	14	7.7	14	5.3
240	6	5.7			14	5	14	9.5	14	6.9	14	7.6	14	5
270	6	5.8			14	5.2	14	9.4	6	7	14	7.9	6	5.1
300	6	5.7			14	5.8	14	9.3	6	6.9	6	7.7	6	5.3
330	6	5.9			14	5.9	14	9.4	14	7	4	7	14	5.4
360	4	4.9			14	5.4	14	9.2	6	6.9	14	7.4	6	5.1
390	4	4.8			14	5.2	14	9.6	4	7	6	7.5	4	4.9
420	2	4.7			14	5.4	14	9.4	6	7.1	10	7	6	5
450	2	4.6			14	5.5	14	8	6	7.5	4	6.9	6	5.1
480	2	4.9			10	5	14	7.7	2	7	4	7.1	2	5.2
510	1	1.5			6	4.1	14	7.5	14	6.7	4	6	14	5.3
540	2	1.4			6	4	14	7.8	6	6.9	4	6.8	6	5
570	0	1.1			6	4.2	14	7.8	2	6.8	2	6.7	2	5
600					6	4	14	7.9	6	6.7	6	6.9	6	5.4
630					6	4	6	5	6	6.9	6	6.7	6	5.4
660					4	3.9	6	4.9	2	7.1	6	6.7	2	5.3
690					6	4.1	6	5.3	6	6.7	2	6.5	14	5.4
720					2	3	6	5.5	6	6.8	2	6	6	5.4
810					4	3.3	6	5.1	6	6.7	2	6.2	6	4.9
900					6	3.1	6	3.4	6	7	2	6.3	6	4.9
990					2	3	2	3.8	6	6.4	0	5	6	4.5
1080					2	2.9	2	3.4	6	6.6	2	4.2	6	5
1170					2	3.2	2	3.3	2	6.6	0	5	2	4.9
1260					2	2.8	2	3.6	2	6	1	5.1	2	4.5
1440					2	2.1	2	2.5	2	6.5	0	4	2	4.6
1530					0	2.3	2	2.4	2	6.6			2	4.4
1620							2	2.3	2	6.2			2	4.6
1800							2	2.8	2	6.4			2	4.5

tion		Quantification		Quantification		Quantification		Quantification		Quantification		Quantification		Quantifica
Time -20 C	DNA H2O Alkaline		DNA H2O Acidic		DNA H2O Neutral (ult		DNA TE		DRY		Ethanol		Filter Paper	
1	14	10	14	10	14	10	14	10	14	10	14	10	14	10
2	14	9.2	14	9.2	14	9.5	14	9.1	14	7	14	8	14	5
3	14	9.2	14	9.1	14	9.3	14	9	14	7.1	14	8.2	14	5.3
4	14	9.1	14	8.9	14	9.1	14	9.2	14	7	14	8	14	5.5
5	14	9.2	14	8.8	14	9.1	14	9	14	7	14	7.8	14	5.6
6	14	8.7	14	8.8	14	9.2	14	9	14	7	14	8.2	14	5.6
7	14	9	14	8.9	14	9.2	14	9.2	14	6.9	14	8.3	14	5.5
8	14	9	14	9.1	14	9.1	14	9.3	14	7.1	14	8	14	5.4
9	14	9	14	9	14	9.2	14	9.4	14	6.9	14	8.1	14	5.8
10	14	9.2	14	9.2	14	9	14	9.2	14	6.8	14	8.3	14	5.7
11	6	8.9	14	9	14	8.8	14	9.3	14	7.1	14	8.2	14	5.6
12	6	8.5	14	9.1	14	9.2	14	9	14	7.2	14	8	14	5.8
13	6	8.4	14	9.2	14	9.1	14	9.1	14	7.4	14	7.8	14	5.7
14	6	9	14	8.8	14	9.1	14	9.3	14	7	14	7.9	14	5.5
21	6	9.1	14	8.9	14	9	14	9.4	14	7.3	14	8	14	5.8
28	6	8.7	14	9	14	8.9	14	8.9	14	7.6	14	7.7	14	5.3
35	6	7.7	14	9.2	14	9.2	14	9.5	14	7.4	14	8.3	14	5
42	6	8.3	14	9.3	14	9.1	14	9.2	14	7.5	14	8.1	14	5.7
49	6	8.7	14	9	14	9	14	9	14	7.3	14	8.3	14	5.6
56	6	8.7	14	9.2	14	8.8	14	9	14	7.2	14	8	14	5.2
63	6	8.8	14	8.8	14	9	14	9	14	7.4	14	7.9	14	5.5
70	6	9	14	8.7	14	9.2	14	9.2	14	7.3	14	7.9	10	5.5
77	6	8.6	14	8.9	14	9	14	9.2	14	7.2	14	8	14	5.5
84	6	8.5	6	8.5	14	9.5	14	9.3	6	7.5	14	7.7	14	5.4
120	6	8.4	6	8	14	9.4	14	9.4	14	7.2	14	8.3	14	5.5
150	6	8.2	14	7.8	14	9.3	14	9.5	6	7.1	14	8	14	5.2
180	2	6.8	2	7.7	14	9	14	9.6	14	7	14	8.1	14	5.7
210	2	6.5	6	7.9	14	8.9	14	9.7	14	7.2	14	7.7	10	5.3
240	2	6.6	2	7.8	14	9	14	9.5	14	6.9	14	7.6	14	5
270	2	6.4	6	7.7	14	9	14	9.4	14	7	14	7.9	14	5.1
300	2	6.5	2	7.5	14	8.9	14	9.3	6	6.9	14	7.7	10	5.3
330	2	6.6	2	6.7	14	8.8	14	9.4	14	7	14	7	6	5.4
360	2	5.4	2	6.1	14	8.8	14	9.2	14	6.9	14	7.4	14	5.1
390	2	5.8	2	4.7	14	8.2	14	9.6	6	7	14	7.5	14	4.9
420	2	5.8	2	3.3	14	8.6	14	9.4	6	7.1	14	7	6	5
450	2	5.3	2	2.5	14	8.4	14	8	6	7.5	14	6.9	10	5.1
480	2	5.8	2	2.2	14	8.7	14	7.7	2	7	14	7.1	14	5.2
510	2	5			14	7.9	14	7.5	14	6.7	14	6	14	5.3
540	2	4			14	8	14	7.8	6	6.9	14	7.2	14	5
570	0	4.3			14	8.1	14	7.8	2	6.8	6	7.7	6	5
600					14	8	14	7.9	4	6.7	6	7.3	6	5.4
630					14	7.9	14	7	6	6.9	6	7.4	5	5.4
660					14	8.3	14	7.1	2	7.1	6	7.5	6	5.3
690					14	8	14	7	6	6.7	6	7.1	14	5.4
720					14	7.8	14	6.9	14	6.8	6	7.4	6	5.4
810					14	7.3	14	6.8	2	6.7	6	7	6	4.9
900					14	6.8	14	7	6	7	6	7.1	14	4.9
990					6	7	14	6.3	6	6.4	6	6.9	14	4.5
1080					6	6.3	6	6.6	6	6.6	6	7	10	5
1170					6	6.6	14	6.4	2	6.6	6	6.4	6	4.9
1260					6	6.4	14	6	6	6	6	6.3	6	4.5
1440					6	6	6	6.1	2	6.5	6	6.7	6	4.6
1530					6	6.1	14	5.9	6	6.6	6	6.3	6	4.4
1620					6	5.9	6	5.5	6	6.2	6	6.4	6	4.6
1800					6	5.5	2	5.7	2	6.4	6	5.9	2	4.5

Appendix B Commercial Preservation Manufacturers' Protocols

DNAstable® Protocol

PRODUCT NOS. 93000-001, 93021-001, 90021-001

PRODUCT DESCRIPTION

DNAstable is a unique storage medium that preserves genomic DNA, plasmids, bacterial artificial chromosomes (BACs), PCR products and oligonucleotides at room temperature. DNAstable allows for long-term stabilization of DNA samples with easy sample recovery by simply adding water.

Each tube or plate contains DNAstable provided as a coating at the bottom of the tube or well, which protects picogram to microgram amounts of DNA. DNAstable is formulated so that upon application of liquid samples, the matrix dissolves and forms a protective coating around the DNA. The sample must then be completely dried for maximum protection and stability for storage at ambient temperatures.

PRECAUTIONS AND DISCLAIMER

This product is for R&D use only, not for drug, household, or other uses. Please consult the Safety Data Sheet for information regarding hazards and safe handling practices.

STORAGE/STABILITY

DNAstable products and kits should be stored dry in their original unopened packaging at ambient laboratory temperatures until ready for use. Prolonged exposure to light may cause fading or color change of DNAstable; however, this will *not* affect the protective properties of the matrix. To prevent color change, store dried samples in a moisture-barrier bag or wrapped in aluminum foil to protect from light.

PROCEDURES

NOTES ON SAMPLE PREPARATION

Types of DNA. All types of DNA can be stored in DNAstable, including genomic DNA, plasmids, oligonucleotides, PCR products, artificial chromosomes (BACs), and DNA from complex sources (e.g. forensics or genetic identify DNA samples.)

Purification Techniques. Most standard molecular biology techniques and/or commercially available kits are compatible with DNAstable storage. Purified DNA that is DNase-free should be resuspended in water or TE buffer (10 mM Tris Cl, 1 mM EDTA) prior to application into DNAstable.

Determining yield. The concentration of the DNA sample should be determined prior to sample application into DNAstable. Although not essential, applying a known amount of DNA into DNAstable for storage can facilitate sample retrieval and subsequent applications. For optimal results, do not exceed 30 µg of total DNA per tube or well in a maximum volume of 50 µL. For oligonucleotides, we recommend storage of 20 µL aliquots, with a concentration of ≤100 µM per oligo (2 nmol of each oligo).

SAMPLE DRYING AND STORAGE

1. Determine the amount of purified DNA in the sample, and calculate the amount to be applied into DNAstable wells or tubes.

2. Gently apply the sample directly into the center of each tube or well containing DNAstable. The final volume of the sample applied to each well should be ≤50 µL.

3. Mix the sample thoroughly with gentle pipetting. Avoid forming air bubbles.

4. Dry the uncovered sample completely at room temperature (15-25 °C). We recommend using a laminar flow hood or drying under a vacuum concentrator to ensure complete drying (see table 1 below for drying times).

Sample Volume (µl)	Drying Times (hrs) Tubes	Drying Times (hrs) (96-well plate)
5	4	4
6–10	6	6
11–20	12	8
21–50	28	18
51–100	56	24
101–125	72	24

Table 1. drying times in a laminar flow hood

5. Store samples with a desiccant packet in the original pouch and heat-sealed. Alternatively, store dried samples in a dry storage cabinet at room temperature.

DNAgard® Protocol

Product Nos. 62001-036 and 62001-046

PRODUCT DESCRIPTION

DNAgard Tissue is designed for room temperature storage and shipment of DNA in biological tissues, such as mammalian cells and organ tissues. DNA in complex samples is protected by the unique stabilization properties of DNAgard Tissue. Samples can be stored in liquid DNAgard Tissue for at least 6 months at room temperature. Samples stored in liquid DNAgard Tissue are ready for immediate processing for DNA recovery via column extraction (following manufacturer's instructions) or using standard lab procedures involving digestion and organic extraction. Purified DNA can be used directly in downstream applications.

PRECAUTIONS AND DISCLAIMER

This product is for R&D use only, not for drug, household, or other uses. Please consult the Safety Data Sheet for information regarding hazards and safe handling practices.

STORAGE/STABILITY

DNAgard Tissue must be stored at room temperature. Use within 6 months of purchase date for optimal product performance. DNAgard Tissue stabilizes genomic DNA in cultured cells and animal tissue samples for at least 6 months at room temperature in a liquid storage format.

PROCEDURES

Sample Storage

Liquid Storage of Tissue Samples in DNAgard Tissue

Prepare tissue samples by dissection. For optimal DNA protection, store tissue fragments less than 75 mg. Small tissue fragments, thinly sliced (at least one edge of the tissue fragment be 5mm or less in length), ensures that DNAgard Tissue permeates rapidly the entire tissue sample. To maintain the integrity of the DNA, tissue fragments should be kept cold during dissection and transferred to DNAgard Tissue as soon as possible.

Submerge tissue fragment in 500 µL DNAgard Tissue solution for shipment or storage. At least 100 µL DNAgard Tissue is required per 10 mg tissue. If sample is to be shipped, it is important

to select a tube size that ensures that the tissue remains submerged during handling. We recommend the use of screw-cap tubes to prevent sample leakage during transport. For general storage, use 2 mL screw-cap tubes.

Store samples at room temperature and protected from light for up to 6 months.

Notes on Sample Recovery (from tissue samples stored as liquid in DNAgard Tissue)

Processing samples for DNA recovery should be done by commercially available column purification technologies or via standard laboratory procedures involving tissue lyses and organic extraction. For ease of use, we recommend removing the DNAgard Tissue solution from the tissue fragment prior to DNA isolation. However, if DNA yield is critical, optimal DNA recovery can be achieved by isolating genomic DNA from the entire DNAgard Tissue sample. Note on tissue disruption: DNA isolation via commercially available column technologies can often be facilitated by disruption of the tissue sample, thereby reducing the time required to fully lyse the tissue and release genomic DNA. We recommend the use of a pestle. Consult the DNA isolation manufacturer's instructions.

Maximal recovery of genomic DNA. For column purification protocols allowing DNA isolation from tissue samples re-suspended in buffer, no additional processing of DNAgard Tissue samples is needed. Follow manufacturer's instructions for DNA isolation, adhering to buffer-to-sample ratio specifications.

Maximal recovery of genomic DNA (modified protocol for column purification kits that initiate from a tissue sample free of liquid). Simply add the kit's initial lyses buffer in a 1:1 ratio with the DNAgard Tissue volume. Scale all other reagents as necessary based on this initial volume (proceed as if the resultant mixture was entirely kit lysis buffer) and process according to the kit specifications.

Maximal DNA isolation involving organic extraction. Tissues stored in DNAgard Tissue can be processed for DNA isolation using standard lab protocols involving tissue lyses and organic extraction. Simply pipette off the DNAgard Tissue solution, being careful to not remove the tissue sample. Add lyses buffers and enzymes according to established protocol.

Notes on Sample Recovery (from tissue culture cells stored as liquid in DNAgard Tissue)

Samples can be processed for DNA recovery directly via commercially available column purification technologies – no additional processing is needed. DNAgard Tissue solution should not be removed prior to sample processing; add lyses buffers and enzymes provided in your DNA isolation kit directly to the DNAgard Tissue sample. Follow manufacturer's instructions for DNA isolation, adhering to buffer-to-sample ratio specifications. Do not use organic extraction methods for DNA isolation (i.e. phenolchloroform extraction).

Maximal recovery of genomic DNA (using a DNA isolation kit that specifies cells be re-suspended in buffer or media). DNAgard Tissue can be treated as if it were any re-suspension buffer or media. Follow manufacturer's instructions for DNA isolation, adhering to reagent ratio specifications.

Maximal recovery of genomic DNA (using a DNA isolation kit that only provides protocol from cell pellet starting point). Do not pellet the DNAgard Tissue-cell suspension (genomic DNA from cells is released into the DNAgard Tissue solution during storage). Simply add the kit's initial lysis buffer in a 1:1 ratio with the DNAgard Tissue volume. Scale all other reagents as necessary based on this initial volume (proceed as if the resultant mixture was entirely kit lyses buffer) and process according to the specifications described in the kit.

Biomeme DNA Preservation

Biomeme's DNA/RNA Preservation Buffer is used to collect and maintain samples during transport and before molecular analysis.

Each order of DNA/RNA Preservation Buffer Tubes includes 100 tubes each filled with 3mL of buffer. (Hyde et al. 2020)

DNA/RNA Shield™

ZYMO RESEARCH
The Beauty of Science is to Make Things Simple

Catalog Nos: R1100-50 (50 ml)
R1100-250 (250 ml)
R1200-25 (25 ml) 2X concentrate
R1200-125 (125 ml) 2X concentrate
Storage: Reagent stable -80°C to 70°C.

Features

- Eliminates cold-chain. Ensures DNA/RNA stability during sample transport/storage at ambient temperatures.
- Inactivates infectious agents *(viral, bacterial, fungal and parasitic)*.
- Easy sample processing. DNA/ RNA can be isolated directly without sample precipitation or reagent removal *(compatible with most DNA and RNA purification kits/ high-throughput workflows)*.

Sample Stability

Samples in DNA/RNA Shield™ are stable for long periods of time before subsequent purification of high-quality DNA/RNA.

Temperature	Time
-20°C and below	Indefinite
4°C – 25°C (ambient)	Minimum 30 days
35-40°C	Up to 7 days

Instructions for Sample Storage/Transport

Transport at ambient temperature
(No cold-chain or dry-ice needed)

Unsure of sample type? Just add 9 volumes of DNA/RNA Shield™.
If sample is viscous, add more DNA/RNA Shield™.

Suggested Volumes

DNA/RNA Shield™	300 µl	600 µl
Cell pellets	10^6	10^7
Tissue	30 mg	60 mg
Biological liquid	100 µl	200 µl

DNA/RNA Shield™ (2X concentrate):
(1) Use only for immediate sample processing/purification.
(2) For sample storage, dilute with nuclease-free water (1:1) prior to use.

DNA/RNA Purification

Samples in DNA/RNA Shield™ are directly compatible with:
- All Zymo Research Purification Kits.
- Most kits and workflows from Qiagen, Roche, Thermo-Fisher, Macherey Nagel, etc.
- High-throughput automated workflows from Hamilton, Tecan, bioMérieux, PerkinElmer, Eppendorf, Promega, etc.

Recommended Purification Kits for DNA/RNA Shield™:

Product / Format	Size	Cat. No.
Quick-DNA/RNA™ Miniprep Plus *Spin Column*	50 preps	D7003
Quick-DNA/RNA™ MagBead *Magnetic Bead*	96 preps 384 preps	R2130 R2131

ZYMO RESEARCH CORP.
Phone: (949) 679-1190 • Toll Free: (888) 882-9682 • Fax: (949) 266-9452 • info@zymoresearch.com • www.zymoresearch.com

Protection from freeze-thaw damage

Are your samples protected from the stress caused by freeze-thaw cycling? DNA/RNA Shield™ is not only beneficial for sample transport, but also for the long-term storage of biological samples. DNA/RNA Shield™ protects DNA/RNA from multiple freeze-thaw cycles, even in the most complex of samples (i.e., whole blood).

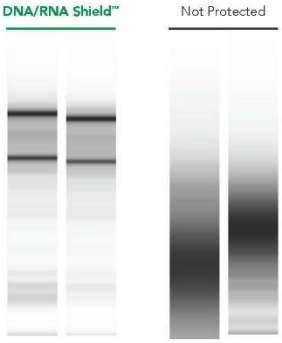

High quality RNA from blood stored in DNA/RNA Shield™ that was freeze-thawed from -80°C to room temperature.

Pathogen Inactivation

DNA/RNA Shield abides by Center for Disease Control's (CDC) guidelines for pathogen inactivation.

Validated organisms by various research groups:

Bacteria	Viruses	Yeast & Eukaryotes
B. subtilis	Parvovirus	*C. albicans*
E. faecalis	Chikungunya Virus	*C. neoformans*
E. coli	Dengue Virus	*S. cerevisiae*
L. fermentum	Ebolavirus	*P. malariae*
L. monocytogenes	Herpes Simplex Virus-1	
M. tuberculosis	Herpes Simplex Virus-2	
P. aeruginosa	Influenza A	
S. enterica	Rhinovirus	
S. aureus	MERS-coronavirus	
S. pneumoniae	West Nile Virus	
X. fastidiosa		

COMPLIANT CDC CENTERS FOR DISEASE CONTROL AND PREVENTION

CERTIFIED BY Eurovir® Hygiene-Labor Antivirale Validierung & Rabies

DNA/RNA Shield™ Collection Devices

Product	Description	Recommended processing
Fecal collection tube R1101	20 x 76 mm container prefilled with 9 ml DNA/RNA Shield™ for the direct collection of up to 1 gram or 1 ml stool. Collection spoon is included in the container screwcap.	ZymoBIOMICS™ DNA/RNA D4301 (spin-column); D4302 (magbead)
Swab & collection tube R1106, R1107, R1108, R1109	12 x 80 mm self-centering screwcap container filled with DNA/RNA Shield™ (1 ml, 2 ml) and a sterile swab for specimen collection.	
Saliva collection kit R1210	Saliva collection tube with funnel and tube filled with 2 ml of DNA/RNA Shield™ for the direct collection of 2 ml saliva.	*Quick*-DNA/RNA™ Plus D7001 (spin-column); R2130 (magbead)
Collection & lysis tube R1102, R1103, R1104, R1105	2 ml screw-cap tube with DNA/RNA Shield™ and Bashing Beads (lysis tubes: microbe, tissue, pathogen) for the collection and homogenization of tough-to-lyse samples.	
Blood collection tube R1150	16 x 100 mm evacuated blood tube filled with 6 ml of DNA/RNA Shield™ for the direct collection of 3 ml whole-blood (human or animal).	*Quick*-DNA/RNA™ Blood Tube R1151 (spin-column); R2130 (magbead)

For bulk reagent, large volume, and custom device requests, please contact Zymo Research directly.

Ordering information

Product	Pack size	Cat. no.
QIAcard FTA Elute Indicating Micro	100	WB120411
QIAcard FTA Elute Indicating Micro	25	WB120412
UniCore Punch Kit 3.0 mm	4 (including 2 cutting mats)	WB100039
UniCore Punch 3.0 mm	25	WB100078
Cutting Mat 2.5" x 3.0"	1	WB100088
Cutting Mat 6.0" x 8.0"	1	WB100020
Multi-Barrier Pouches, 3.75" x 3"	100	WB100036
Indicating Desiccant Pack (1000)	1000 (1 g each)	WB100003
Investigator Lyse&Spin Basket	50	19597
Investigator Lyse&Spin Basket	250	19598

Document Revision History

Date	Changes
11/2020	Initial release

Appendix C: Dps Purified Protein

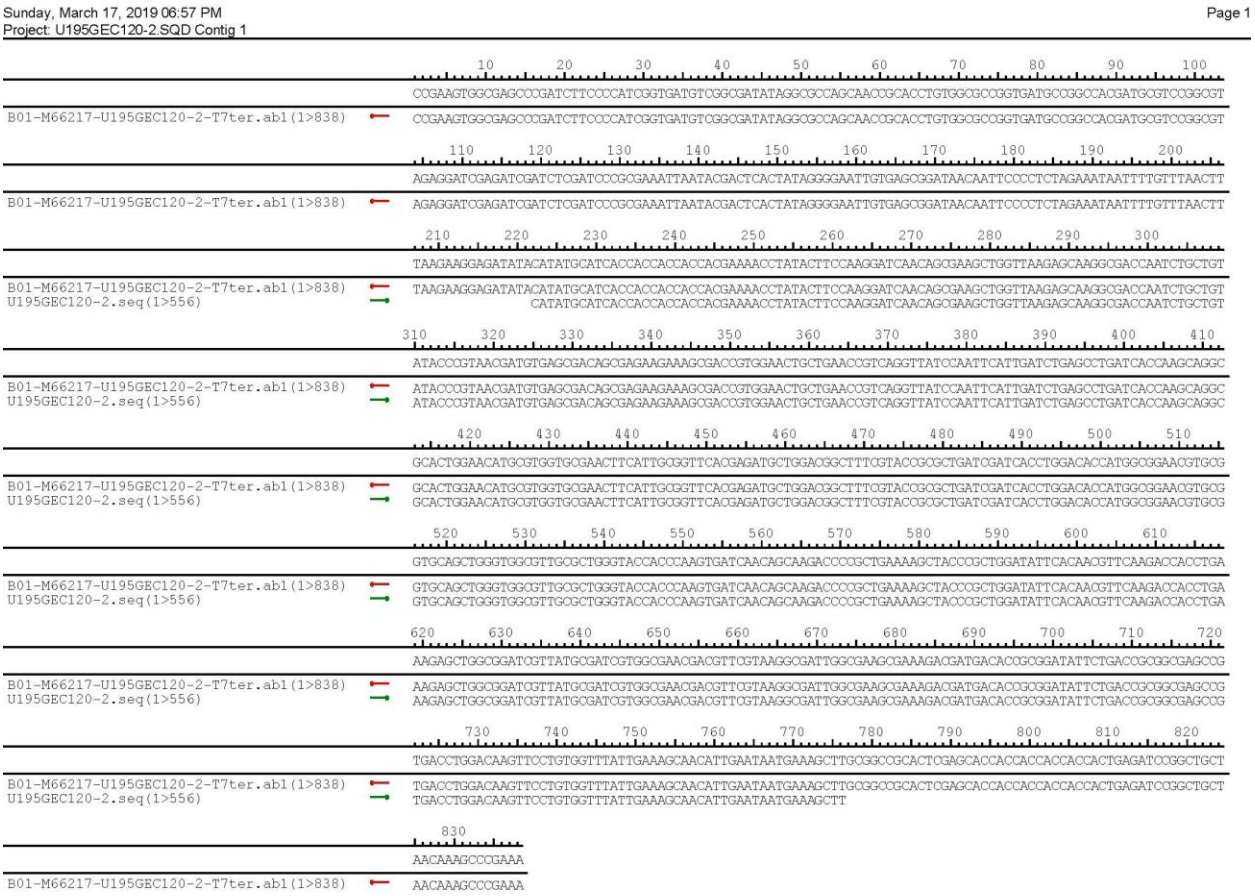

Attachment 1

Plasmid Construct Map

The gene was cloned in pET-30a(+) by NdeI / HindIII.

NdeI — **U195GEC120-2** — HindIII

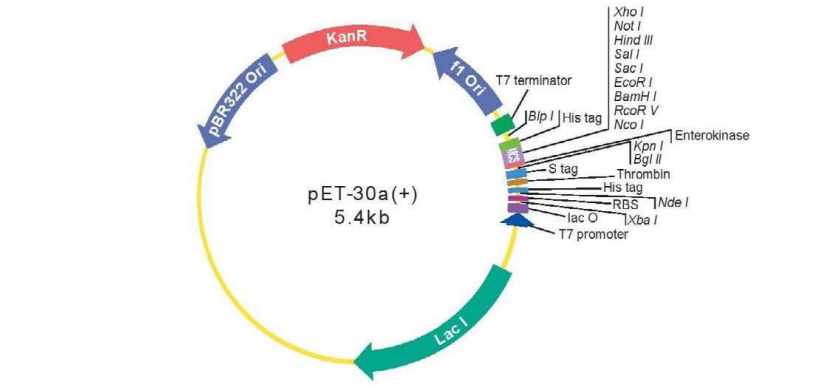

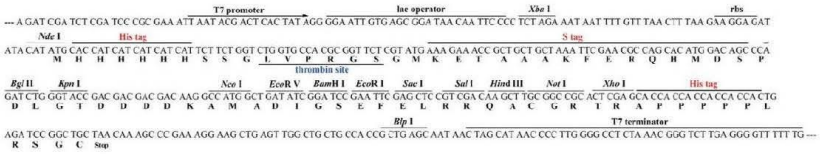

Notes: This map is based on a commercial vector. Some of the clone sites may be lost after cloning.

Enzyme Digestion

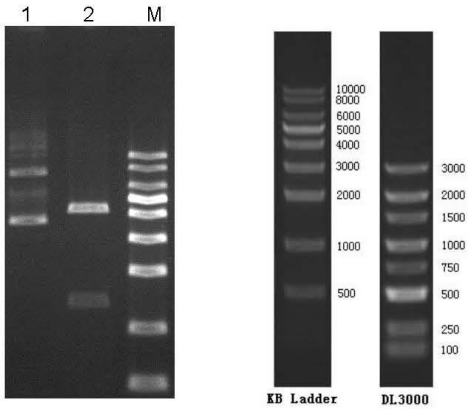

Lane M: KB Ladder
Lane 1:U195GEC120-2 plasmid
Lane 2:U195GEC120-2 plasmid digested by MluI and HindIII

Digestion Conditions:

About 300ng plasmid digested
Digestion in water-bath,37℃ for 40 minutes
1% Agarose Gel

For research use only

Certificate of Analysis

Project ID: U195GEC120-2

Construct Information:

Gene Name:	U9698EC110-1 (Dps protein) pET-30a(+)		
Clone ID:	M66217	**Gene Length:**	555 bp
Cloning Vector:	pET-30a(+)	**Cloning Strategy:**	NdeI / HindIII

Growth in Bacteria:

Plasmid resistance:	Kanamycin
Suggested competent cell:	TOP10
Growth Temperature:	37℃

Sequencing primer(s) *:

T7: TAATACGACTCACTATAGGG

T7ter: TGCTAGTTATTGCTCAGCGG

*: The primers are located at the 5'and/or 3'sides of MCS region.

Default	Shipping at	Plasmid Storing at	Bacstab Storing at	Glycerol Stock Storing at
Lyophilized	Room Temperature	-20℃	4℃	-80℃

QC Items	Specifications	Results	
Sequencing Alignment	Sequencing results are consistent with the targeted insert sequence.	Pass	Consistent
Vector Sequence	The flanking sequences of the cloning site are correct.	Pass	Correct Shown in the SQD file
Restriction Digests	The size of inserted fragment is correct and free of unexpected bands suggesting contamination.	Pass	Correct Shown in attachment 1
DNA Quality	Miniprep: 4 ug OD260/280=1.8~2.0 Free of contamination	Pass	⩾ 4 ug OD260/280=1.82 Pure
Quality Grade	Research Grade	Pass	Research Grade
Appearance	Clear and free of foreign particles.	Pass	Clear Free of foreign particles
Additional Test		N/A	

Certified by: Morgan **Date:** 03/19/2019

860 Centennial Ave., Piscataway, NJ 08854, USA
Toll-Free: 1-877-436-7274 Tel: 1-732-885-9188 Fax: 1-732-210-0262 Email: order@genscript.com Web: www.genscript.com